



LIBRARY

NBS REPORT

7238

THE PREDICTION OF SERVICE VOLUMES FOR
AIR NAVIGATION FACILITIES

by

RESEARCH INSTITUTE LIBRARY
SAN ANTONIO, TEXAS

G. D. Gierhart, J. S. Miller,
M. E. Johnson, and A. P. Barsis



U. S. DEPARTMENT OF COMMERCE
NATIONAL BUREAU OF STANDARDS
BOULDER LABORATORIES
Boulder, Colorado

THE NATIONAL BUREAU OF STANDARDS

Functions and Activities

The functions of the National Bureau of Standards are set forth in the Act of Congress, March 3, 1901, as amended by Congress in Public Law 619, 1950. These include the development and maintenance of the national standards of measurement and the provision of means and methods for making measurements consistent with these standards: the determination of physical constants and properties of materials; the development of methods and instruments for testing materials, devices, and structures; advisory services to government agencies on scientific and technical problems; invention and development of devices to serve special needs of the Government; and the development of standard practices, codes, and specifications. The work includes basic and applied research, development, engineering, instrumentation, testing, evaluation, calibration services, and various consultation and information services. Research projects are also performed for other government agencies when the work relates to and supplements the basic program of the Bureau or when the Bureau's unique competence is required. The scope of activities is suggested by the listing of divisions and sections on the inside of the back cover.

Publications

The results of the Bureau's work take the form of either actual equipment and devices or published papers. These papers appear either in the Bureau's own series of publications or in the journals of professional and scientific societies. The Bureau itself publishes three periodicals available from the Government Printing Office: The Journal of Research, published in four separate sections, presents complete scientific and technical papers; the Technical News Bulletin presents summary and preliminary reports on work in progress; and Basic Radio Propagation Predictions provides data for determining the best frequencies to use for radio communications throughout the world. There are also five series of nonperiodical publications: Monographs, Applied Mathematics Series, Handbooks, Miscellaneous Publications, and Technical Notes.

Information on the Bureau's publications can be found in NBS Circular 460, Publications of the National Bureau of Standards (\$1.25) and its Supplement (\$1.50), available from the Superintendent of Documents, Government Printing Office, Washington 25, D.C.

NATIONAL BUREAU OF STANDARDS REPORT

NBS PROJECT

NBS REPORT

8370-12-83478

7238

March 26, 1962

THE PREDICTION OF SERVICE VOLUMES FOR AIR NAVIGATION FACILITIES

by

G. D. Gierhart, J. S. Miller,
M. E. Johnson, and A. P. Barsis

This study was sponsored by
the Federal Aviation Agency.



U. S. DEPARTMENT OF COMMERCE
NATIONAL BUREAU OF STANDARDS
BOULDER LABORATORIES
Boulder, Colorado

IMPORTANT NOTICE

NATIONAL BUREAU OF STANDARDS
documents intended for use within
is subjected to additional evaluation,
tion, or open-literature listing
mission is obtained in writing
25, D. C. Such permission is
been specifically prepared if

Approved for public release by the
Director of the National Institute of
Standards and Technology (NIST) on
October 9, 2015.

progress accounting documents
is formally published in
ation, reprinting, reproduction,
not authorized unless permission
of Standards, Washington, D. C.
y for which the Report has been
es for its own use.

TABLE OF CONTENTS

	<u>Page No.</u>
ABSTRACT	1
1. INTRODUCTION	1
2. TRANSMISSION LOSS CALCULATIONS	3
3. INTERFERENCE BETWEEN TWO STATIONS	8
4. SYSTEM PARAMETERS	10
5. COMPUTER PROGRAMS	11
6. RESULTS OF THE STUDY	13
a. Service Limitations Due to Noise	13
b. Service Limitation Due to Co-Channel Interference	14
c. Signal-to-Interference Ratio Curves	15
7. COMPARISON OF THE RESULTS WITH PREVIOUS STUDIES	19
8. ACKNOWLEDGEMENTS	20
 <u>APPENDIX</u>	
1. VOR PROPAGATION MODEL	I-1
2. TACAN PROPAGATION MODEL	I-11
3. COMPUTATION PROCEDURES	I-17
a. General Methods and VOR Calculations	I-17
b. TACAN Calculations	I-25
c. Extension of the Program to the Case of Multiple-Station Interference	I-26

REFERENCES

THE PREDICTION OF SERVICE VOLUMES FOR AIR NAVIGATION FACILITIES

by

G. D. Gierhart, J. S. Miller,
M. E. Johnson, and A. P. Barsis

ABSTRACT

This report deals with the prediction of service volumes (i. e., service ranges in three dimensions) for VOR and TACAN air navigation facilities in the presence of noise and interfering stations. Propagation mechanisms applicable to the frequency ranges employed are discussed first, together with calculation of transmission loss and its variability. Second, the statistical treatment of the interference problem is explained. Finally, it is shown how service volumes are determined based on transmission loss and its variations, specified or assumed criteria on signal-to-noise and signal-to-interference ratio, and the spatial relations of the aircraft, the desired facility, and the undesired facility. The results of the entire study are presented in graphical form.

Detailed procedures, mathematical formulas, and computer programs used are discussed in the Appendix.

1. INTRODUCTION

Increasing air traffic density together with fast, high-flying jets have made the use of reliable air navigation aids more imperative than ever before. In expanding the present complex of navigation aids to meet future demands consideration must be given to potential interference between facilities operating on the same or on adjacent channels. The amount of interference is a function of the desired-to-undesired signal ratio at the aircraft antenna terminals; as both signals vary with time and aircraft location, the ratio varies as well, and the

interference becomes dependent on time and location. Due to the nature of radio wave propagation in the frequency ranges used, the variations of the received signals and of the interference ratios are best described statistically. The large number of possible conditions dictates the use of a digital computer with programs that take into account all variables as well as the fixed equipment parameters.

The navigation aids treated here, namely VOR and TACAN operate in the 100 and 1,000 Mc/s frequency ranges, respectively. In these ranges, propagation of radio frequency energy is affected principally by the lower atmosphere (the troposphere), specifically by variations in the refractive index of the atmosphere. The terrain along and in the vicinity of the great circle path between transmitter and receiver also plays an important part.

Within the last decade a number of methods and procedures have been developed to calculate field strength and its variability. In this report procedures are followed which have been used at the National Bureau of Standards to predict in a statistical manner the effects of terrain and atmosphere on the variability of field strength and on the performance of radio systems; see for example Barsis, Norton, Rice, and Elder [1961], and NBS Report 6767 [1961]. It is also convenient to use the concept of transmission loss [Norton, 1953 and 1959], which is the ratio of power transmitted to the power available at the receiving antenna terminals, usually expressed in decibels. Methods used for its calculation as a function of path length, terminal heights, and carrier frequency are discussed below.

All fixed and variable parameters for either the VOR or the TACAN system are assembled into essentially one general computer program which yields signal-to-noise and signal-to-interference ratios for given probability-of-service values as functions of aircraft location

in relation to the desired and the undesired transmitting facility and equipment parameters. From these results, boundaries of service volumes have been established corresponding to points in space where the specified desired-to-undesired signal strength ratios will be exceeded with a probability of 0.95.

For the time being, only one interfering station has been considered in any particular case, and the study is restricted to conditions along a common great circle path between the desired station, the aircraft, and the undesired station.

2. TRANSMISSION LOSS CALCULATIONS

Figure 1 shows a typical configuration of the aircraft (representing the receiving terminal), a desired navigational transmitting facility, and an undesired navigational transmitting facility. All three are aligned along a great circle path, and for simplicity assumed to be above a smooth surface. In the example drawn, the aircraft is within the radio horizon of the desired facility, but beyond the radio horizon of the interfering station. The distances along the great circle path from a point vertically below the aircraft to the desired and the undesired station are denoted by d_D and d_U , respectively. The aircraft is at a height h_2 above the terrain. The angle θ between the horizon rays from the aircraft and the interfering station is an important parameter in the calculation of transmission loss for beyond-line-of-sight paths [Norton, Rice, and Vogler, 1955]. For the assumption of a smooth spherical earth, θ is also the distance between radio horizons expressed in angular measure, and it is therefore called the "angular distance," as indicated on Fig. 1. As is customary in the analysis of tropospheric propagation paths, first order allowance for

the refraction effects of the atmosphere is accounted for by assuming an earth radius $4/3$ times the actual radius. This permits radio rays to be drawn as straight lines, and simplifies the determination of geometric parameters.

Transmission loss calculations are accomplished in three steps for the application to air navigation problems, as follows:

- (a) A reference value of basic transmission loss is calculated in accordance with methods given in NBS Report 6767 [1961]. This reference value, as explained by Norton, et al. [1955], represents the conditions on an average winter afternoon in the northern temperate zone. More specifically, it is the median of all hourly medians within "Time Block 2," representing the hours 1:00 p.m. to 6:00 p.m., November through April. The term "basic transmission" loss means that for the purpose of these calculations the antennas at the terminals are considered to be isotropic with unity power or voltage gain in all directions. Actual antenna characteristics are brought in later on when converting from basic transmission loss to transmission loss.

Within the radio horizon, basic transmission loss is calculated using geometric optics methods including interference between the direct and the ground-reflected ray. For the VOR propagation model in the 110 Mc/s frequency range, a specular reflection was assumed with effective reflection coefficients on the order of 0.9. In the case of TACAN with frequencies in the 1100 Mc/s range it is more appropriate to assume that the ground-reflected ray is

made up of a large number of components having random relative phase. The total contribution from these components can be represented statistically by a Rayleigh distribution [Decker, 1957; McGavin and Maloney, 1959]. Norton, Vogler, Mansfield, and Short [1955] have shown how this Rayleigh-distributed reflected component can be combined with a fixed component representing the direct ray in order to arrive at the resulting distribution of basic transmission loss at the receiver.

Beyond the radio horizon, basic transmission loss is calculated using smooth-earth diffraction or forward scatter models, depending on the path distance involved. The diffracted field decreases very rapidly for distances beyond the radio horizon, especially at the TACAN frequencies, so that the forward scatter model is the more important one. Calculations for both models, and the method of properly combining diffraction and scatter fields if they are of comparable magnitude, are based on procedures contained in NBS Report 6767 [1961].

- (b) Long-term variations in basic transmission loss are estimated by means of time variability functions $V(p, \theta)$ or $V(p, d)$ for VOR, and $V(p, d)$ for TACAN. These empirical functions were calculated in accordance with methods given in NBS Report 6767 [1961]. The $V(p, \theta)$ curves were derived from data mostly in the 100 Mc/s range and at distances beyond the radio horizon, and were therefore thought well applicable to the VOR frequencies at angular distances greater than 10 milliradians, whereas the $V(p, d)$

functions contain a frequency factor, and are based on a more extensive data sample extending up to the frequency range of TACAN, and are also more suitable for distances within and slightly beyond the radio horizon than the $V(p, \theta)$ curves. Thus the $V(p, d)$ functions were used for VOR at distances corresponding to $\theta < 10$ milliradians, and for TACAN at all distances.

Either one of the $V(p, \theta)$ or $V(p, d)$ functions are used to determine the cumulative distribution with time of hourly median basic transmission loss values relative to the reference values calculated under (a) above. The results for VOR and TACAN consist in expected distributions of all hourly median basic transmission loss values during the year as functions of path length, angular distance, terminal height, and carrier frequency.

- (c) In addition to the distributions of hourly medians representing long-term variations, short-term (usually within-the-hour) distributions of the received signal levels have to be considered. Short-term variations in this particular application are principally due to two causes. One is the inherent short-term fluctuation of the tropospheric signal ascribed to the phase interference of rays reflected from small layers or scattered from refractive index discontinuities, or to reflections from ground irregularities. The other cause is the pattern of the aircraft antenna: the numerous small lobes and gain changes with varying bearings are best represented by a cumulative distribution of effective antenna gain with time as the aircraft moves through space.

This is actually a variation in transmission loss and not in basic transmission loss as it concerns the gain of the receiving antenna in the aircraft. However, the actual calculations for both VOR and TACAN are handled most efficiently by including the gain of the transmitting antenna (ground facility) in the auxiliary propagation curves developed for the model, and by treating the variable gain of the receiving antenna as an additional time variability, which has to be combined with the short-term fluctuations due to propagation and the long-term variability of hourly medians in order to arrive at a complete picture of time variations which can be used for the service and interference analysis. This will be discussed in more detail in the Appendix, where the mechanics of combining cumulative distribution will be explained.

Both the calculation of service volumes limited by receiver noise only and the calculation of service volumes under various conditions of interference require a knowledge of the time distribution of transmission loss or field strength at many points in space; therefore time variability calculations have to be performed for these points with distance from the desired and undesired station, aircraft height, spacing of desired and undesired ground facilities, carrier frequency, and antenna patterns as parameters.

It should be noted here that the one-hour period taken as the dividing line between long-term and short-term variations is somewhat arbitrary. It is convenient in view of the available empirical time variability functions.

3. INTERFERENCE BETWEEN TWO STATIONS

As shown by Fig. 1, both the desired and the undesired signals arrive at the aircraft over propagation paths characterized by the distances d_D and d_U , respectively, and by the aircraft height. The distances are measured along the great circle path. Both signals vary with time, and the distributions of signal levels are calculated in accordance with the procedures outlined in the preceding section. The next step is the determination of ratios of desired to undesired signal exceeded for given percentage-of-time values when the aircraft is at a particular location in space. A desired ratio value cannot be obtained directly for a desired percentage value of time; thus, ratio values are determined for a finite number of points scattered over the potential service volume for 95% time availability, and the location of the three-dimensional 95% time availability contour for a given ratio value is determined by interpolation. This procedure has to be repeated for each set of parameters such as spacing between co-channel ground facilities, or aircraft altitudes.

The ratio of desired-to-undesired signal can be expressed as a decibel difference of desired and undesired signal levels, which are obtained directly from the calculated transmission loss values and the system parameters. The distribution of the ratio will be denoted $D/U(p, d)$. This notation, besides the separately specified aircraft height and the spacing between the desired and the undesired ground station, implies a percentage-of-time value, p , as well as a distance parameter, d , which has to be identified in each specific case. The percentage value, p , is that percentage of time during which the given value of D/U is exceeded. By virtue of the aircraft being in motion, time variations also include variations in space. As the actual time

distribution of D/U may vary from installation to installation due to terrain characteristics and other factors not taken into account in this analysis, the time availability p may be interpreted as an expression of reliability for an average installation. The concepts of prediction uncertainty and service probability in the sense defined by Barsis, et al. [1961] are not used here explicitly. Because the calculations are based on smooth earth, the standard deviation characterizing a prediction uncertainty can be assumed to be quite small; therefore, the expected value corresponding to a service probability of 0.5 and used here is very little, if any, different from values applicable to a high degree of service probability. It should, however, be understood that installations in very rough terrain would show somewhat different results, if analyzed in detail. This consideration is applicable to any value of the time availability p considered; the 0.5 service probability has no relation to the percentage of time used, and may approximately be identified with the results obtained for an average installation over relatively smooth terrain.

As an example, $D/U(95, d_U) = 10$ db means that for the average installation the ratio of the desired to the undesired signal is equal to or greater than 10 db during 95% of the time at a distance d_U from the interfering station for a given aircraft height and spacing between the desired and the undesired station.

In order to solve for the time availability of the desired-to-undesired ratios at any point in space, time distributions of the individual power or signal levels (expressed in decibels) have to be combined in a similar way as was done to obtain the total time variability of transmission loss. Thus a time distribution of the decibel differences (representing the power ratios) can be obtained, from which the time availability of the specified ratio value can be determined for

each point in space. The method of combining cumulative distributions will be illustrated in the Appendix, as mentioned before.

4. SYSTEM PARAMETERS

System parameters are based on a standard VORTAC ground installation, and passenger-jet aircraft antennas. A 52 ft diameter counterpoise, 12 ft above ground, is used at the ground station for both the VOR and the TACAN antenna. Other parameters are as follows:

TABLE I
System Parameters

	<u>VOR</u>	<u>TACAN</u>
Carrier Frequency Used in the Calculations	113 Mc/s	1150 Mc/s
Transmitter Power	23 dbw	-
Transmission Line Losses	6 db	3 db
Effective Radiated Power	-	39, 43, & 48 dbw
Polarization	Horizontal	Vertical
Ground Antenna Type	Four-loop Alford Array	Center Array
Maximum Antenna Gain Relative to Isotropic Antenna	2.15 db	8.15 db
Horizontal Pattern	Appr. Circular	Appr. Circular
Vertical Pattern	Appr. like Dipole	See Fig. 3
Antenna Height above Counterpoise	4 ft	18 ft
Antenna Height above Ground	16 ft	30 ft
Aircraft Antenna Type	E-Cavity	Annular Slot
Aircraft Antenna Gain	See Fig. 2	See Fig. 4
Required Receiver Input		
Class I	5 μ V into 50 ohms	-109 dbw
Class II	10 μ V into 50 ohms	-103 dbw

For the VOR system, the 6 db line loss figure includes transmitting and receiving transmission line and associated losses. The gain of the aircraft antenna was determined as a function of azimuth and vertical angle from a modeling study based on an E-cavity type VOR antenna in the vertical stabilizer of a passenger-type jet aircraft [Conviar, 1959]. Fig. 2 shows the distribution of antenna gains at various vertical angles, together with the measurement points from which the principal distribution was derived.

The several values of effective radiated power assumed for the TACAN model include the line losses in the ground station and the transmitter power; therefore, the line loss figures given in Table I are the losses in the aircraft receiving system. The ground antenna was taken to be the typical center array shown by Casabona [1956], with its free-space vertical radiation pattern shown on Fig. 3. The gain of the aircraft antenna again was obtained from modeling studies based on an annular slot type DME antenna mounted on the bottom fuselage center line forward of the landing gear of a passenger jet aircraft. Pertinent distributions of antenna gain values for several vertical angles are shown on Fig. 4, together with the results of available measurements [Commercial Jetstar, 1959].

5. COMPUTER PROGRAMS

Calculations necessary to produce all desired distributions of transmission loss values or power levels as well as the processes involving the combination of various distributions are so numerous and complex that the use of a large electronic computer is mandatory. Computer programs were organized in the following manner.

- (a) Existing programs were modified and new programs were developed to calculate reference basic transmission loss values including the effect of the transmitting antenna as a function of distance and aircraft height for both, VOR and TACAN separately. The resulting propagation curves were reduced to tabular form, and made available to the computer as "data" for subsequent procedure.
- (b) Subroutines were developed for the combination of various cumulative time distributions. These served either to combine the various variability distributions, or, with changed sign, to obtain the final result of the computer programs, namely the distribution of desired-to-undesired signal ratios.
- (c) Short-term and long-term time distribution functions were made available to the computer in tabular form as "data" separately for VOR and TACAN. Distributions of receiving antenna gain values were handled in a similar way.
- (d) The main computer program used all the "data" assembled by the subroutines described, and delivered tables of interference ratios for various values of time availability as a function of the aircraft position and various distances between the desired and the undesired facilities. From these tables, auxiliary graphs were plotted, and the 95% time availability values determined which are the results of the study, and will be shown in graphical form in the next section.

The final program step, after check-out and after assembly of all subroutines and all "data," consumed about 15 hours of computer time. It is not possible to estimate the number of man hours required to accomplish the same object by the use of slide rule and desk calculator.

6. RESULTS OF THE STUDY

The results are in the form of prediction curves. Three types of curves are presented, which involve service limitations due to: (1) receiver sensitivity and transmitter power output only, i. e., the service is limited by noise; (2) interference from one co-channel station; and (3) proximity to an undesired station which may be operating on an adjacent channel.

a. Service Limitations Due to Noise

Curves of the first type are shown as solid lines on Figs. 5 and 6 labeled "VORTAC (or TACAN) Service Volume without Interference" and as dashed lines on Figs. 7 through 12 labeled "VOR (or TACAN) Service Volumes with Interference from One Co-Channel Station." In the volume defined by the revolution of the appropriate curve about the ordinate axis (the desired station is near the origin) service as defined in Section 3 is predicted to be available during 95% of the time. This may be called a conservative estimate, as interference conditions are based on the values obtained on the direct path between the desired and the undesired station; for other points on the surface of revolution there is obviously less interfering signal. The appropriate curve is determined by: (1) system type (VOR or TACAN), (2) receiver sensitivity (Class I or Class II), and (3) ground station power (VOR, 23 dbw transmitter power; TACAN, 48, 43, or 39 dbw effective radiated power).

The system parameters have been described in Section 4 above; however, the ground station power output for the "standard" TACAN curves on Fig. 5 was taken as the 48 dbw E.R.P. (effective radiated power) value. The effect of changes in the values of the E.R.P. are illustrated on Fig. 6, which shows Class I and Class II TACAN service volumes for the additional 39 and 43 dbw E.R.P. values, constituting noise-limited service volumes.

The Class I and Class II noise-limit curves for VOR and standard TACAN (48 dbw E.R.P.) are repeated on Figs. 7 through 9 and 10 through 12, respectively in order to show where noise is more restrictive than co-channel interference.

All figures discussed so far show also the distance to the radio horizon as a function of aircraft altitude, based on the antenna heights over a smooth earth and a standard atmosphere. Due to the higher elevation of the TACAN antenna, its radio horizon extends about two miles further for each aircraft altitude than the VOR horizon.

b. Service Limitation Due to Co-Channel Interference

The second type of curves, shown on Figs. 7, 8, and 9 for VOR and 10, 11, and 12 for TACAN, illustrates the effect of co-channel interference on the service volume when the aircraft is located above the great circle path between the desired and the undesired station at a distance d_D from the desired station. The geometry involved is shown by a small diagram on each curve sheet. Station separations, S , ranging from 70 to 695 nautical miles were considered along with aircraft altitudes ranging from 1,000 to 100,000 feet. Each curve sheet is applicable to a different signal-to-interference ratio, $D/U(95, d)$. For example, $D/U(95, d) = 14$ db means that the desired signal is at least 14 db greater for 95% of the time along the solid

curve which forms the boundary of service volume closest to the interfering station. On these figures the limitation imposed by ground station power output and receiver sensitivity is described only by the dashed lines labeled Class I or Class II.

The volume defined by rotating the appropriate curve about the ordinate axis represents a volume in which service reliability in the sense defined in Section 3 is 95% or greater (by virtue of each curve representing the smallest station separation). Similarly, if service is limited by interference from several co-channel stations, the volume defined by rotating the most restrictive curve (which is the curve appropriate to the closest interfering station) about the ordinate axis represents a volume in which the service reliability is generally 95% or greater, when an average installation (in the sense described above) is considered.

Figures 7, 8, and 9 describe VOR service volumes with one co-channel interfering station for signal-to-interference ratios of $D/U(95, d) = 14, 20, \text{ and } 26$, respectively.

Figures 10, 11, and 12 describe TACAN service volumes with one co-channel interfering station for signal-to-interference ratios of $D/U(95, d) = 8, 14, \text{ and } 20 \text{ db}$, respectively.

c. Signal-to-Interference Ratio Curves

The third type of curves shows signal-to-interference ratios in the neighborhood of an undesired station. The distance, d_U , from the undesired station is used to locate the aircraft in the same manner as d_D was used for the service volume curves in the preceding figures. This geometry is shown by the small diagram on each curve sheet. Signal-to-interference ratio values of $D/U(95, d)$ are used as the ordinate, with emphasis on negative values. Curves applicable to

station separations ranging from 25 to 175 nautical miles are presented on some of the graphs. There is a separate figure for each system-altitude combination with the altitudes ranging from 1,000 to 100,000 feet. As an example, the intersection of the $D/U(95, d) = -20$ db ordinate on Fig. 13 with the curve labeled $S = 70$ means that for 95% of the time the interfering signal exceeds the desired signal by at least 20 db at a distance of 27 miles from the undesired station and for the 1,000 ft aircraft height represented by Fig. 13. If, in an application to an adjacent channel interference problem, the undesired signal just causes trouble when it is greater than the desired signal by 20 db, service is available 95% of the time where the $D/U(95, d)$ curve for the appropriate station separation does not become more negative than -20 db.

The curve sheets developed for signal ratios near an undesired station are arranged as shown on Table II:

TABLE II

Index of Curve Sheets

<u>Figure Number</u>		<u>Aircraft Altitude</u>
<u>VOR</u>	<u>TACAN</u>	<u>In Feet</u>
13	26	1,000
14	27	5,000
15	28	10,000
16	29	15,000
17	30	20,000
18	31	30,000
19	32	40,000
20	33	50,000
21	34	60,000
22	35	70,000
23	36	80,000
24	37	90,000
25	38	100,000

The curves on Figs. 13-38 do not show the effect of interference beyond the undesired station or at locations not on the great circle path connecting the stations; i. e. the distance d_U shown on the abscissa scales locates the aircraft on the great circle path between the desired and the undesired station. However, a method of approximating the locus of a constant interference ratio $D/U(95, d_U)$ as a circle about the undesired station has been developed. For a given aircraft altitude this circle is centered on the extension of the line connecting the ground stations concerned, but on the "far" side of the undesired station. The pertinent geometry is shown in a top and a side view on Fig. 39. Generally service may be regarded as being unsatisfactory within this circle, even though some locations having satisfactory service may exist above the undesired station due to the vertical pattern of the ground antenna.

Two basic assumptions have to be made as follows:

- (a) The geometry represented by Fig. 39 may be considered plane geometry; thus the earth is assumed to be flat and the projection of the slant ranges r_U and r_D onto the horizontal plane is approximately equal to the actual ranges r_U and r_D .
- (b) The interference ratio $D/U(95, d_U)$ is proportional to the logarithm of the ratio of the ranges r_D/r_U . In the terminology used in the appendix, this may be written for any percentage value p :

$$D/U(p, d_U) = L(p, d_U) * [-L(p, d_D)] = M \log(r_D/r_U) \quad (1)$$

where M is a constant.

Assumption (a) is reasonable if $d_D > d_U \geq (\text{aircraft altitude}/1600)$, where the distances d_D and d_U are in nautical miles and the aircraft altitude is in feet. Hence, the problem of finding the locus of $r_D/r_U = \text{constant}$ may be solved using plane geometry. This locus is found to be a circle, described by the parameters C and R defined on Fig. 39, and given by the following equations which contain an additional auxiliary parameter B :

$$B = d_D/d_U = (S - d_U)/d_U \cong r_D/r_U \quad (2)$$

$$C = \frac{S(B^2 + 1)}{2(B^2 - 1)} \quad (3)$$

$$R = \frac{SB}{B^2 - 1} \quad (4)$$

As an example, use the separation $S = 150$ miles for the VOR graph of Fig. 16, representing an aircraft height of 15,000 ft. For a desired-to-undesired signal ratio $D/U(95, d_D) = -40$ db which may very well constitute the adjacent-channel interference threshold in a practical case, the distance $d_U = 20$ miles from the undesired station (with $d_D = 130$ miles) is read from Fig. 16. The results are:

$$B = \frac{130}{20} = 6.5$$

$$C = 75 (43/41) = 79 \text{ miles}$$

$$R = 975/41 = 24 \text{ miles}$$

Thus, inside a circle of 24 miles radius centered at a point 4 miles beyond the undesired station, VOR service at 15,000 ft aircraft altitude would be expected to be sub-standard.

It should not be overlooked that this method is only approximate. The second assumption, (b), would be violated by lobing in the transmission loss versus distance curve, which may occur at any constant altitude due to ground reflections or due to the ground antenna pattern. The assumption (b) would also be violated by a change in the slope of the transmission loss versus distance curve which, as an example, occurs in the vicinity of the radio horizon. However, the use of the largest d_U read for a particular station spacing and a particular signal ratio from Figs. 13-38 avoids the ambiguity due to lobing. Furthermore, in most applications service is limited by noise rather than by interference if ranges beyond the radio horizon of the desired station are considered.

7. COMPARISON OF THE RESULTS WITH PREVIOUS STUDIES

Staras, Rice, and Herbstreit [1951] have previously predicted VOR service volumes. The curves they developed are not in overall agreement with curves presented here. Although the antennas, both ground and air, used in the two predictions were not identical, they were so similar that only minor differences between prediction curves would be likely because of different antennas. However, since 1951 more refined methods for calculating transmission loss beyond the radio horizon and for estimating time variability have been developed. Thus, major differences in prediction curves are most likely caused by different variability estimates, and different predicted median fields beyond the radio horizon. The power output for VOR used in the

earlier study was 3 db lower than that used here, but only the curves for service without interference would be affected by this difference.

The TACAN curves developed by Decker [1956] also differ from the curves presented here. The same ground station antenna was used in both studies, but in the earlier study it was placed 100 feet above the ground, whereas in this study a height of 30 feet was used. Although the method used to account for ground reflections was almost identical, the actual numbers involved were different, because of the different ground antenna height and different estimates of the effective ground reflection coefficient. This may account for minor differences in the prediction curves, but different estimates of long-term variability, $V(p, d)$, were found to be more significant. Decker's probability of service curves applicable to interference limited service also included limitations due to noise (transmitter power and receiver sensitivity), whereas in the present study interference and noise limitations were treated separately.

8. ACKNOWLEDGEMENTS

This entire study was sponsored by the Aviation Facilities Service of the Federal Aviation Agency. The authors wish to acknowledge the participation of personnel in the Propagation-Terrain Effects Section of the National Bureau of Standards in all calculations and in the preparation of data for the machine programs. Drafting work was done by J. C. Harman and his group, and the manuscript was typed by Mrs. D. J. Hunt.

The authors also wish to thank Messrs R. S. Kirby and M. T. Decker for their review and suggestions.

SKETCH SHOWING RELATIVE POSITIONS OF AIRCRAFT AND
OF NAVIGATIONAL FACILITIES OVER A SMOOTH SPHERICAL EARTH

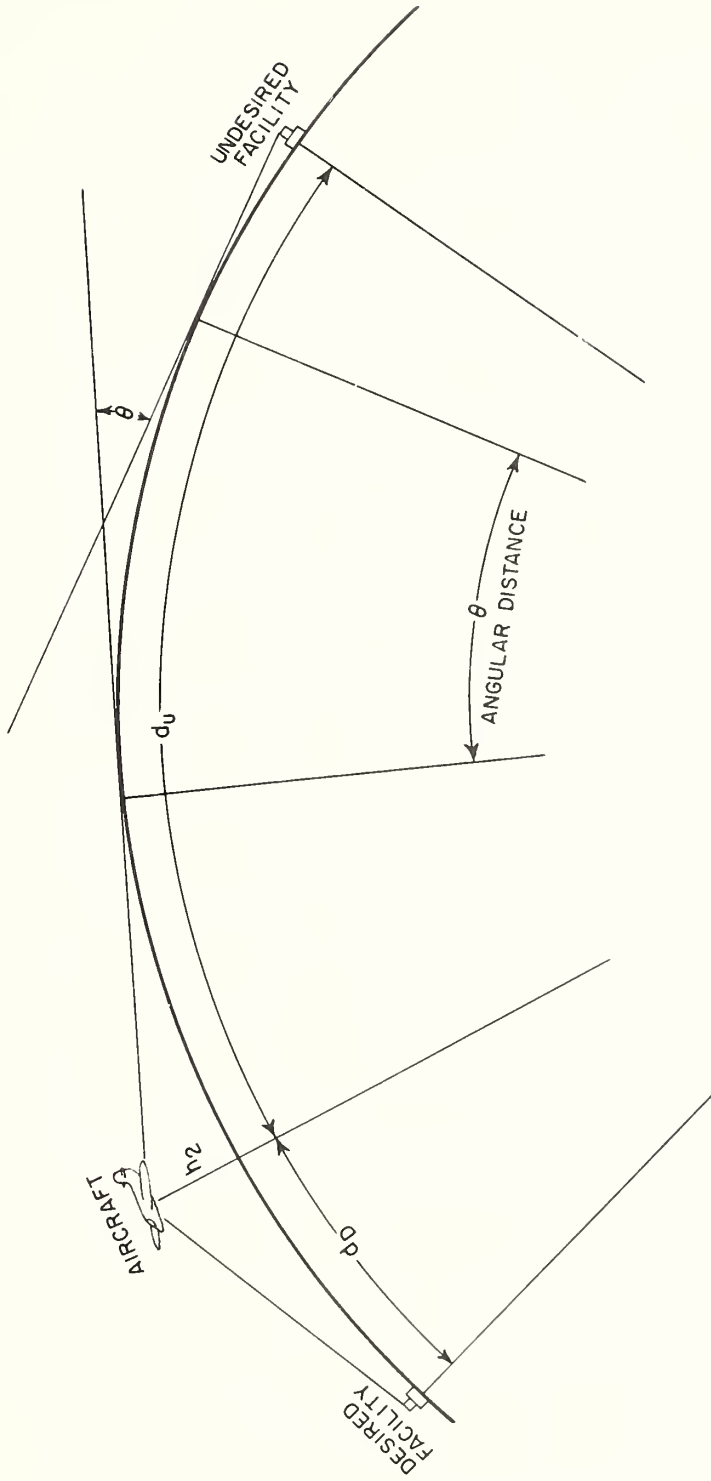


Figure 1

CUMULATIVE DISTRIBUTION OF AIRCRAFT ANTENNA GAIN
 VOR, STABILIZER MOUNTED E-CAVITY, HORIZONTAL POLARIZATION, 113 MC/S

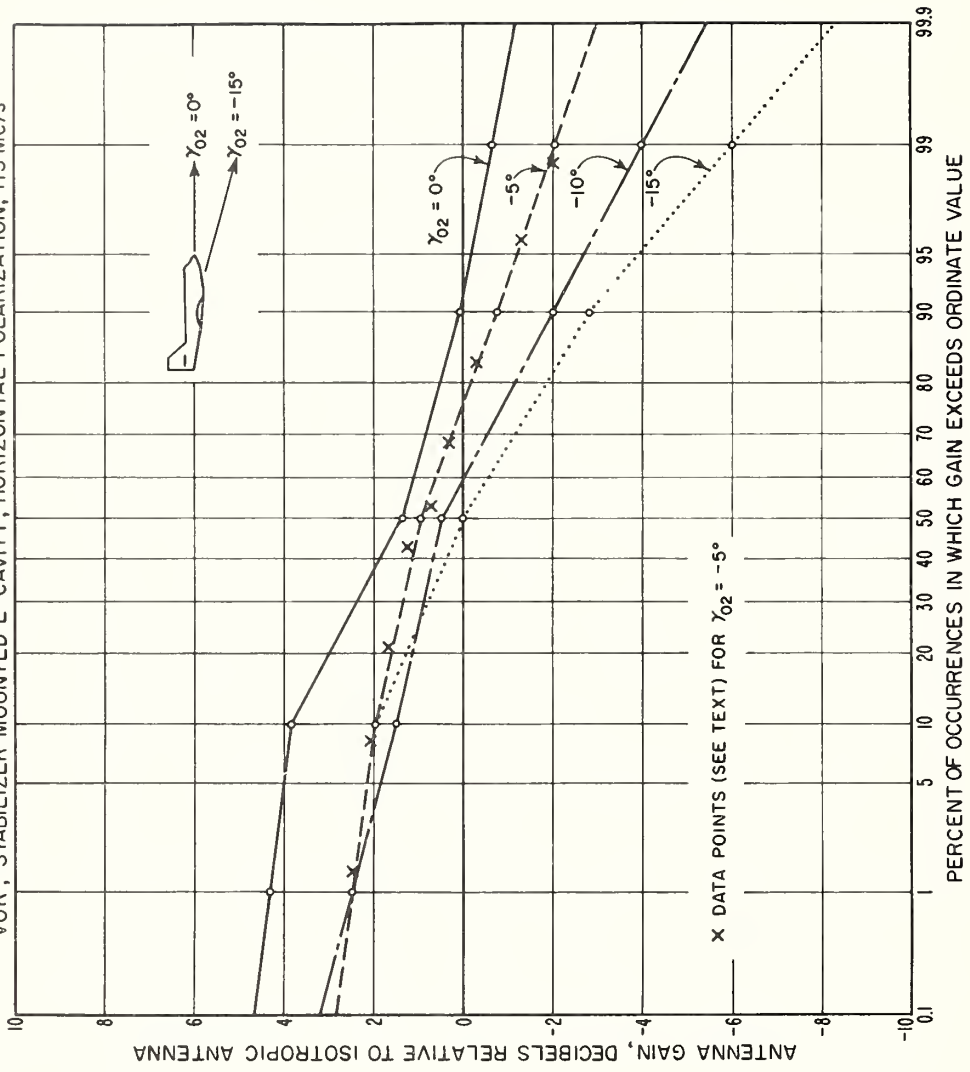


Figure 2

TYPICAL URN-3 ANTENNA PATTERN
Free Space Radiation in the Vertical Plane

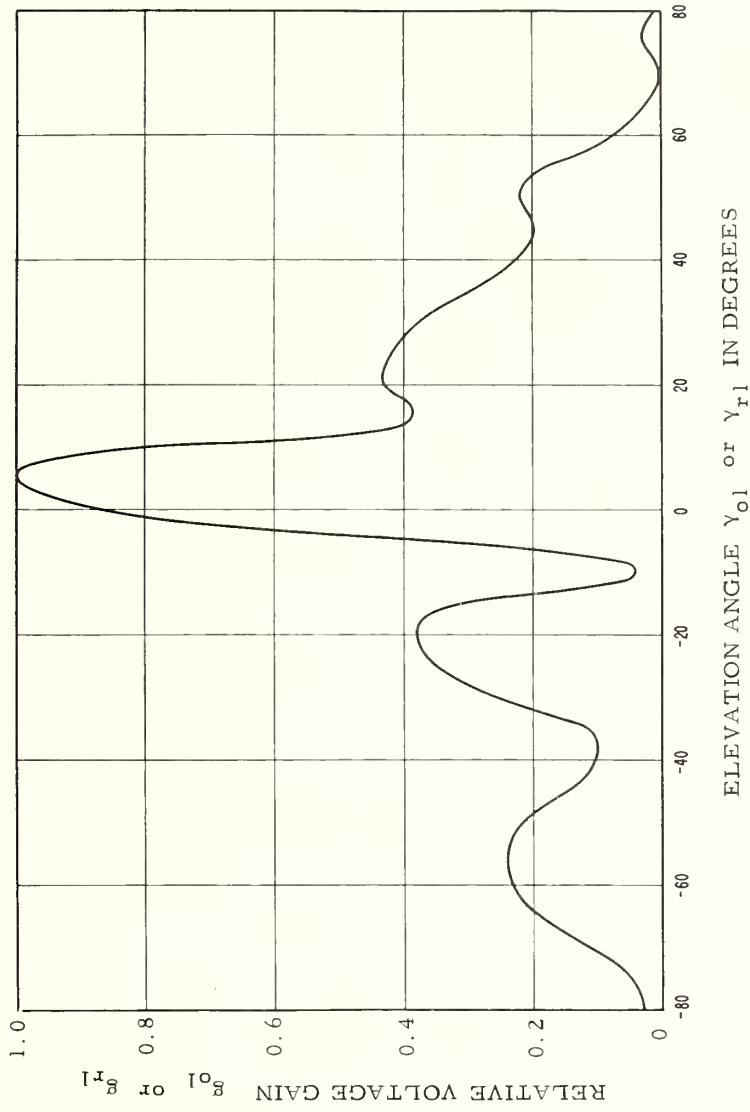


Figure 3

CUMULATIVE DISTRIBUTION OF AIRCRAFT ANTENNA GAIN
 TACAN, BELLY MOUNTED ANNULAR SLOT, VERTICAL POLARIZATION, 1150 Mc/S

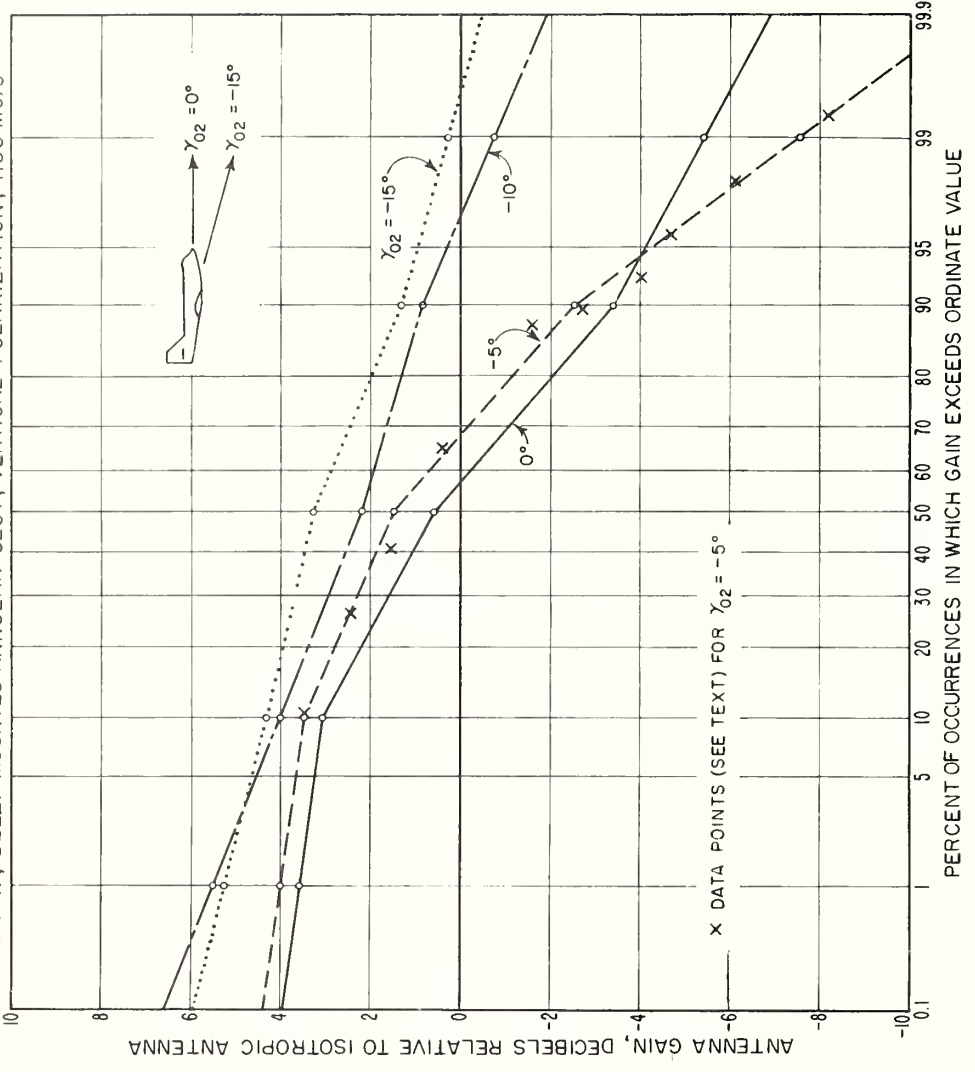


Figure 4

VORTAC SERVICE VOLUME WITHOUT INTERFERENCE
95% RELIABILITY

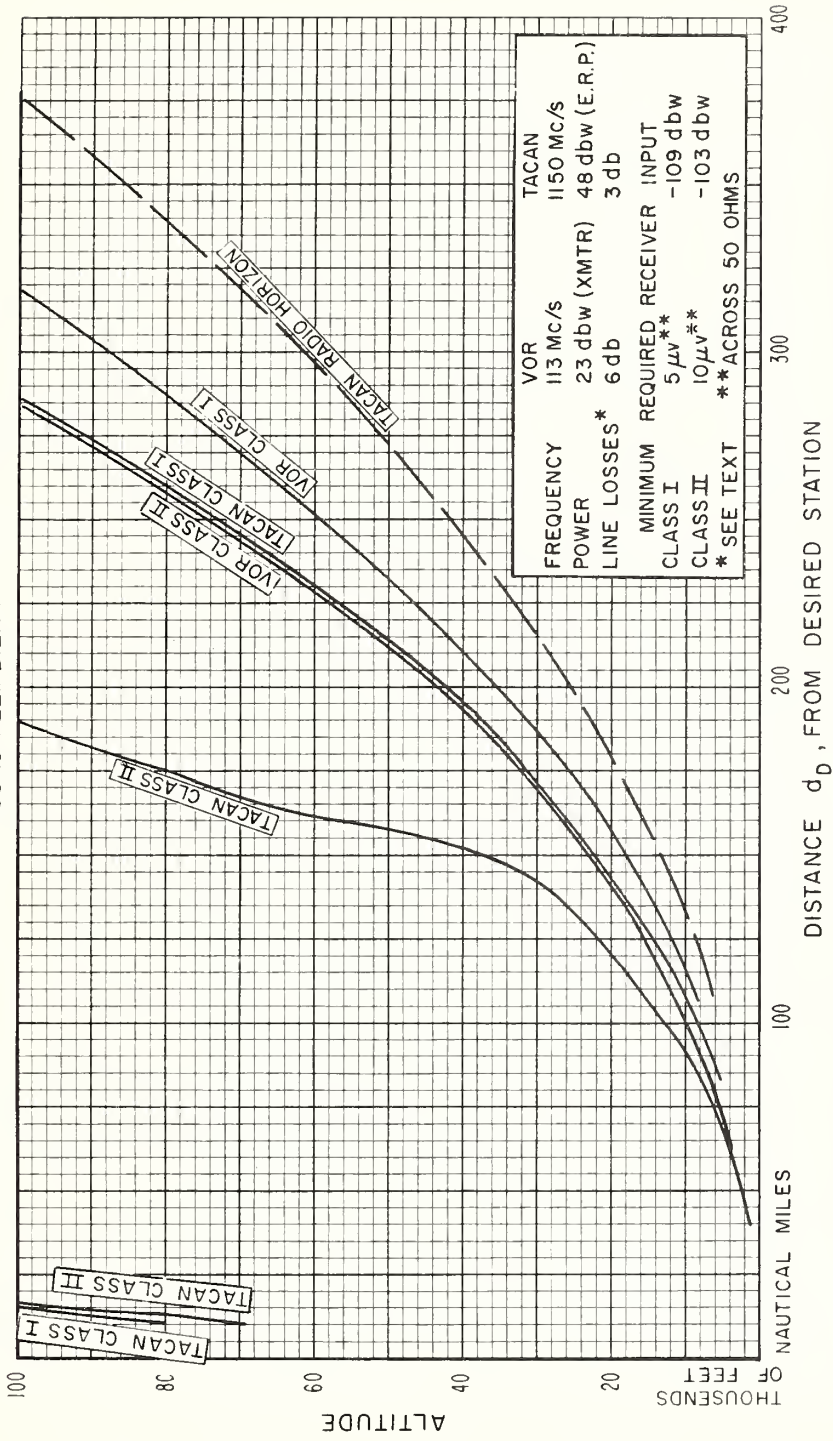


Figure 5

TACAN SERVICE VOLUME WITHOUT INTERFERENCE

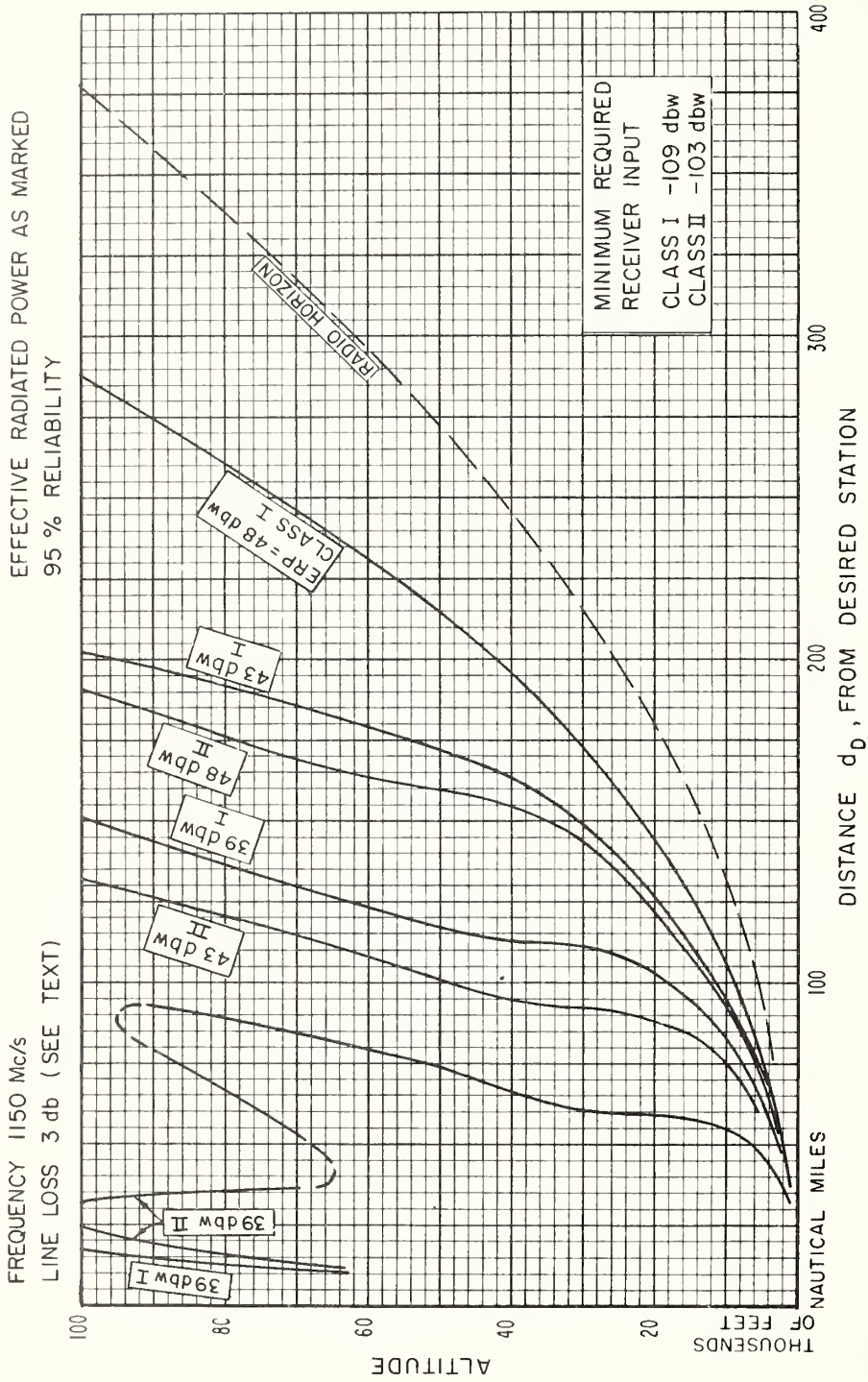


Figure 6

VOR SERVICE VOLUMES WITH INTERFERENCE FROM ONE CO-CHANNEL STATION

FREQUENCY 113 Mc/s
 D/U (95, d) = 14 db

STATION SEPARATION, S, AS LABELED
 95% RELIABILITY

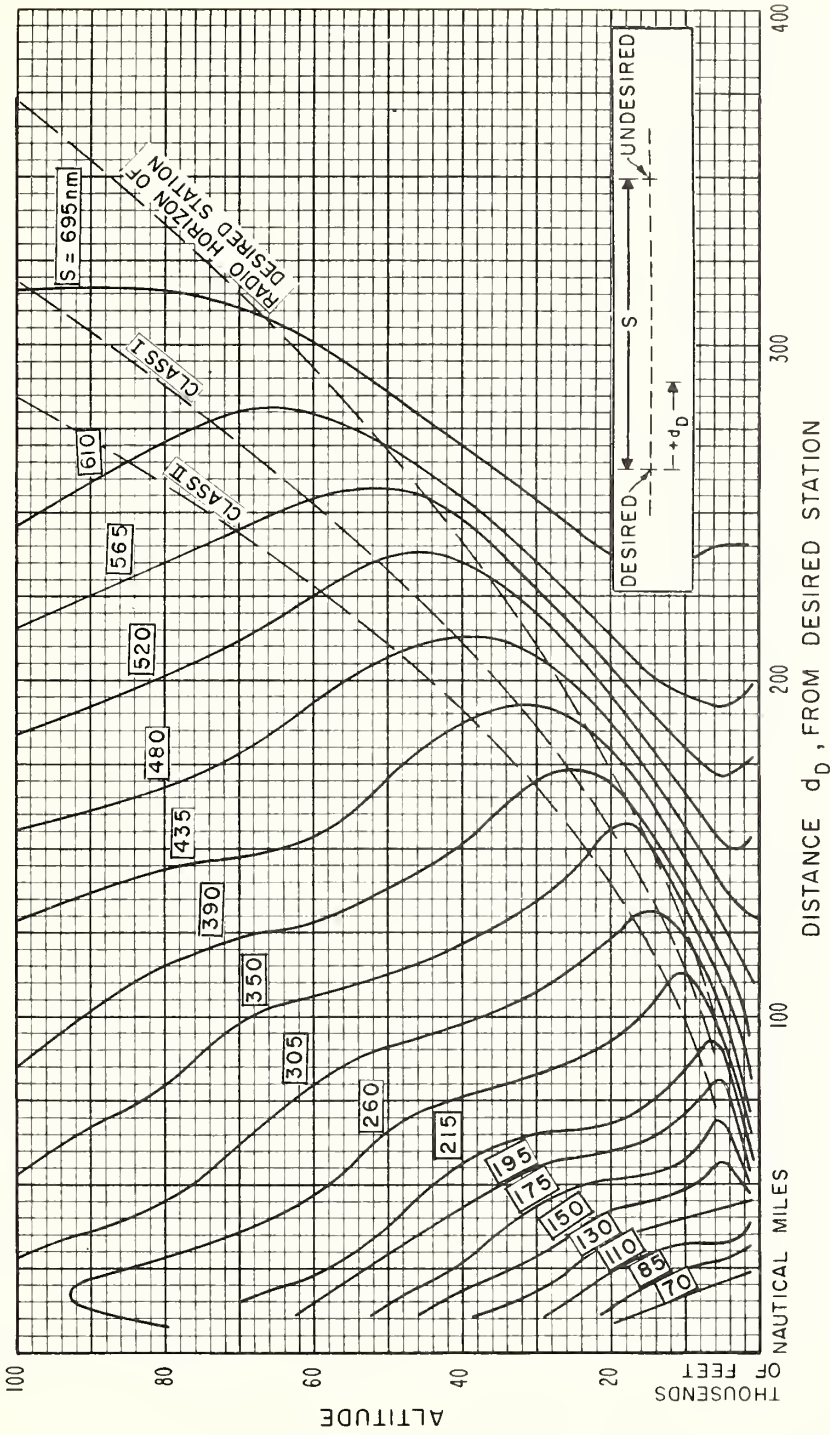


Figure 7

VOR SERVICE VOLUMES WITH INTERFERENCE FROM ONE CO-CHANNEL STATION

FREQUENCY 113 Mc/s
 D/U (95, d) = 20 db

STATION SEPARATION, S, AS LABELED
 95% RELIABILITY

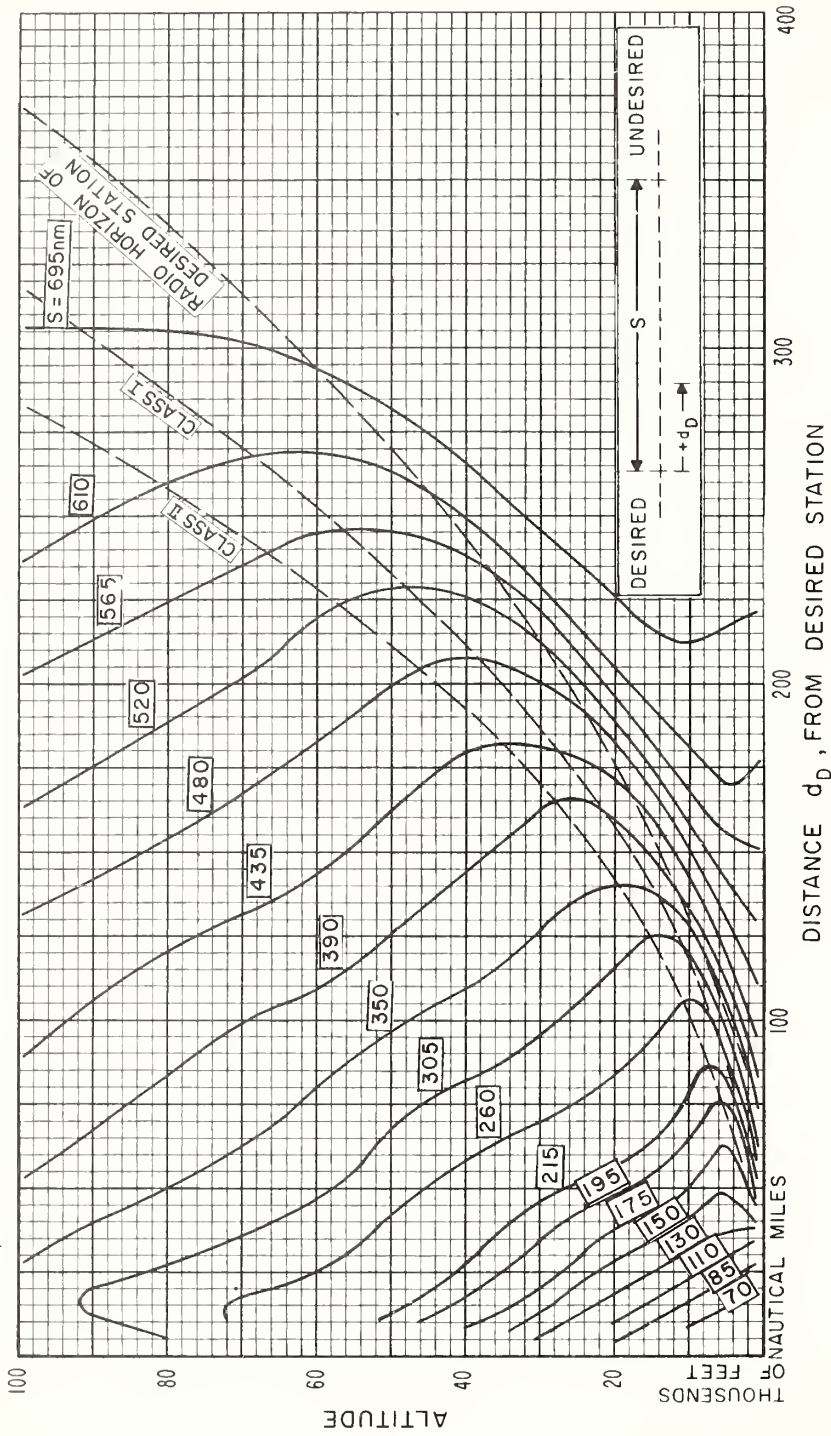


Figure 8

VOR SERVICE VOLUMES WITH INTERFERENCE FROM ONE CO-CHANNEL STATION

FREQUENCY 113 Mc/s
 D/U (95, d) = 26 db

STATION SEPARATION, S, AS LABELED
 95% RELIABILITY

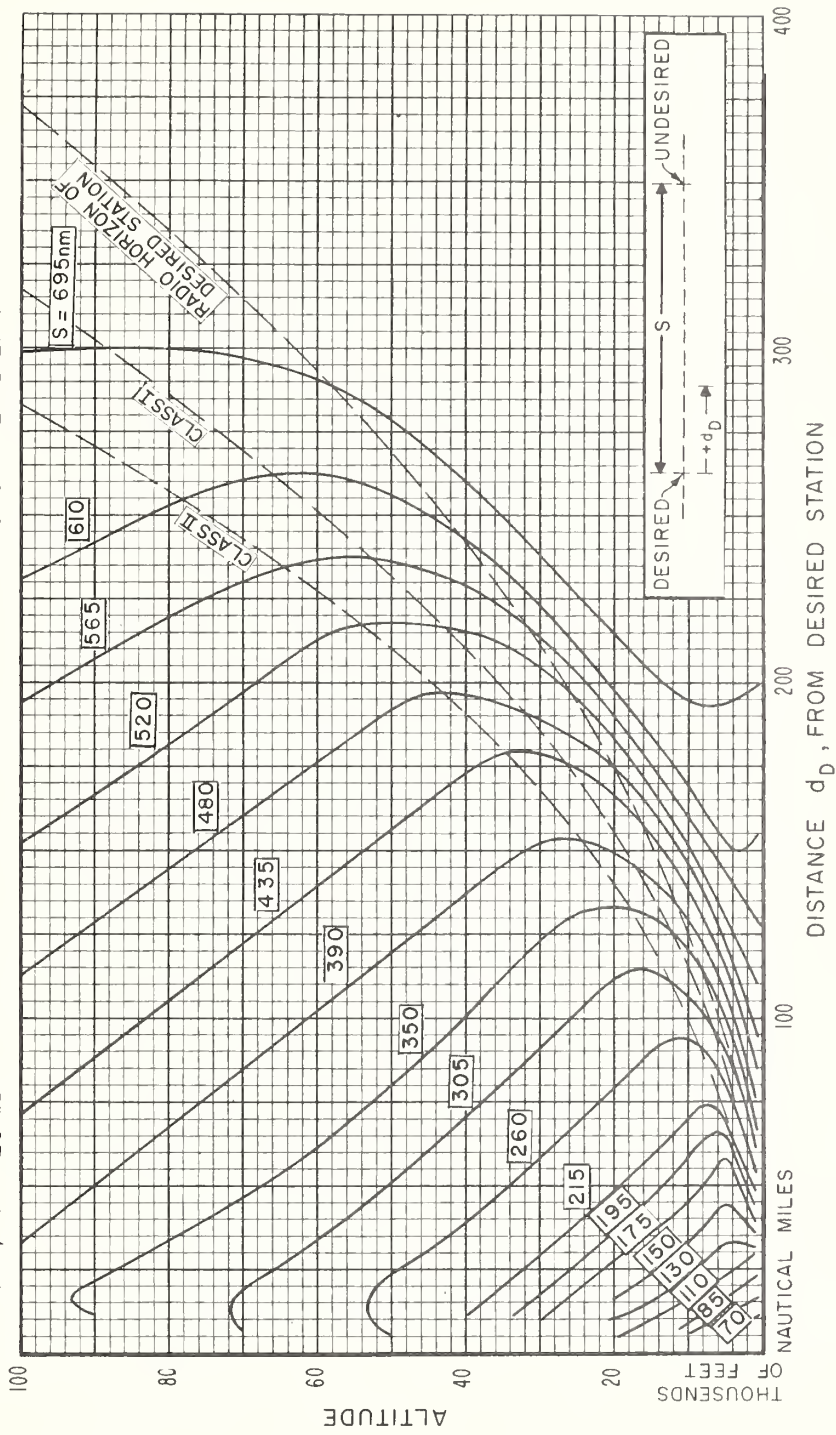


Figure 9

TACAN SERVICE VOLUMES WITH INTERFERENCE FROM ON CO-CHANNEL STATION

FREQUENCY 1150 Mc/s
 D/U (95, d) = 8 db
 STATION SEPARATION, S, AS LABELED
 95% RELIABILITY

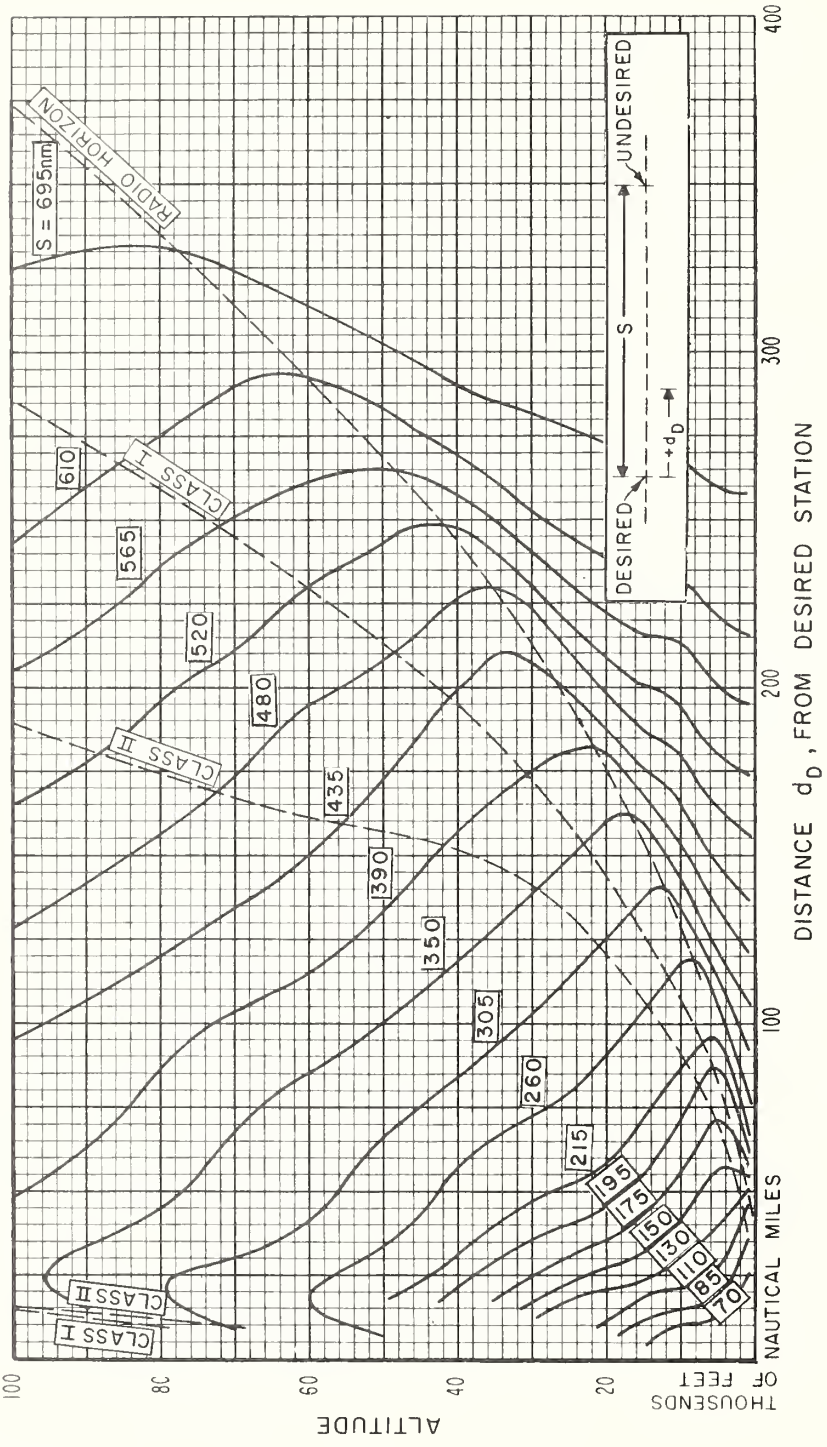


Figure 10

TACAN SERVICE VOLUMES WITH INTERFERENCE FROM ONE CO-CHANNEL STATION

FREQUENCY 1150 Mc/s
 $D/U (95, d) = 14 \text{ db}$

STATION SEPARATION, S , AS LABELED
 95% RELIABILITY

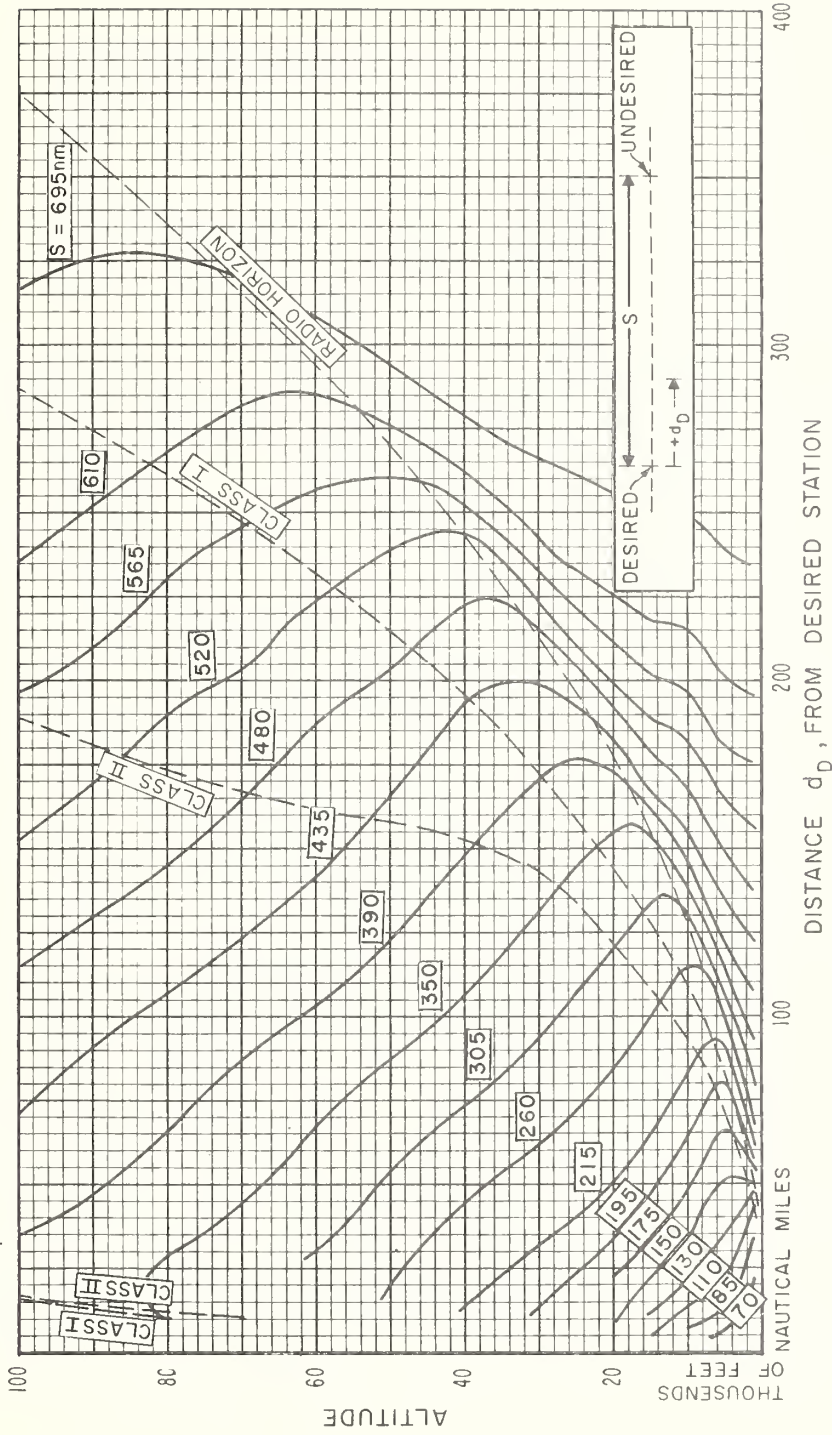


Figure 11

TACAN SERVICE VOLUMES WITH INTERFERENCE FROM ONE CO-CHANNEL STATION

FREQUENCY 1150 Mc/s
 D/U (95, d) = 20 db
 STATION SEPARATION, S, AS LABELED
 95% RELIABILITY

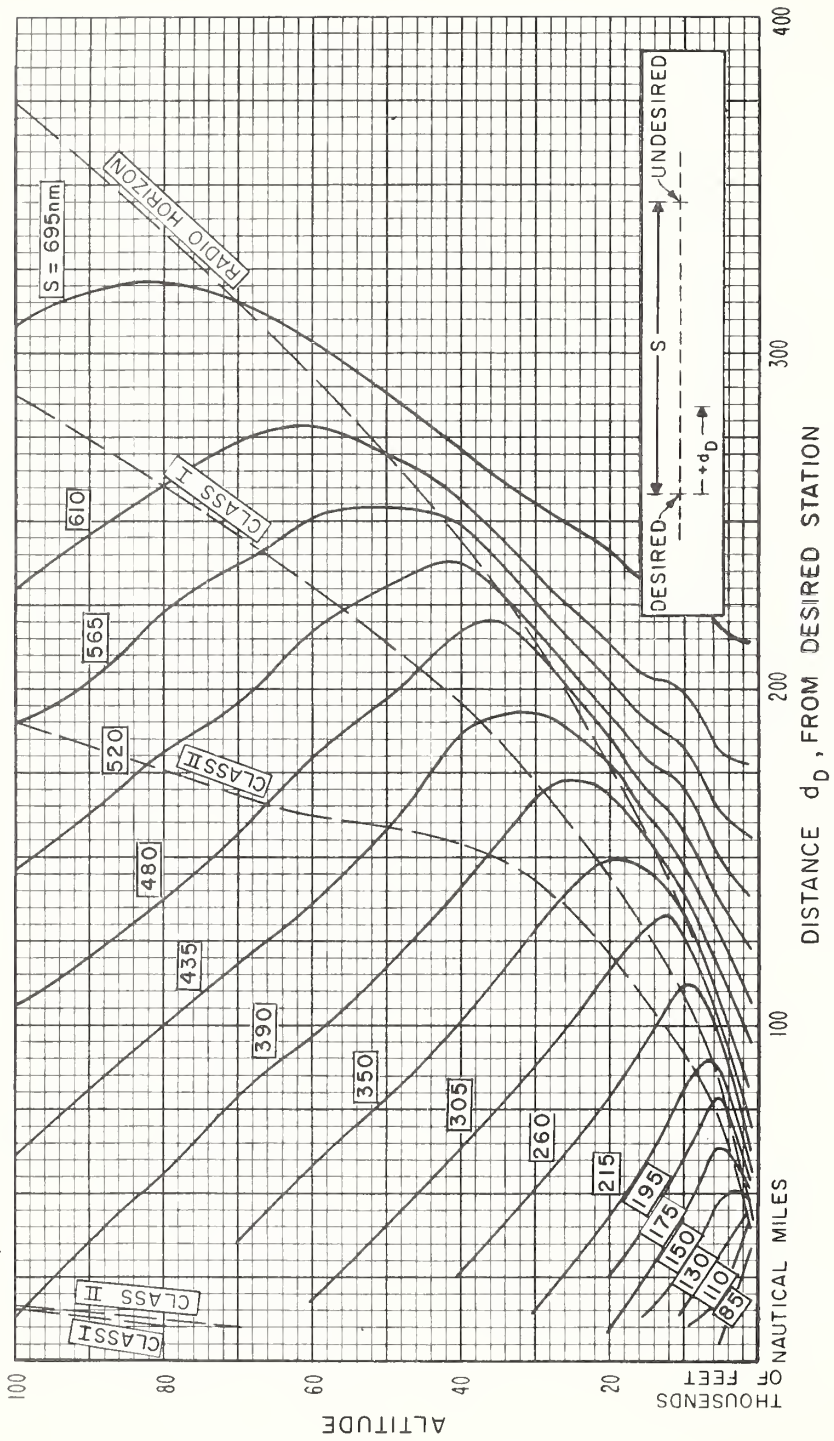


Figure 12

VOR SIGNAL RATIOS NEAR AN INTERFERING STATION

STATION SEPARATION, S , AS LABELED
95% RELIABILITY

FREQUENCY 113 Mc/s
ALTITUDE 1,000 FEET

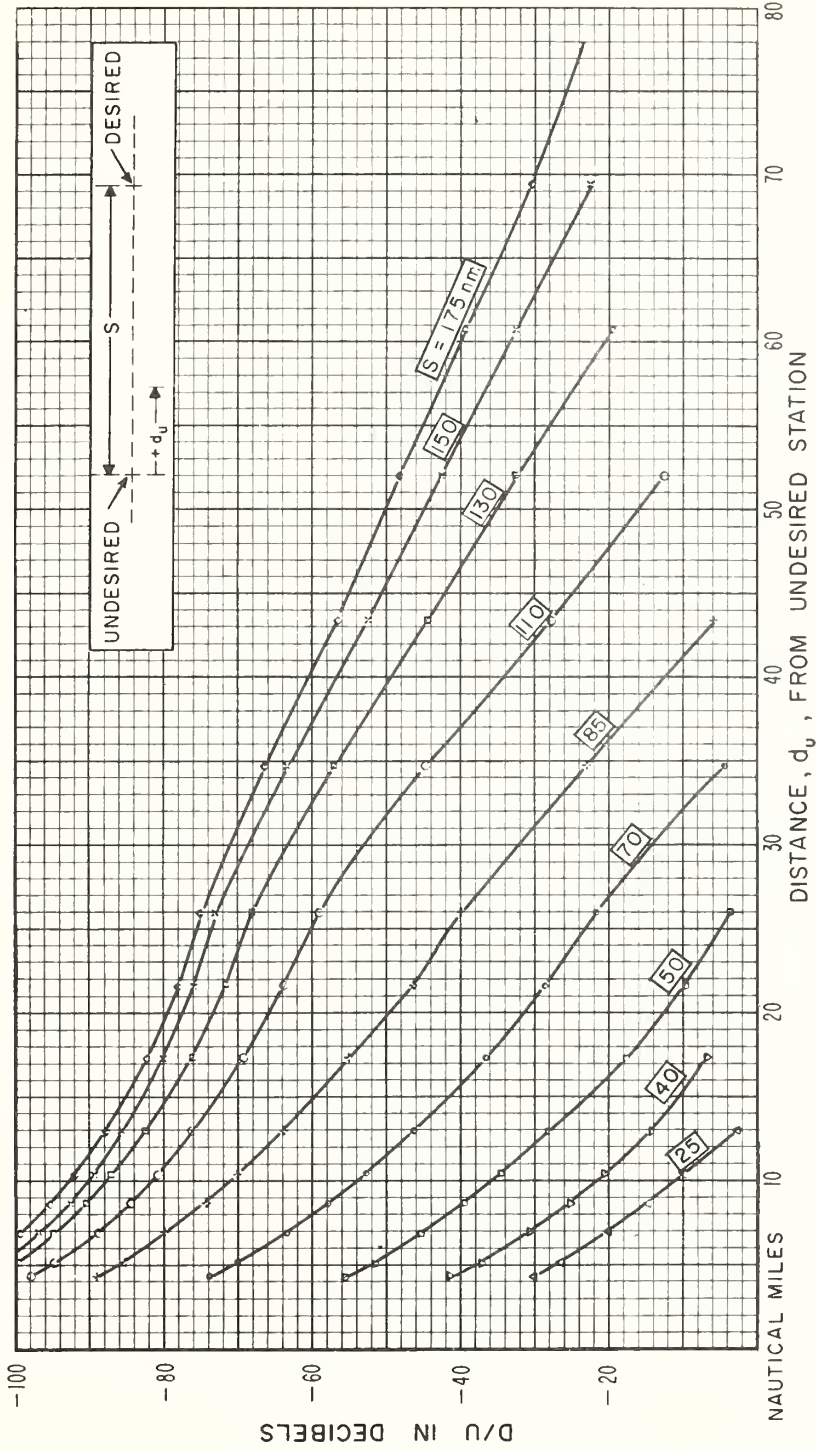


Figure 13

VOR SIGNAL RATIOS NEAR AN INTERFERING STATION

FREQUENCY 113 Mc/s
 ALTITUDE 5,000 FEET

STATION SEPARATION, S , AS LABELED
 95% RELIABILITY

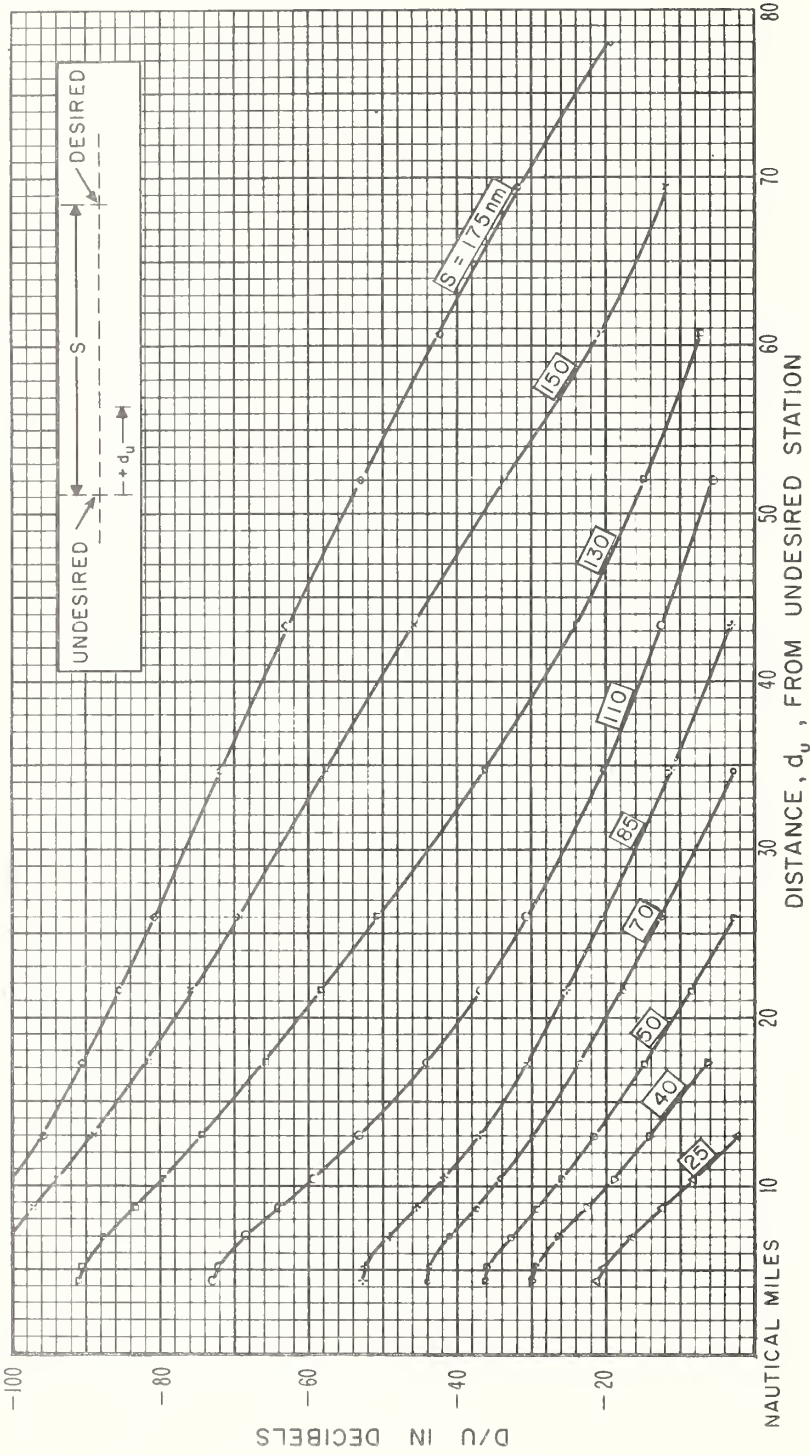


Figure 14

VOR SIGNAL RATIOS NEAR AN INTERFERING STATION

FREQUENCY 113 Mc/s
 ALTITUDE 10,000 FEET
 STATION SEPARATION, S, AS LABELED
 95 % RELIABILITY

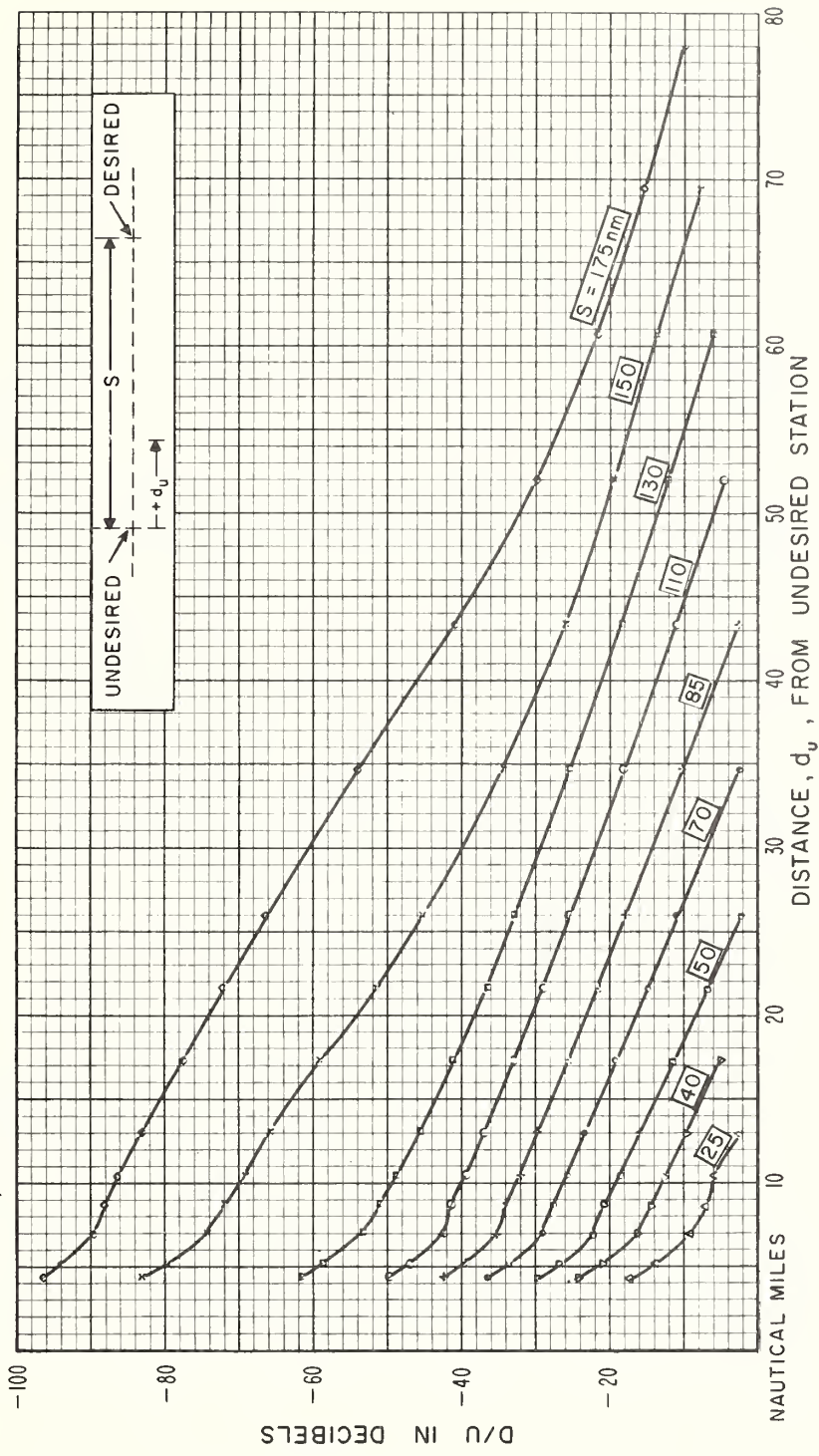


Figure 15

VOR SIGNAL RATIOS NEAR AN INTERFERING STATION

FREQUENCY 113 Mc/s
 ALTITUDE 15,000 FEET
 STATION SEPARATION, S, AS LABELED
 95% RELIABILITY

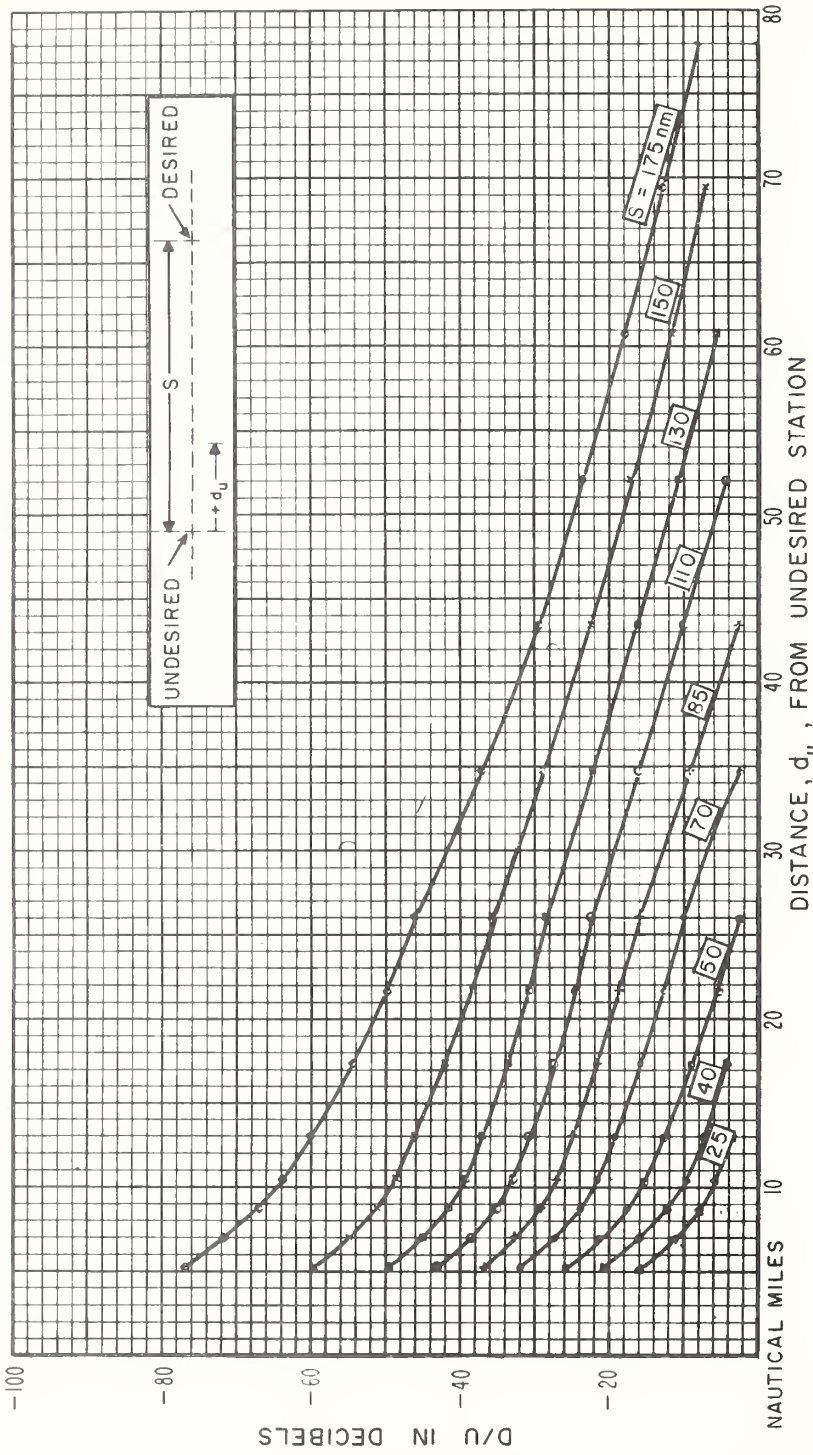


Figure 16

VOR SIGNAL RATIOS NEAR AN INTERFERING STATION

FREQUENCY 113 Mc/s
 ALTITUDE 20,000 FEET
 STATION SEPARATION, S, AS LABELED
 95 % RELIABILITY

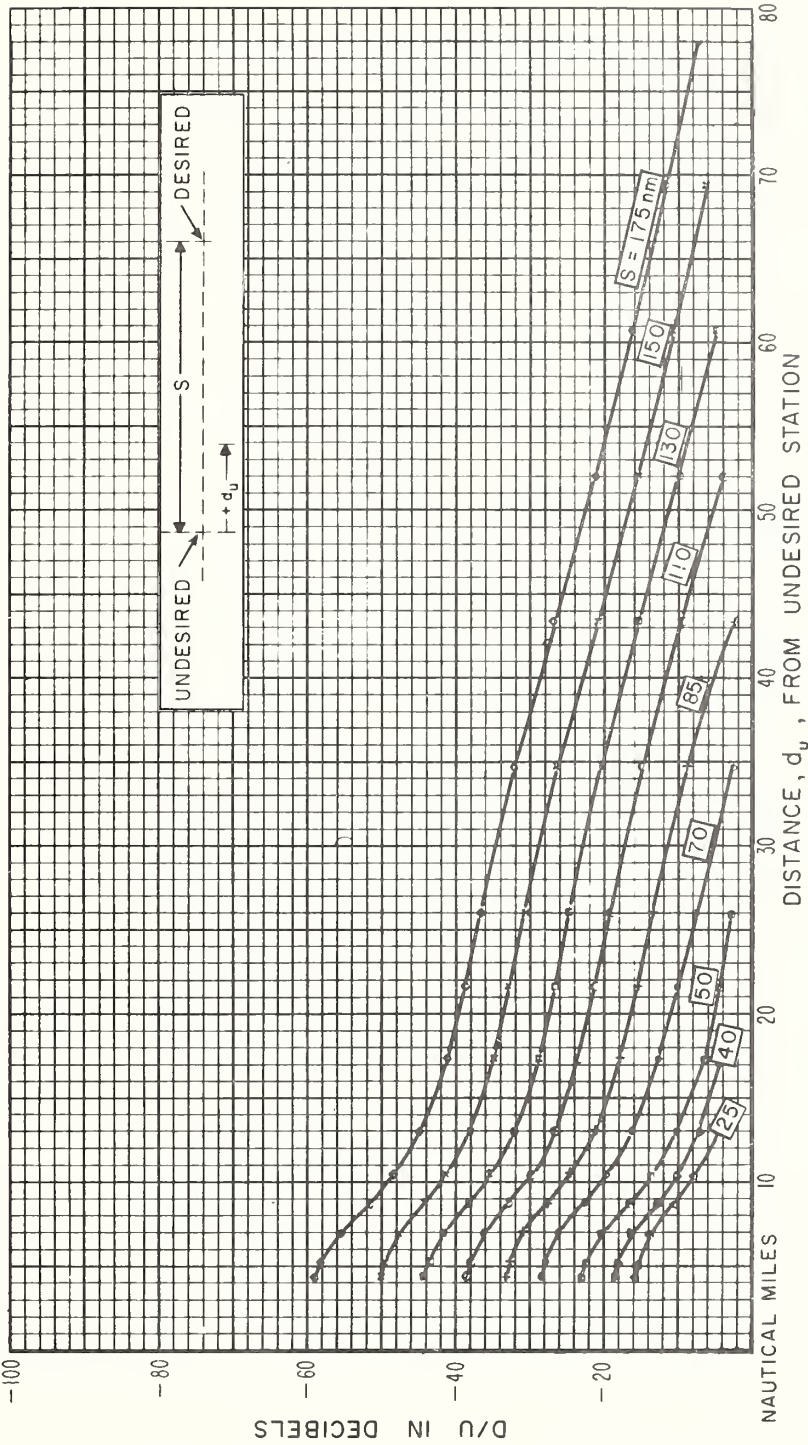


Figure 17

VOR SIGNAL RATIOS NEAR AN INTERFERING STATION

FREQUENCY 113 Mc/s
 ALTITUDE 30,000 FEET

STATION SEPARATION, S , AS LABELED
 95% RELIABILITY

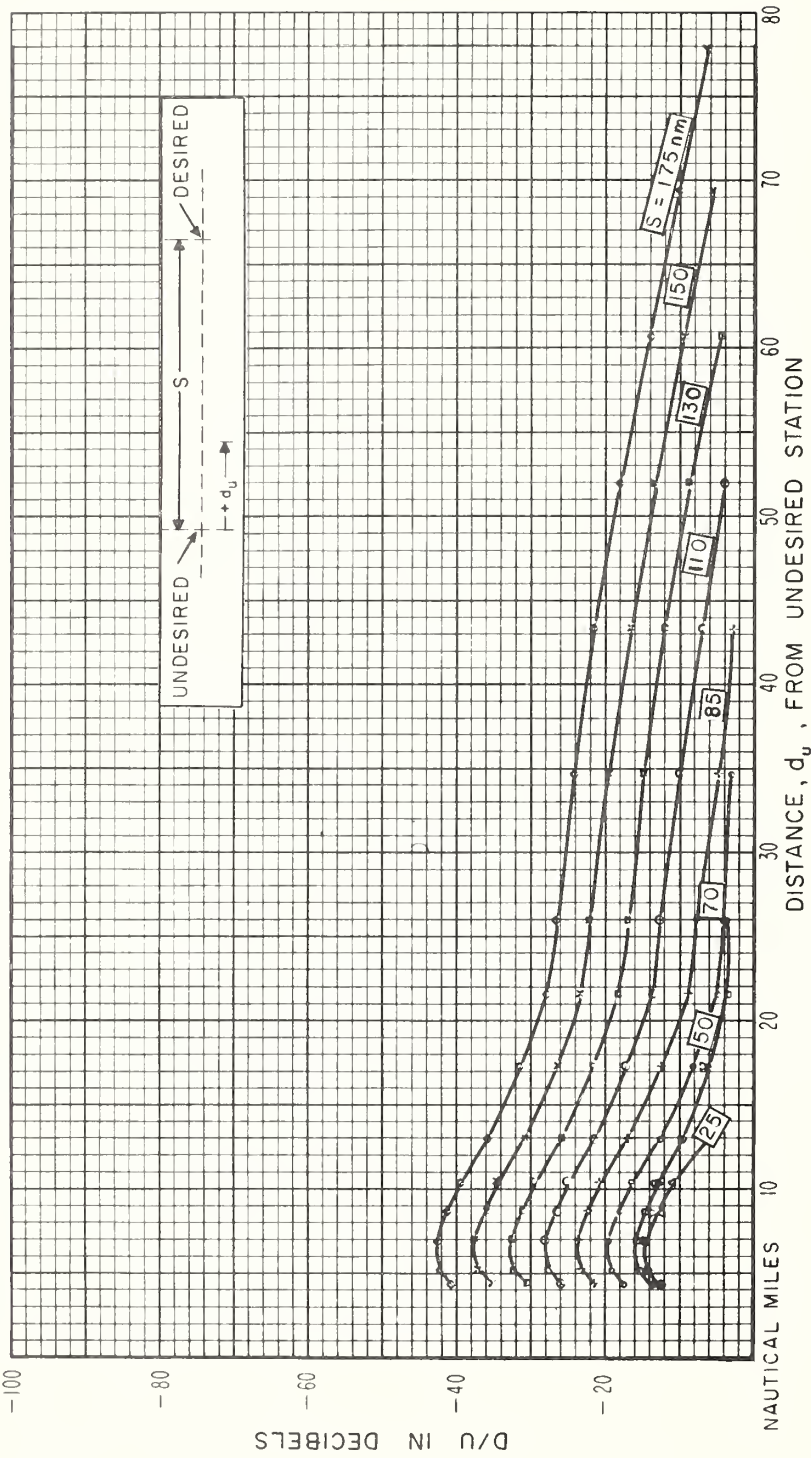


Figure 18

VOR SIGNAL RATIOS NEAR AN INTERFERING STATION

FREQUENCY 113 Mc/s
 ALTITUDE 40,000 FEET

STATION SEPARATION, S, AS LABELED
 95% RELIABILITY

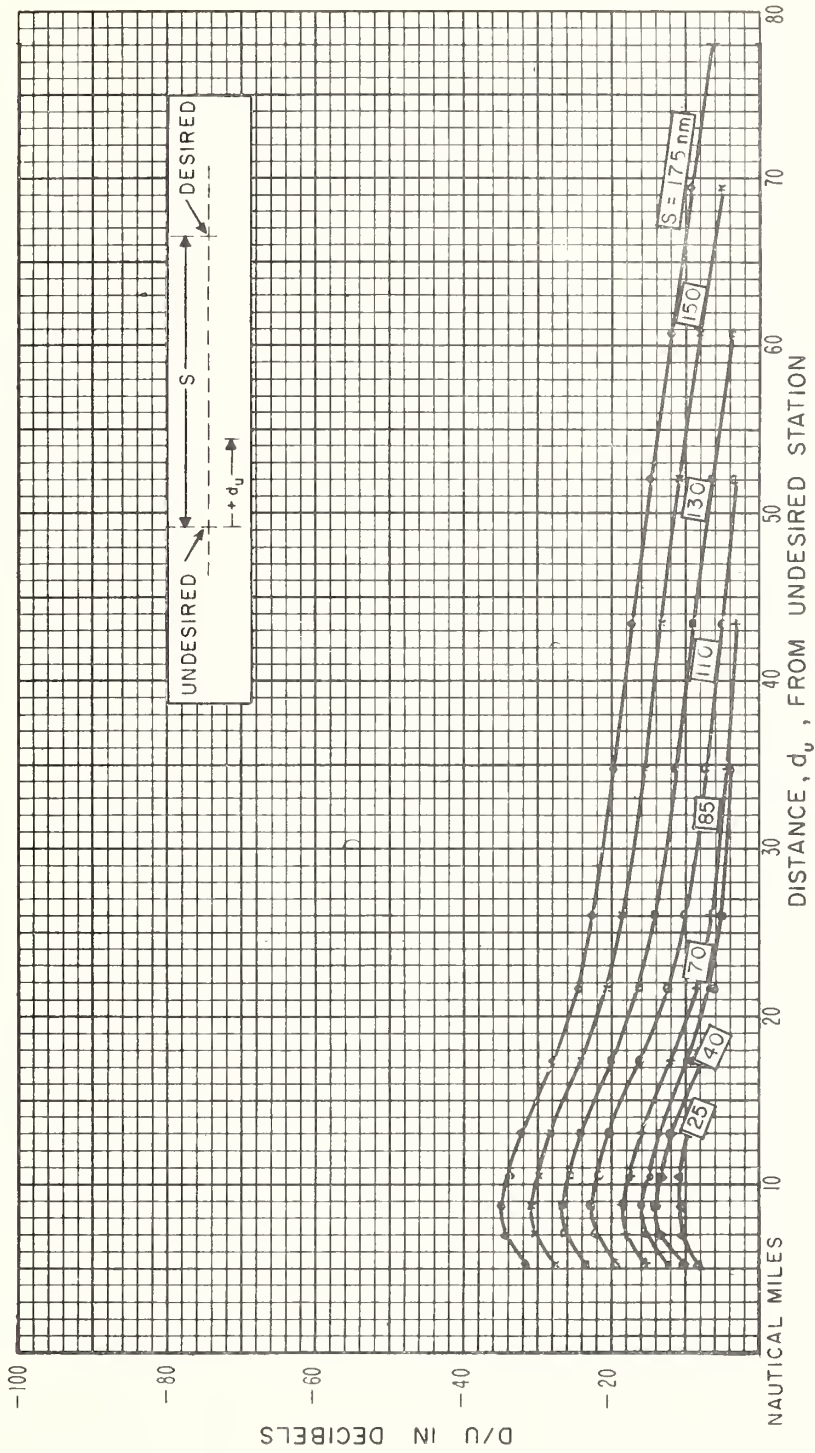


Figure 19

VOR SIGNAL RATIOS NEAR AN INTERFERING STATION

FREQUENCY 113 Kc/s
 ALTITUDE 50,000 FEET

STATION SEPARATION, S , AS LABELED
 95% RELIABILITY

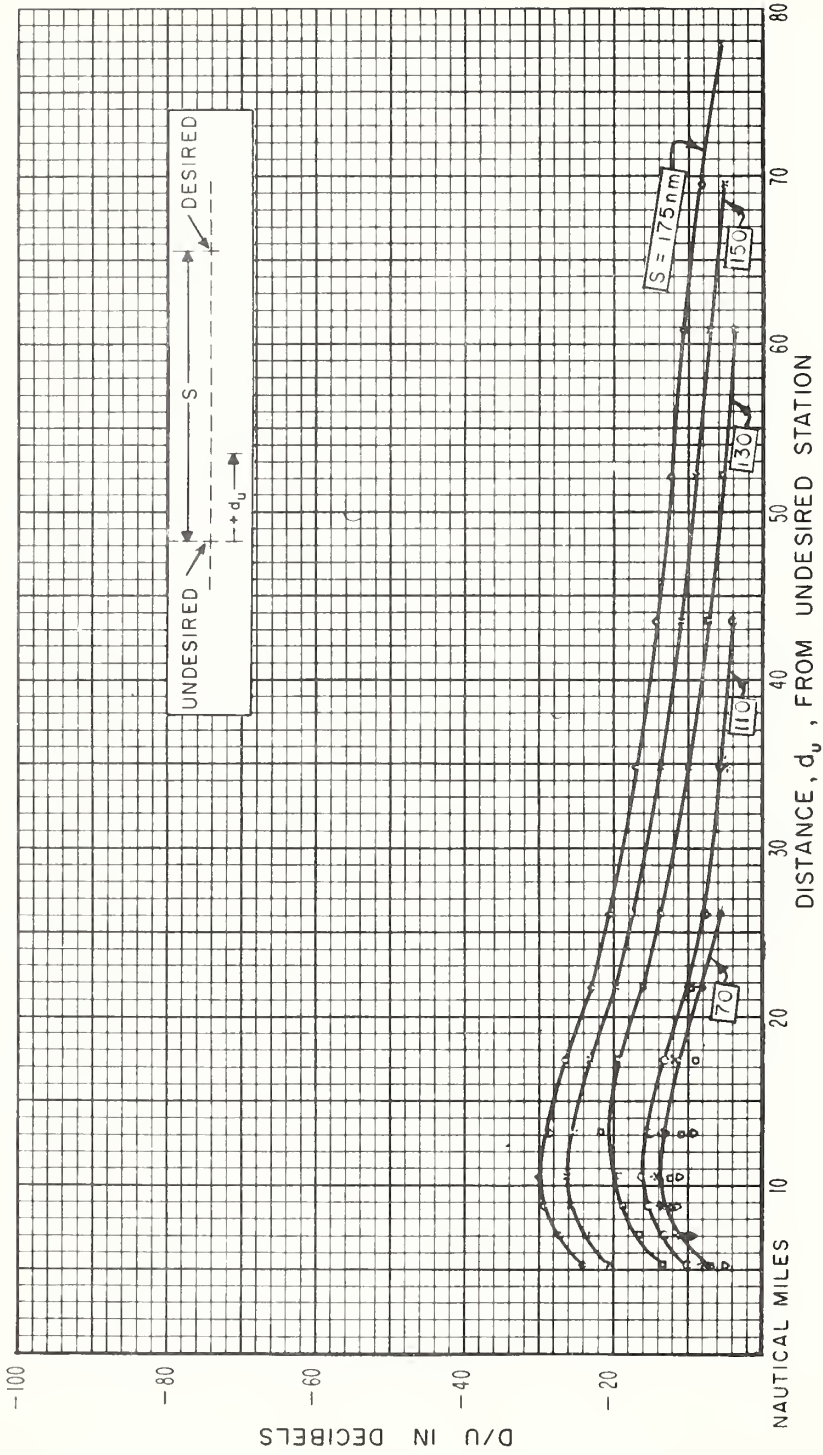


Figure 20

VOR SIGNAL RATIOS NEAR AN INTERFERING STATION

FREQUENCY 113 Mc/s
 ALTITUDE 60,000 FEET
 STATION SEPARATION, S, AS LABELED
 95 % RELIABILITY

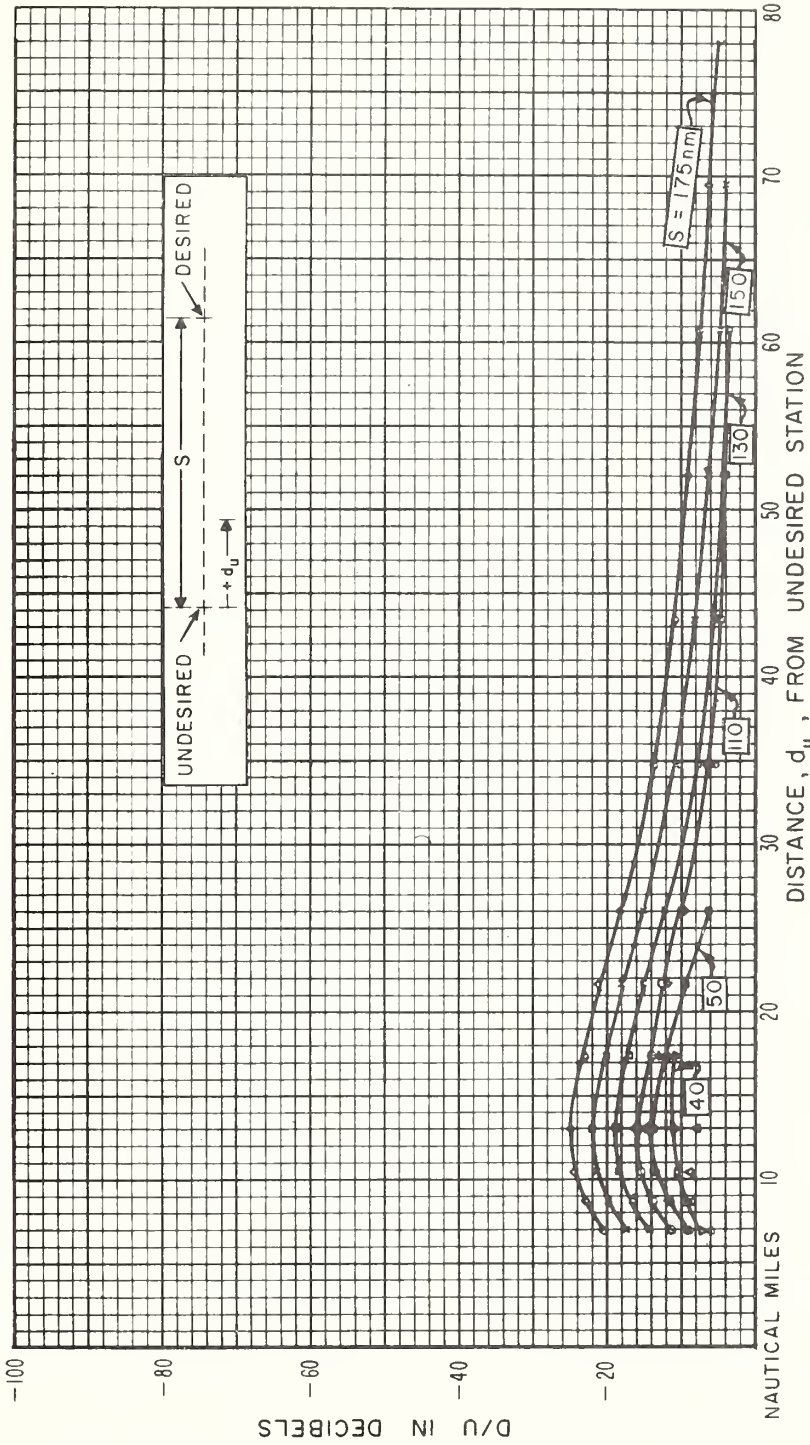


Figure 21

VOR SIGNAL RATIOS NEAR AN INTERFERING STATION

FREQUENCY 113 Mc/s
 ALTITUDE 70,000 FEET

STATION SEPARATION, S, AS LABELED
 95 % RELIABILITY

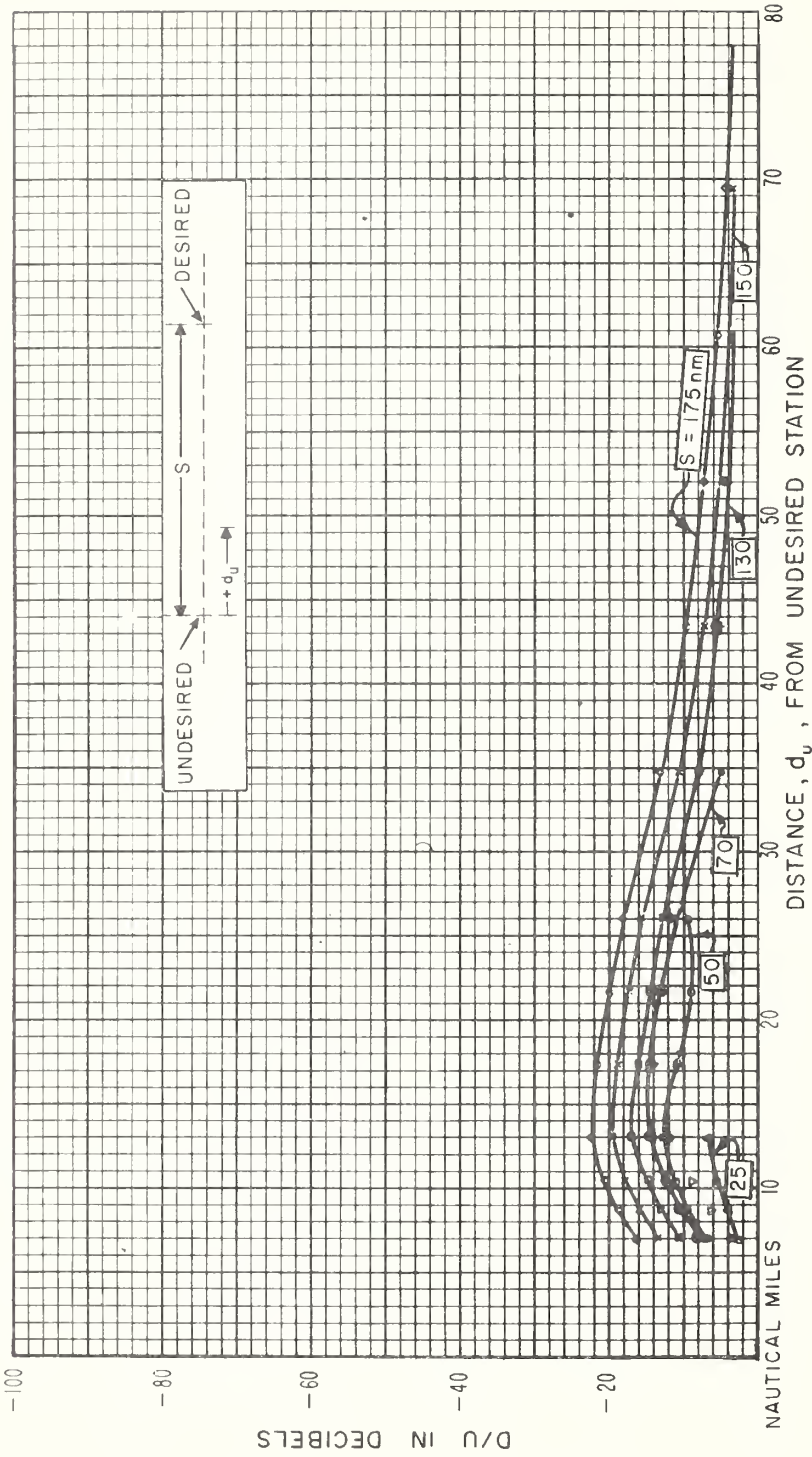


Figure 22

VOR SIGNAL RATIOS NEAR AN INTERFERING STATION

FREQUENCY 113 Mc/s

ALTITUDE 80,000 FEET

STATION SEPARATION, S, AS LABELED

95% RELIABILITY

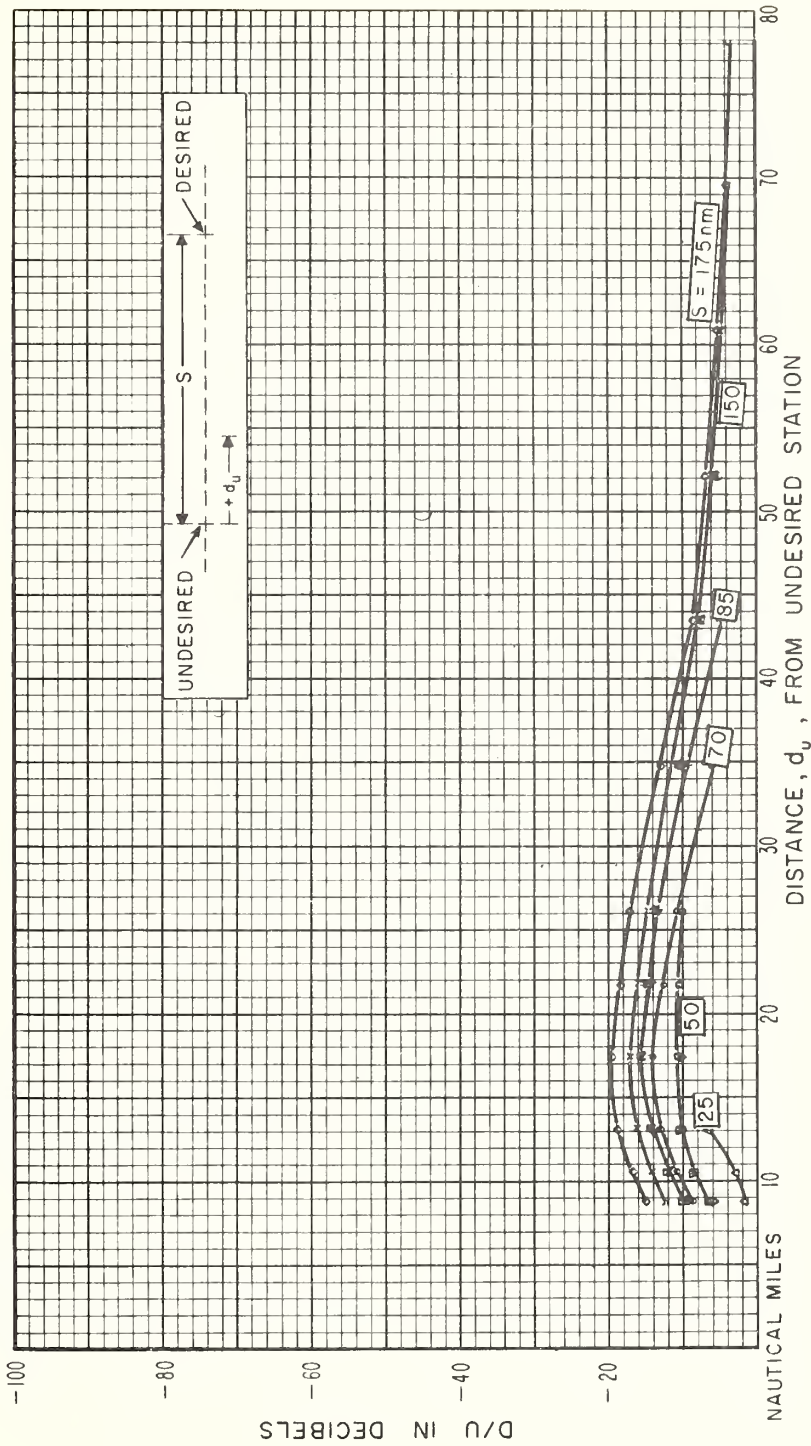


Figure 23

VOR SIGNAL RATIOS NEAR AN INTERFERING STATION

FREQUENCY 113 Kc/s
 ALTITUDE 90,000 FEET
 STATION SEPARATION, S, AS LABELED
 95% RELIABILITY

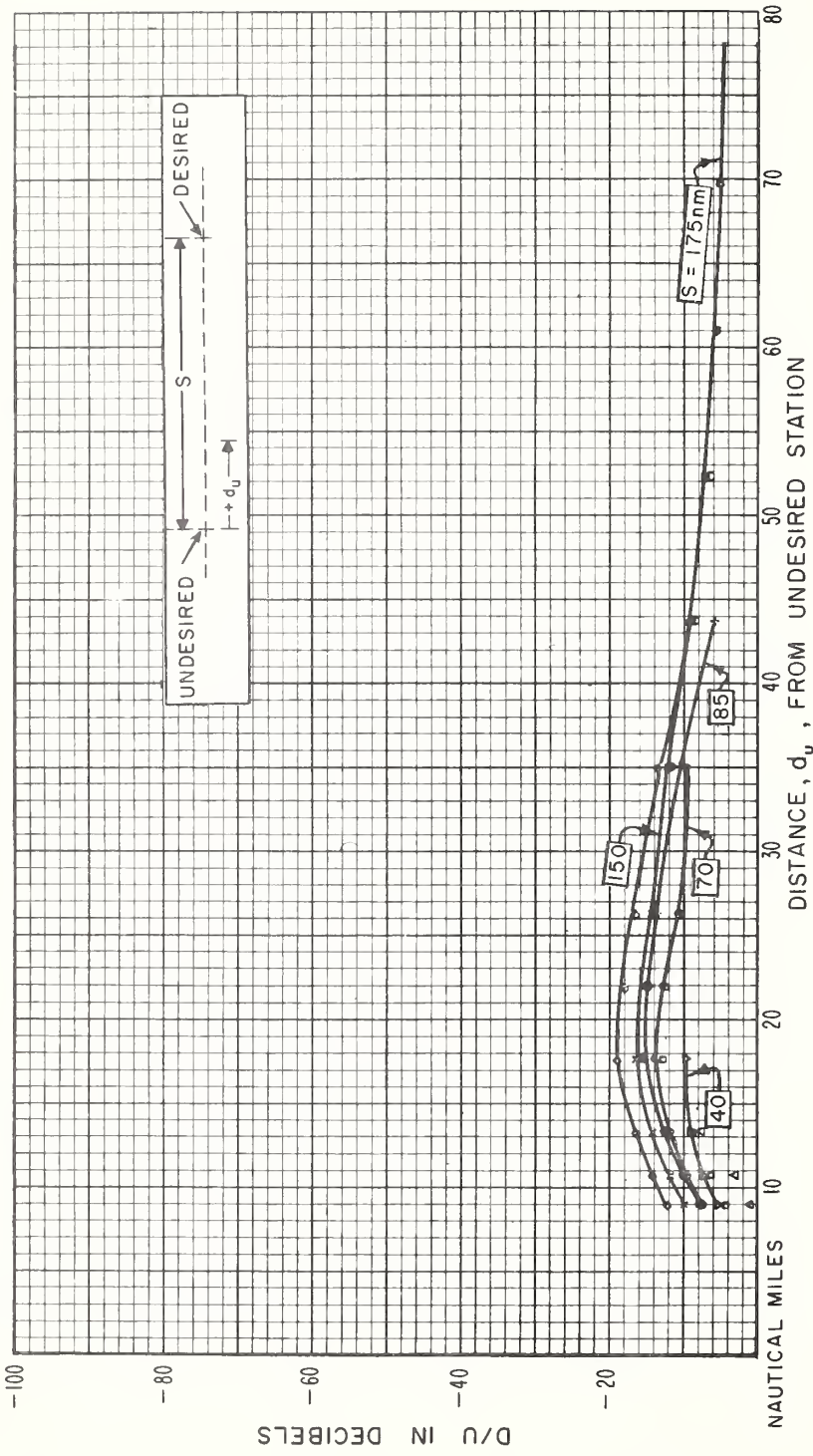


Figure 24

VOR SIGNAL RATIOS NEAR AN INTERFERING STATION

FREQUENCY 113 Mc/s
 ALTITUDE 100,000 FEET

STATION SEPARATION, S , AS LABELED
 95% RELIABILITY

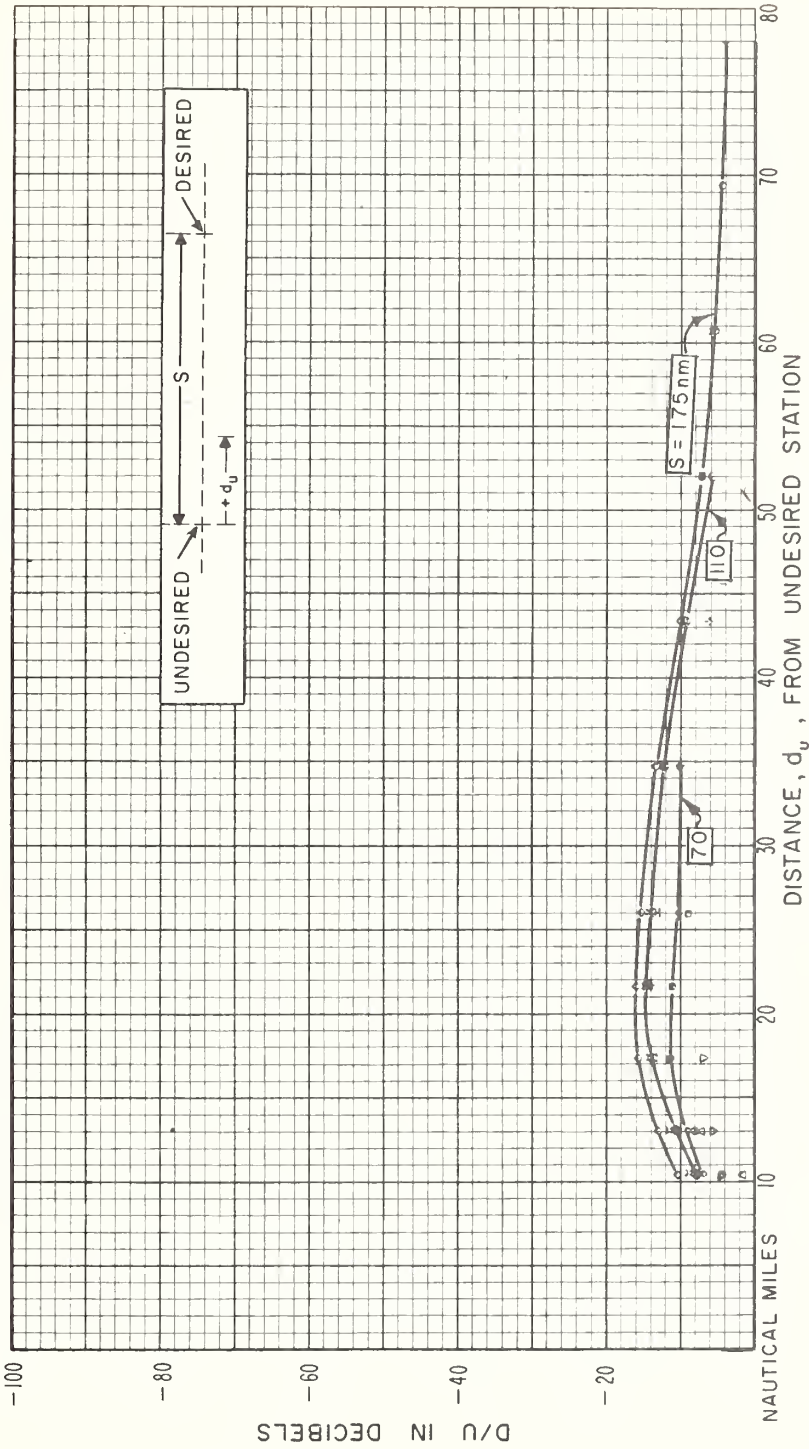


Figure 25

TACAN SIGNAL RATIOS NEAR AN INTERFERING STATION

FREQUENCY 1150 MC/S
 ALTITUDE 1,000 FEET
 STATION SEPARATION, S, AS LABELED
 95% RELIABILITY

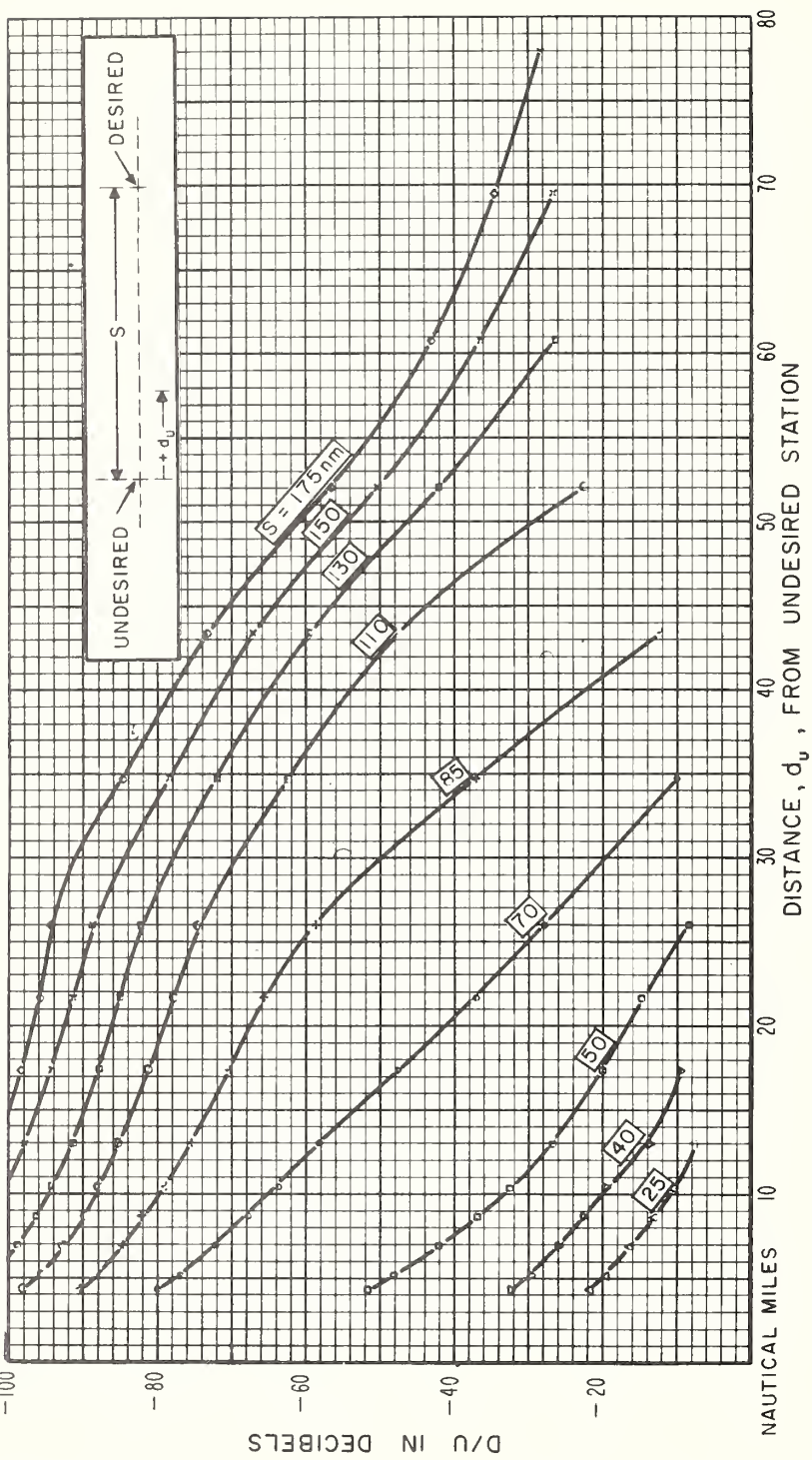


Figure 26

TACAN SIGNAL RATIOS NEAR AN INTERFERING STATION

FREQUENCY 1150 Mc/s
 ALTITUDE 5,000 FEET
 STATION SEPARATION, S, AS LABELED
 95% RELIABILITY

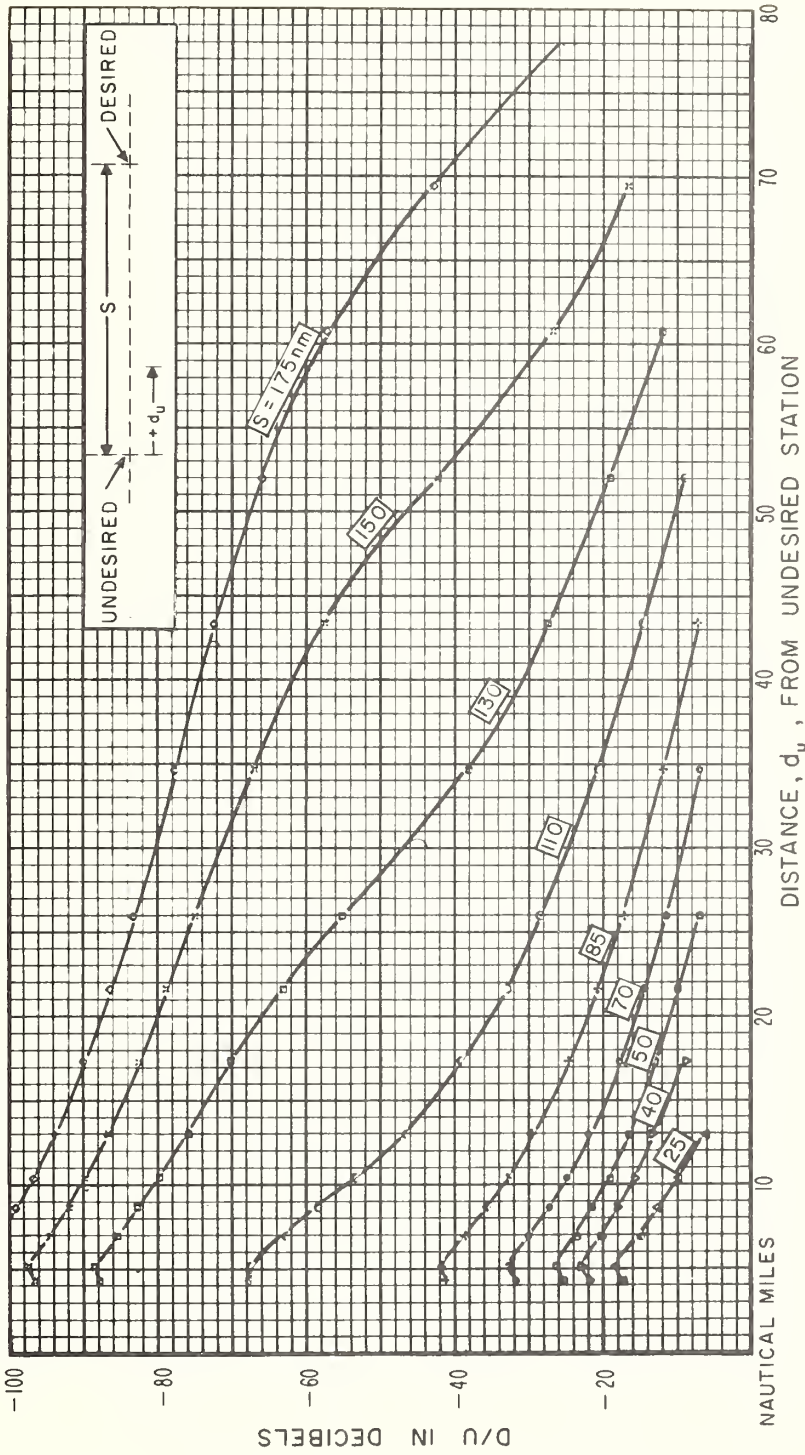


Figure 27

TACAN SIGNAL RATIOS NEAR AN INTERFERING STATION

FREQUENCY 1150 Mc/s
 ALTITUDE 10,000 FEET
 STATION SEPARATION, S, AS LABELED
 95% RELIABILITY

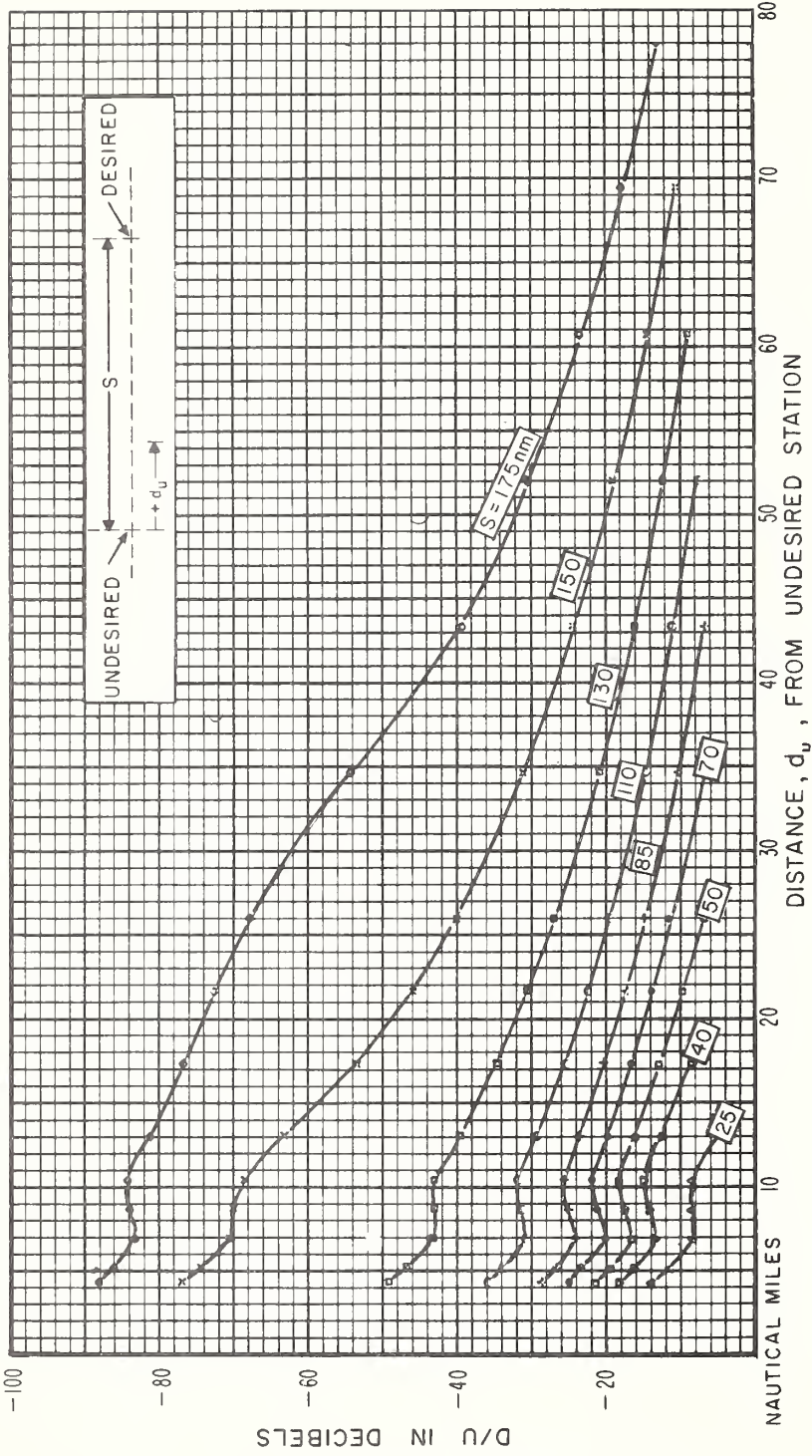


Figure 28

TACAN SIGNAL RATIOS NEAR AN INTERFERING STATION

STATION SEPARATION, S , AS LABELED
95% RELIABILITY

FREQUENCY 1150 Mc/s
ALTITUDE 15,000 FEET

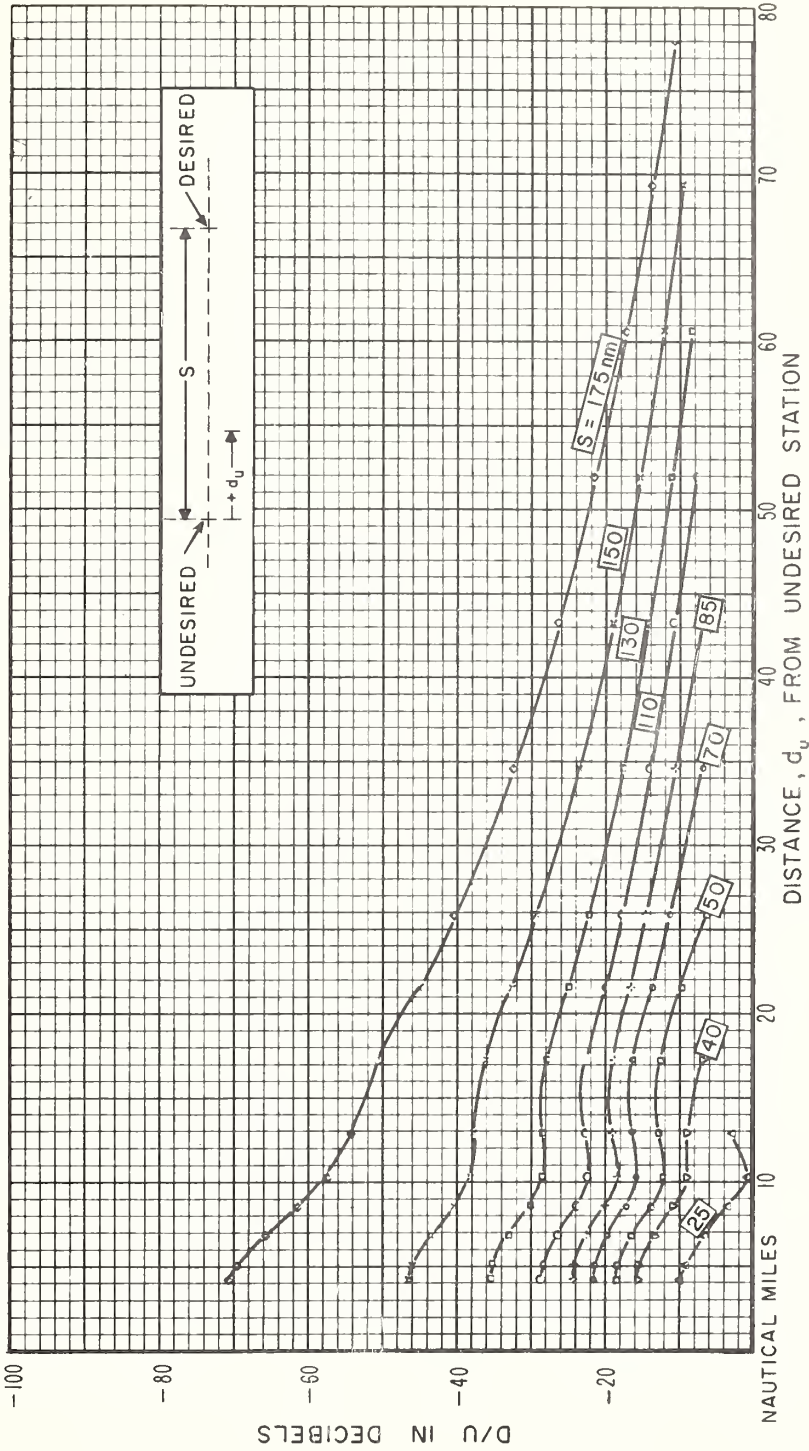


Figure 29

TACAN SIGNAL RATIOS NEAR AN INTERFERING STATION

FREQUENCY 1150 Mc/s
 ALTITUDE 20,000 FEET

STATION SEPARATION, S , AS LABELED
 95% RELIABILITY

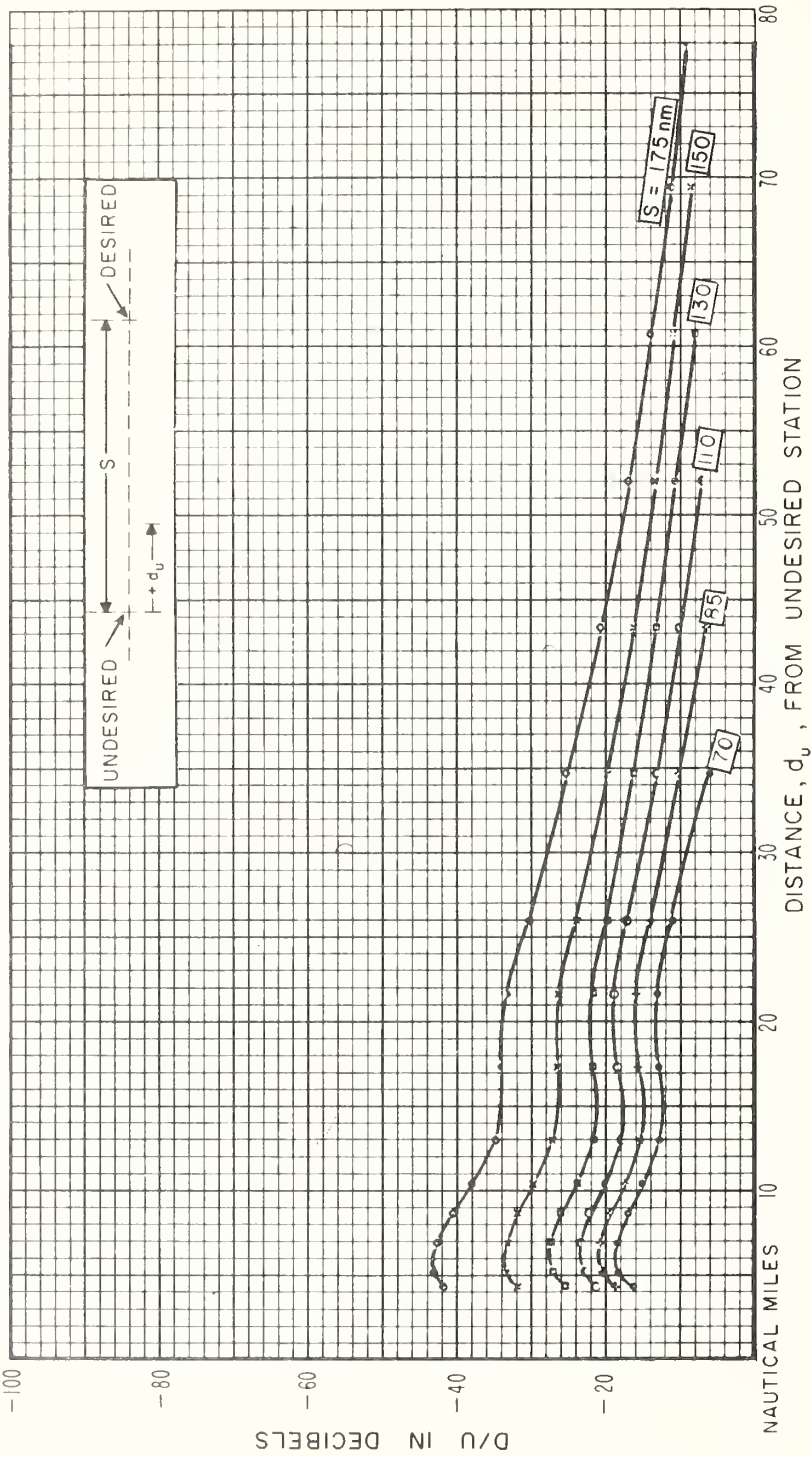


Figure 30

TACAN SIGNAL RATIOS NEAR AN INTERFERING STATION

FREQUENCY 1150 Mc/s
 ALTITUDE 30,000 FEET
 STATION SEPARATION, S, AS LABELED
 95% RELIABILITY

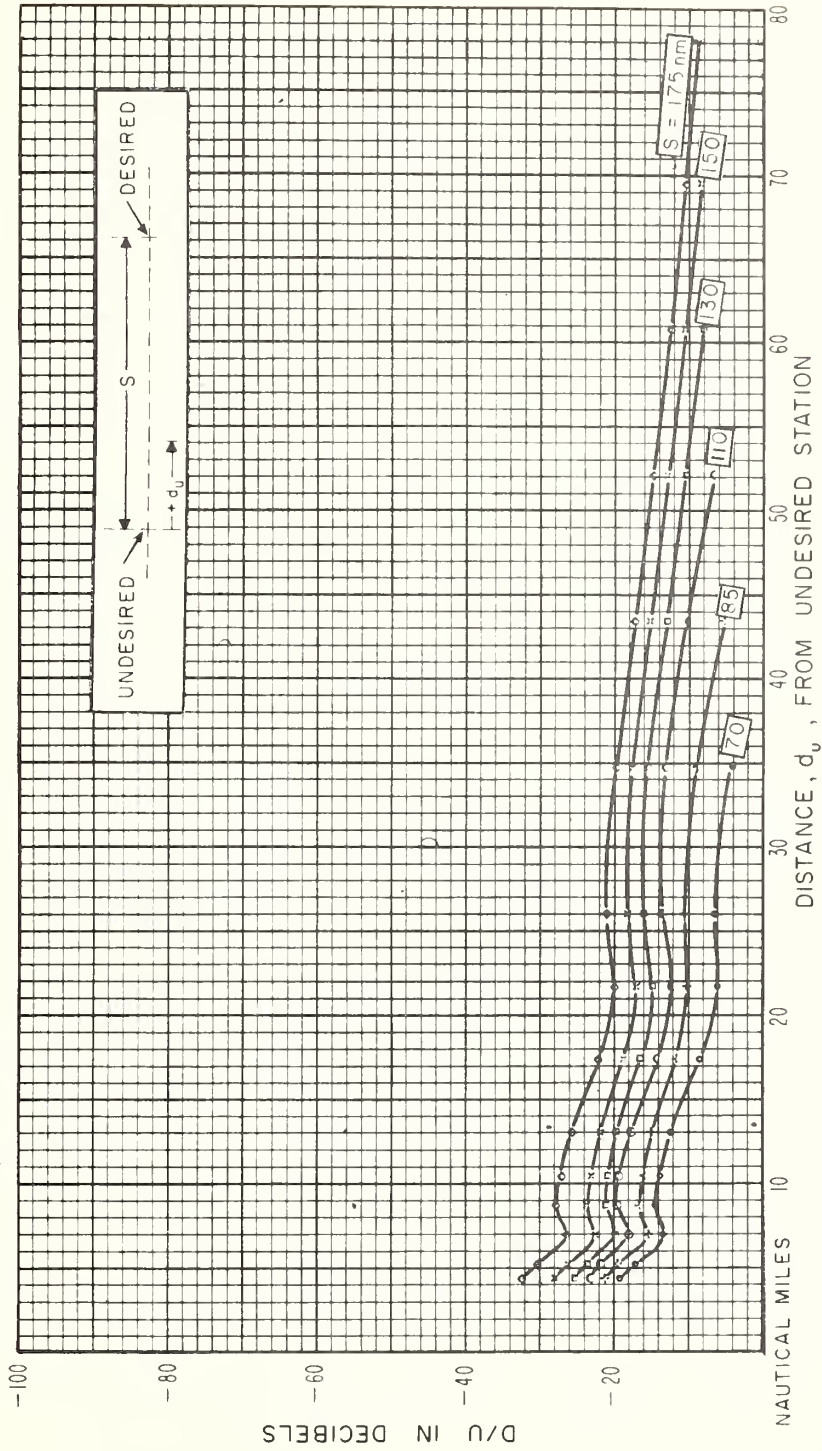


Figure 31

TACAN SIGNAL RATIOS NEAR AN INTERFERING STATION

FREQUENCY 1150 Mc/s
 ALTITUDE 40,000 FEET

STATION SEPARATION, S , AS LABELED
 95% RELIABILITY

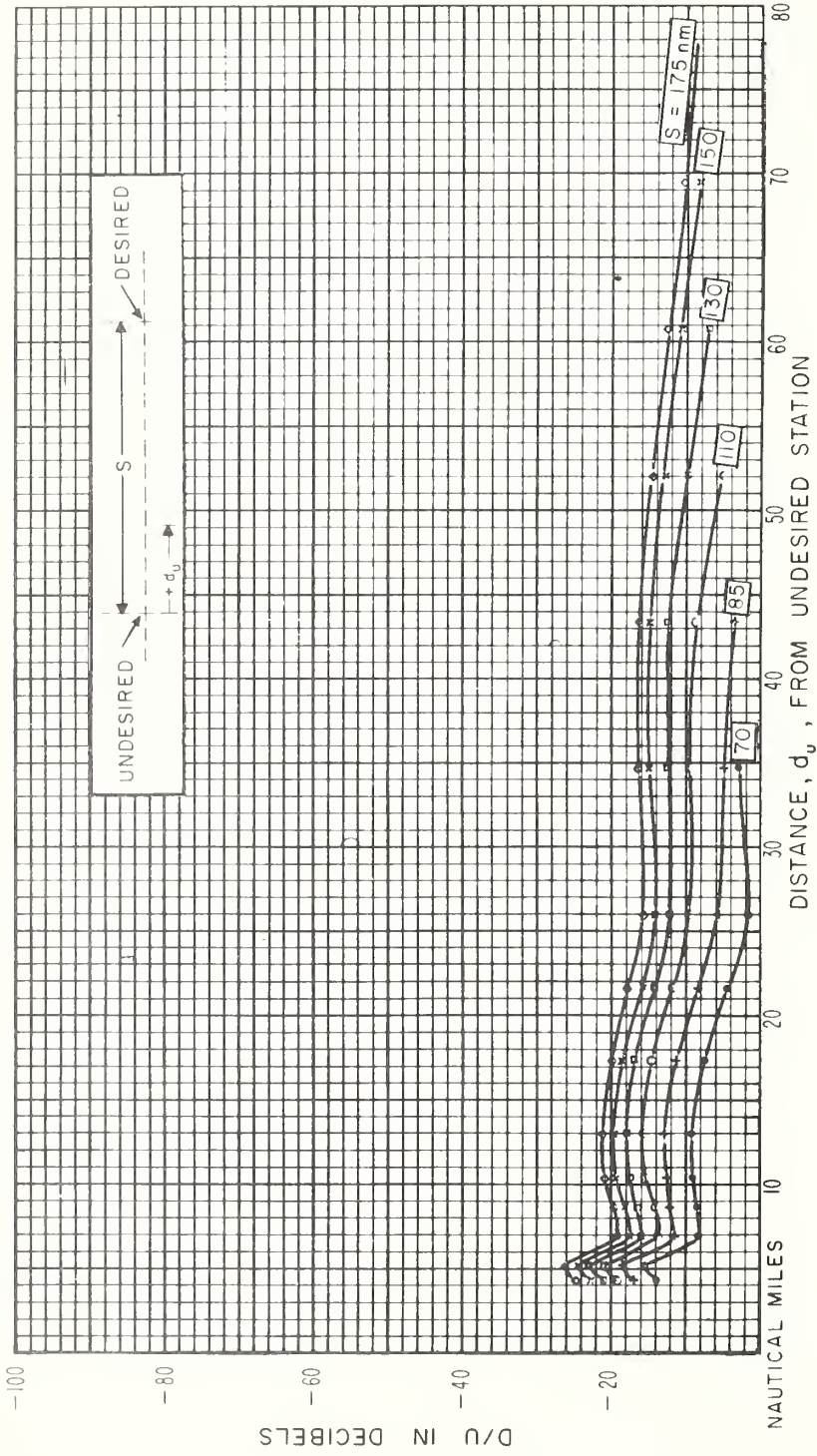


Figure 32

TACAN SIGNAL RATIOS NEAR AN INTERFERING STATION

STATION SEPARATION, S , AS LABELED
95% RELIABILITY

FREQUENCY 1150 Mc/s
ALTITUDE 50,000 FEET

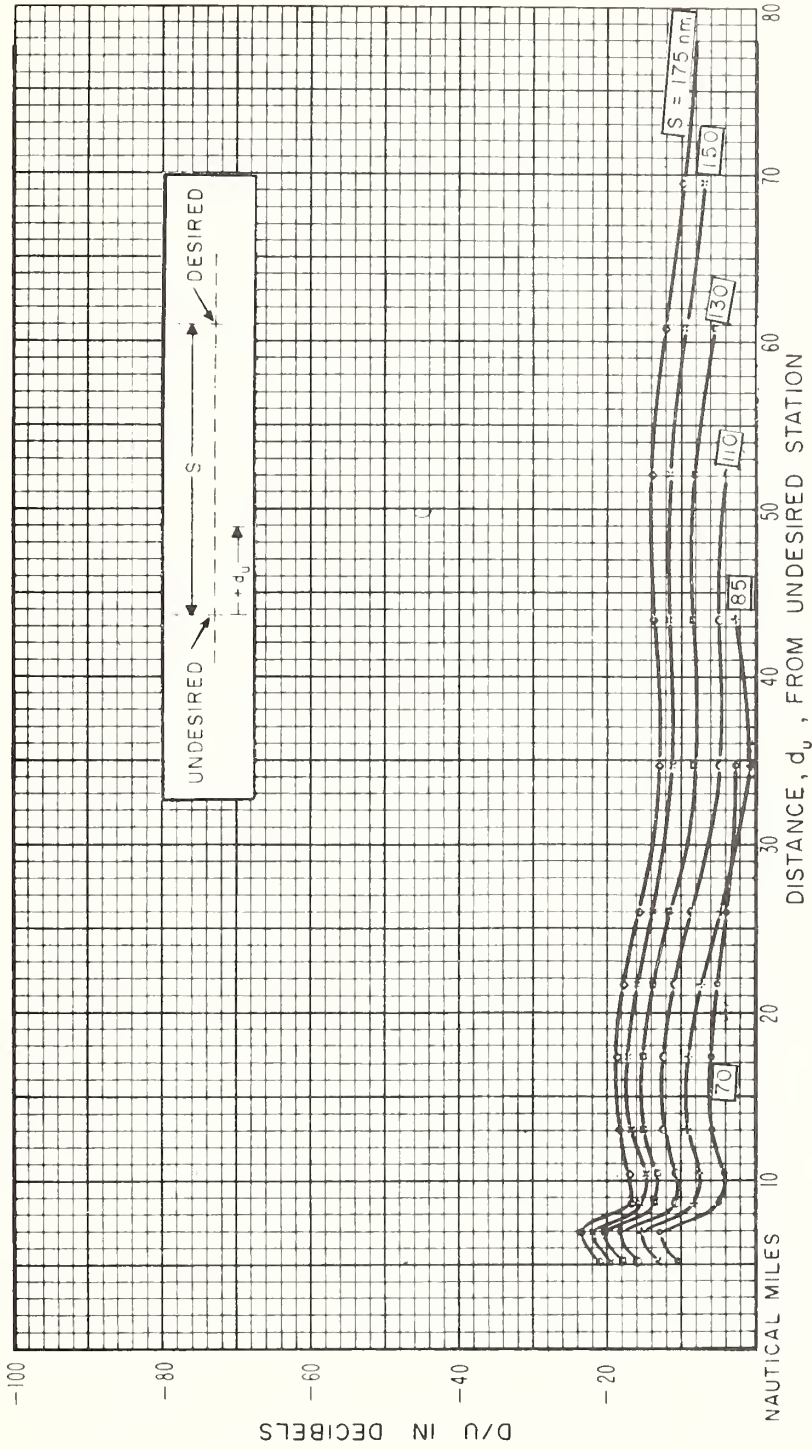


Figure 33

TACAN SIGNAL RATIOS NEAR AN INTERFERING STATION

FREQUENCY 1150 Mc/s
 ALTITUDE 60,000 FEET
 STATION SEPARATION, S , AS LABELED
 95% RELIABILITY

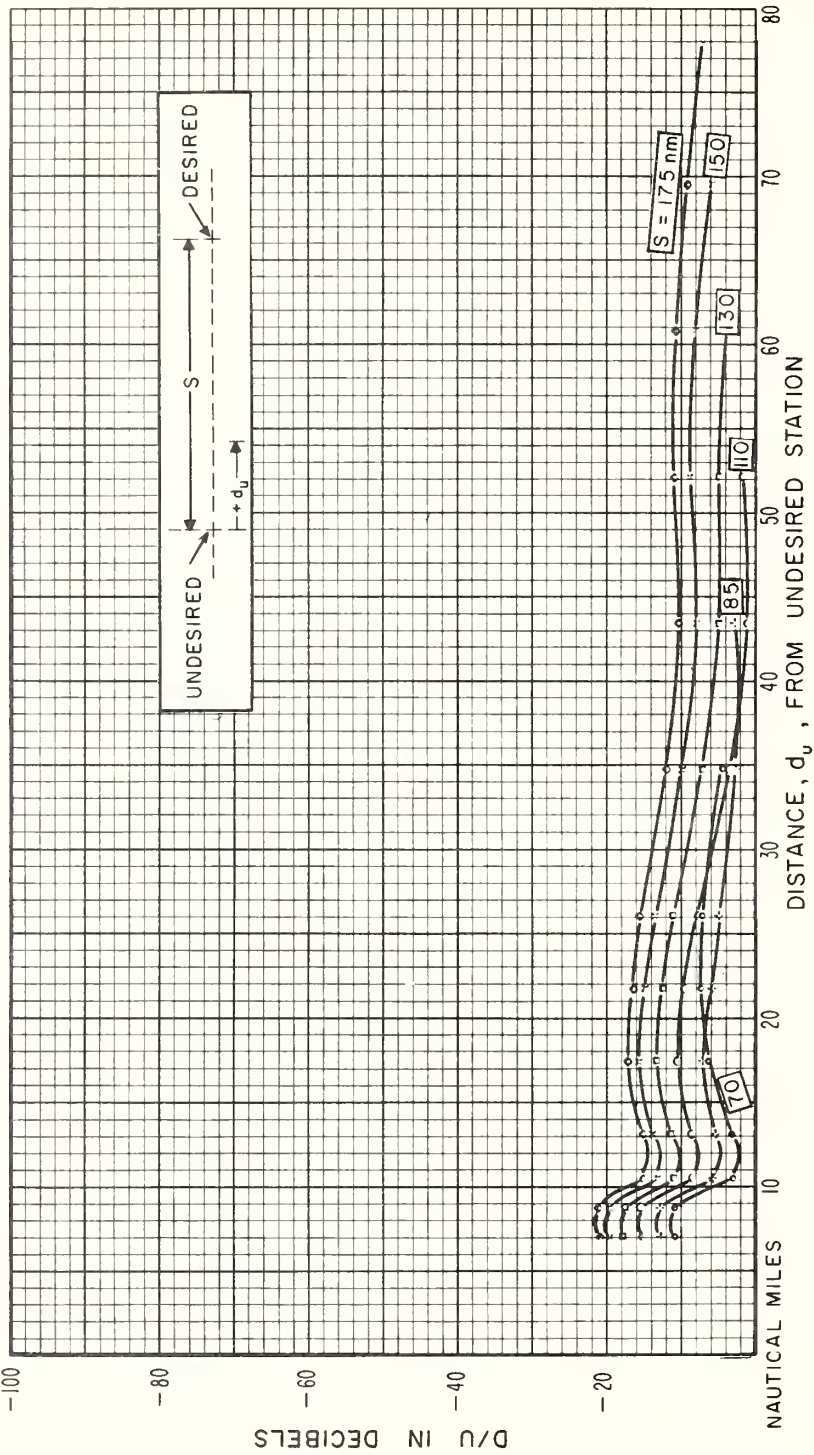


Figure 34

TACAN SIGNAL RATIOS NEAR AN INTERFERING STATION

FREQUENCY 1150 Mc/s
 ALTITUDE 70,000 FEET
 STATION SEPARATION, S, AS LABELED
 95% RELIABILITY

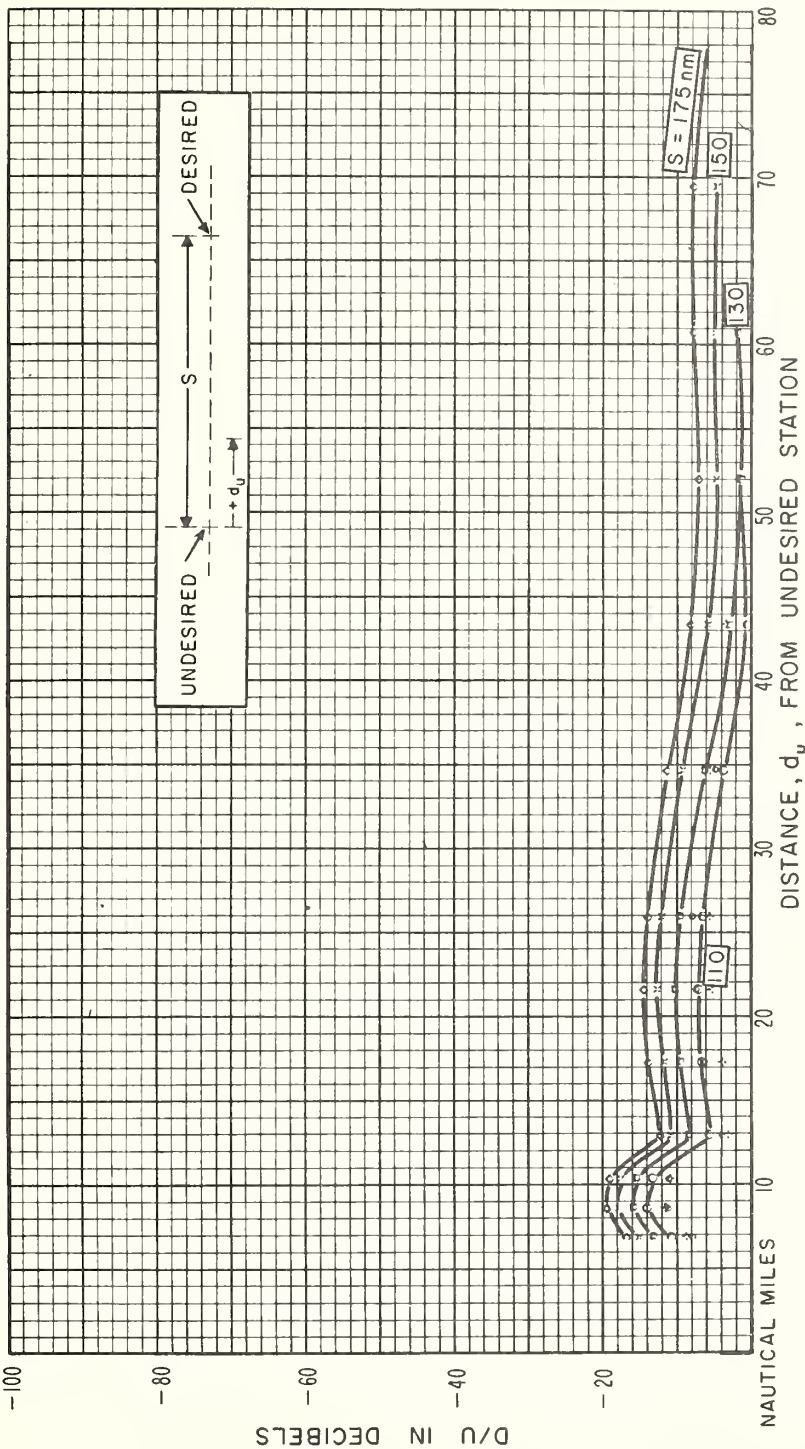


Figure 35

TACAN SIGNAL RATIOS NEAR AN INTERFERING STATION

FREQUENCY 1150 Mc/s
 ALTITUDE 80,000 FEET
 STATION SEPARATION, S, AS LABELED
 95% RELIABILITY

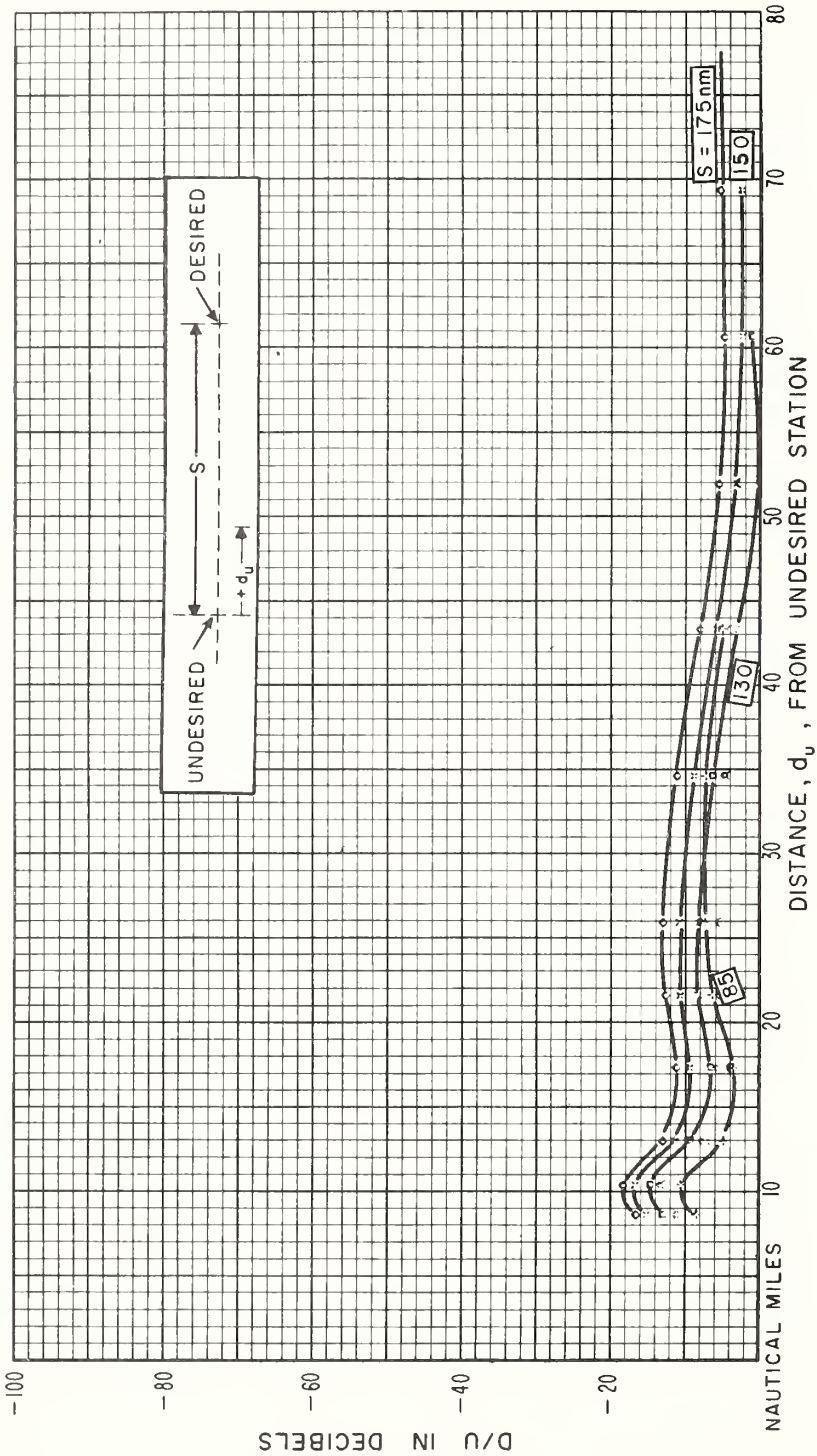


Figure 36

TACAN SIGNAL RATIOS NEAR AN INTERFERING STATION

FREQUENCY 1150 Mc/s
 ALTITUDE 90,000 FEET

STATION SEPARATION, S , AS LABELED
 95% RELIABILITY

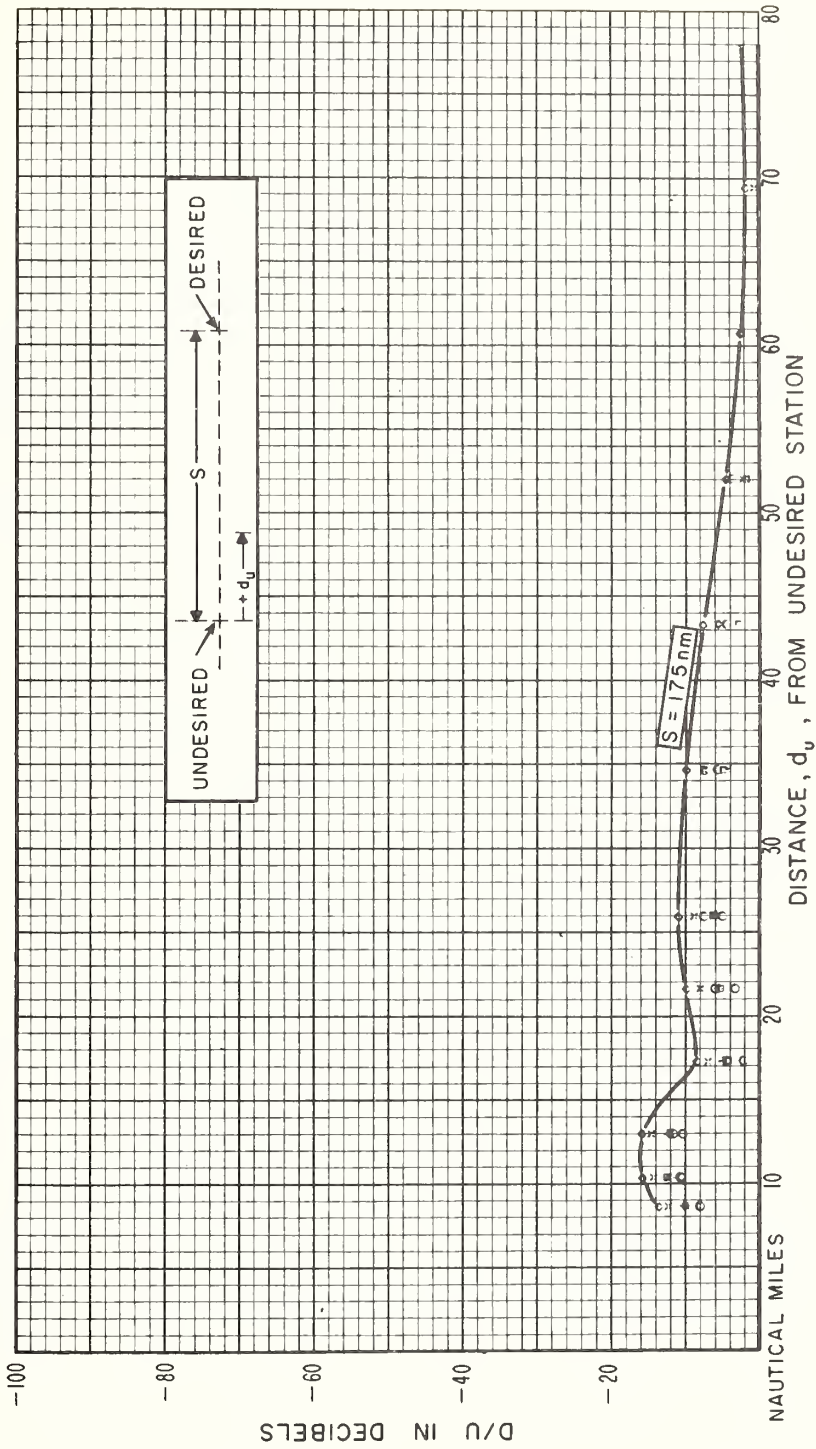


Figure 37

TACAN SIGNAL RATIOS NEAR AN INTERFERING STATION

FREQUENCY 1150 Mc/s
 ALTITUDE 100,000 FEET
 STATION SEPARATION, S, AS LABELED
 95 % RELIABILITY

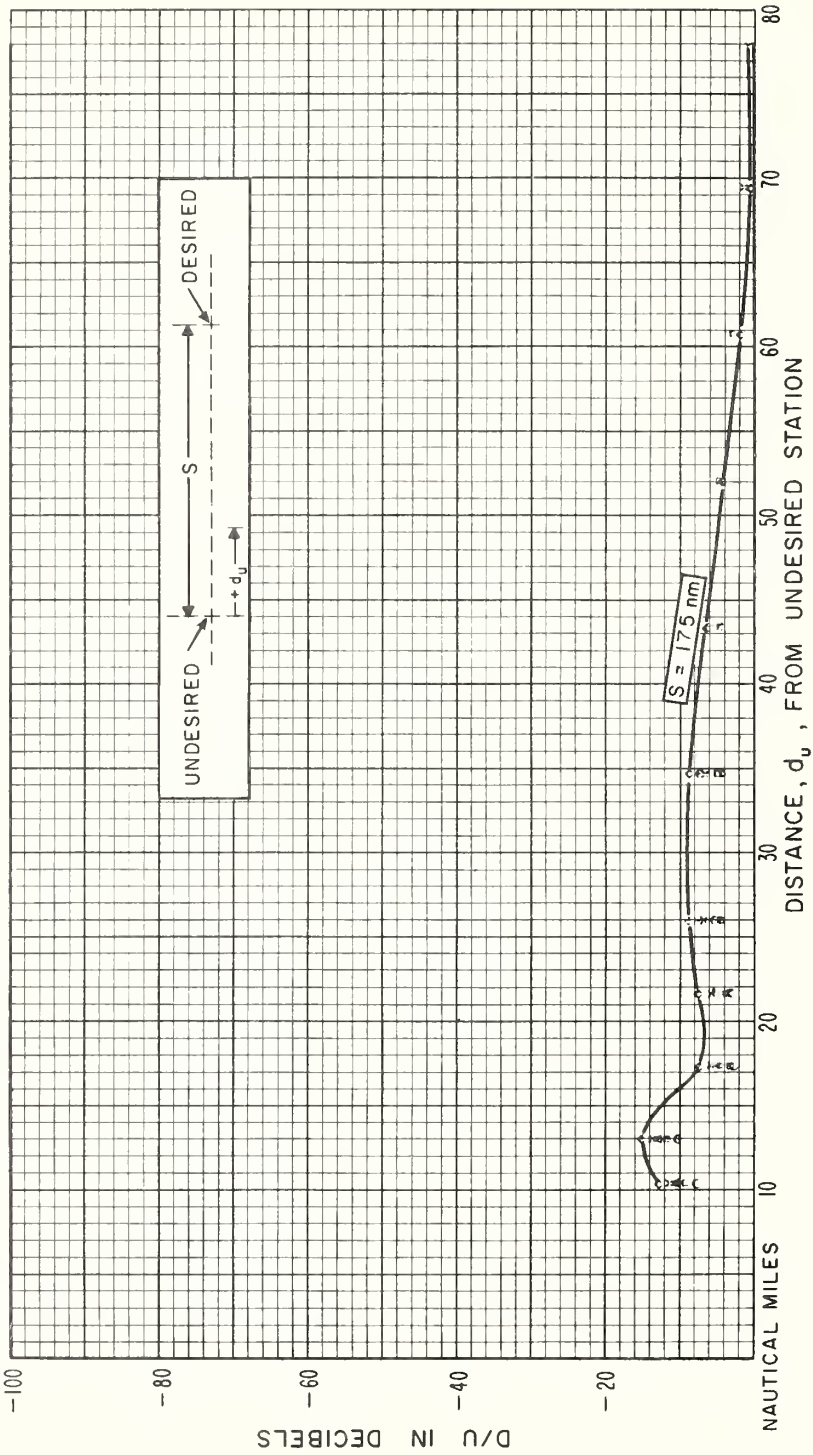


Figure 38

APPENDIX

1. VOR PROPAGATION MODEL

As mentioned briefly in Section 2 of the main body of this report, the smooth, spherical earth model was used to calculate transmission loss for the VOR system at 113 Mc/s. A linear-gradient atmosphere was assumed for the initial calculations, so that for a first approximation radio rays could be considered to be straight lines above an earth having an effective radius k times its actual value. Where appropriate, ray tracing methods were used for final calculations. In conformance with usual practice, the effective earth radius factor, k , was assumed to be $4/3$ for the "standard" atmosphere. Calculation methods are based on material contained in NBS Report 6767 [1961].

It was found convenient to include only the gain of the transmitting antenna in the definition of transmission loss as used in these calculations. Usually, the term transmission loss includes the antenna gains at both path terminals, whereas the term "basic transmission loss" excludes all antenna gains [Norton, 1953 and 1959]. In this study, an hourly median transmission loss, L_m , is defined to include the free-space gain of the transmitting antenna as a function of the elevation angle above ground as well as the effect of reflections from the counterpoise and from the ground. The transmitting antenna at the ground VOR station is a standard horizontally polarized Alford loop array 4 ft above the center of a 52 ft diameter counterpoise, which in turn is 12 ft above ground level.

Within the radio horizon, values of the hourly median transmission loss, L_m , were calculated using geometrical optics methods [Kirby, Herbstreit, and Norton, 1952]. These methods take into

account the interference between the direct and the ground-reflected ray. Fig. I-1 shows the geometry for this ray interference problem, and defines many of the symbols used in the analysis. Using this geometry, two curves of L_m versus distance were calculated for each assumed aircraft altitude. One curve applies to reflections from the counterpoise, where applicable, and the other to reflections from the ground. Both curves were blended in the region where the assumed specular reflection point is close to the edge of the counterpoise. In order to facilitate this blending, the curves were calculated so that they extended beyond their region of validity.

For reflections from the counterpoise, calculated for elevation angles greater than 5 degrees, the effective earth radius is increased by the height of the counterpoise above ground so that a sphere through the level of the counterpoise becomes the reflecting surface. For the calculations, all heights and distances are expressed in statute miles, and all angles in radians. The following constants and relationships were used, with most of the symbols defined on Fig. I-1.

- a effective earth radius = $4/3$ times the actual radius of the earth ($a = 5280$ statute miles).
- a_c effective earth radius for reflections from the counterpoise ($a_c = a + 12$ ft, but is also expressed in statute miles).
- h_1 height of the transmitting antenna above the reflecting surface ($h_1 = 4$ ft for reflections from the counterpoise, and 16 ft for reflections from the ground).
- h_2 aircraft altitude above the reflecting surface (h_2 is the aircraft altitude above ground for reflections from the ground, and the altitude minus 12 ft for reflections from the counterpoise).

- $|R|$ magnitude of the reflection coefficient, assumed to be 0.95 for counterpoise reflections and 0.9 for ground reflections.
- c phase angle of the reflection coefficient relative to π , and assumed to be zero for both cases.
- D divergence factor, assumed to be unity for reflections from the counterpoise.
- d distance along the great circle path to a point on the reflecting surface below the aircraft.
- r_0 length of the direct ray path.
- $r_1 + r_2$ length of the reflected ray path.
- d_1 distance from transmitting antenna to reflection point.
- d_2 distance from aircraft to reflection point.
- ψ grazing angle at reflection point.

The first step was the determination of the grazing angle ψ . The constant a shown in the equations below refers to reflections from the ground ($\psi < 15^\circ$); for reflections from the counterpoise ($\psi > 5^\circ$), the effective earth radius a_c was used instead of a , and the heights h_1 and h_2 were changed accordingly. Initial values of the linear distance d are estimates, which were checked later by ray-tracing methods, and changed if necessary:

$$d = d_1 + d_2 \quad (\text{I-1})$$

$$h_1' = h_1 - d_1^2/2a \quad (\text{I-2a})$$

$$h_2' = h_2 - d_2^2/2a \quad (\text{I-2b})$$

$$\tan \psi = h_1'/d_1 = h_2'/d_2 \quad (\text{I-3})$$

Equations (I-2a), (I-2b), and (I-3) are approximate relations. In order to utilize the electronic computer in solving the above expressions for the grazing angle ψ , an iteration method was used, assuming for each d different values of d_1 until the equations were satisfied within the desired limits of accuracy, which was $\pm 10^{-6}$ miles in this case. Final values for ψ for each assumed total distance d were then used to calculate various auxiliary angles and quantities to be used in the ray-tracing problem and in the final calculation of the transmission loss L_m . For reflections from the counterpoise h_1' may be assumed equal to h_1 , d_2 to equal d , and ψ can be determined directly without iteration.

Referring to Fig. I-1, the ray path portion r_1 for reflections from the counterpoise can be very closely approximated by:

$$r_1 \cong h_1 / \sin \psi, \quad (\text{I-4})$$

as the distance to the reflection point is extremely small. By the same reasoning,

$$\theta_1 \cong (r_1 \cos \psi) / a_c \quad (\text{I-5})$$

Other needed quantities are calculated as follows:

$$\sin \phi_2 = (a_c \cos \psi) / (a_c + h_2) \quad (\text{I-6})$$

$$\theta_2 = \pi/2 - \psi - \phi_2 \quad (\text{I-7})$$

$$\theta_o = \theta_1 + \theta_2 \quad (\text{I-8})$$

$$r_2 = (a_c \sin \theta_2) / (\sin \phi_2) \quad (\text{I-9})$$

$$r_o = \sqrt{(h_1 - h_2)^2 + 4(a_c + h_1)(a_c + h_2) \sin(\theta_o/2)} \quad (\text{I-10})$$

The total angular distance θ_o is now used to obtain the corrected great-circle distance d from

$$d = a \theta_o, \quad (\text{I-11})$$

which may differ slightly from the first assumption given by (I-1).

For the reflections from the ground, the approximations (I-4) and (I-5) can no longer be used, because the reflection point may not be close enough to the transmitting antenna. Referring again to Fig. I-1, the following relations are established, again after first obtaining the grazing angle ψ :

$$\sin \phi_1 = (a \cos \psi) / (a + h_1) \quad (\text{I-12})$$

$$\sin \phi_2 = (a \cos \psi) / (a + h_2) \quad (\text{I-13})$$

$$\theta_1 = \pi/2 - \psi - \phi_1 \quad (\text{I-14})$$

$$\theta_2 = \pi/2 - \psi - \phi_2 \quad (\text{I-15})$$

$$r_1 = (a \sin \theta_1) / (\sin \phi_1) \quad (\text{I-16})$$

$$r_2 = (a \sin \theta_2) / (\sin \phi_2) \quad (\text{I-17})$$

$$\theta_o = \theta_1 + \theta_2 \quad (\text{I-8})$$

$$r_o = \sqrt{(h_1 - h_2)^2 + 4(a + h_1)(a + h_2) \sin(\theta_o/2)} \quad (\text{I-18})$$

Again the corrected great circle distance d is obtained using (I-11). For this case of reflections from the ground, a divergence factor D is now calculated using:

$$D = \frac{a(r_1 + r_2) \cos \psi}{(a + h_1)(a + h_2)} \sqrt{\frac{\sin \psi}{\sin \theta_o (\sin \theta_1 \cos \phi_2 + \sin \theta_2 \cos \phi_1)}} \quad (\text{I-19})$$

Before calculating the transmission loss values as a function of distance for reflections from the counterpoise ($\psi > 5^\circ$) as well as for reflections from the ground ($\psi < 15^\circ$), it is necessary to determine the angles γ_{o1} and γ_{r1} for which the voltage gain of the ground antenna is used. From Fig. I-1,

$$\sin \beta = [r_2 \sin(\pi - 2\psi)] / r_o \quad (\text{I-20})$$

$$\gamma_{o1} = \beta - \psi - \theta_1 \quad (\text{I-21})$$

$$\gamma_{r1} = -(\psi + \theta_1) \quad (\text{I-22})$$

The voltage gains g_{o1} and g_{o2} of the ground antenna relative to that of an isotropic radiator are given by 1.28 times the cosine of the elevation angle of the direct and the ground-reflected rays, respectively:

$$g_{o1} = 1.28 \cos \gamma_{o1} \quad (\text{I-23a})$$

$$g_{o2} = 1.28 \cos \gamma_{o2} \quad (\text{I-23b})$$

All quantities necessary in the calculation of L_m have now been determined (r_o , r_1 , r_2 , $|R|$, c , g_{o1} , g_{o2} , D , and d), except the relative phase angle between the direct ray r_o and the ground-reflected ray, r_1 . This phase angle Δ , in radians, can be expressed by:

$$\Delta = 33.73 f_{Mc} (r_1 + r_2 - r_o) - c, \quad (\text{I-24})$$

where $f_{Mc} = 113 \text{ Mc/s}$ is the carrier frequency of the signal, taken at the center of the VOR band.

Finally, the formula for L_m can be written as follows, where the actual lengths of the ray paths r_o , r_1 , and r_2 are used instead of the great circle distance d . The great circle distance, however, is used as an abscissa parameter in plotting L_m , and for subsequent applications.

$$L_m = 36.58 + 20 \log_{10} f_{Mc} + 20 \log_{10} r_o - 10 \log_{10} \left\{ g_{o1}^2 + \left[\frac{r_o D |R| g_{r1}}{r_1 + r_2} \right]^2 - \frac{2 r_o D |R| g_{o1} g_{r1} \cos \Delta}{r_1 + r_2} \right\} \quad (\text{I-25})$$

For large distances and low angles the linear gradient atmosphere predicts too much bending [Bean and Thayer, 1959]. To correct for this, a ray leaving the ground station antenna at the same angle, γ_{01} , as the direct ray calculated using a linear gradient atmosphere was traced through an exponential atmosphere until it reached the aircraft altitude. The great circle distance below the ray was then used in the final calculations instead of the distance d obtained by (I-11). The angle, γ_{02} , at which the direct ray arrived at the aircraft was also determined by this ray tracing procedure. The exponential atmosphere used corresponds to the reference atmosphere given by Rice, Longley, and Norton [1959] with a surface refractivity of $N_s = 301$.

Calculations of transmission loss beyond the radio horizon were made by combining smooth-earth diffraction with tropospheric scatter. The short-cut method of Vogler [1961] was used for diffraction computations, as it specifically applies to horizontal polarization. Scatter computations and methods of combining the two mechanisms follow the work by Rice, et al. [1959].

Calculations for the beyond-the-horizon case are based on the same exponential atmosphere used for within-the-horizon computations. For the beyond-the-horizon case the effect of the finite counterpoise can be neglected, as the grazing angles involved are very low or zero; thus the transmitting antenna was treated as a single loop 16 ft above ground. The electrical constants of the ground assumed for calculations of the diffracted wave were a dielectric constant, $\epsilon = 15$, and a conductivity value, $\sigma = 5$ millimhos per meter. At the carrier frequency used, however, the effect of ground constants is small.

Finally, from a large number of computations both within and beyond the radio horizon, a set of curves was drawn for discrete aircraft altitudes showing the expected median transmission loss as a function of the great circle distance, d , and assuming the antenna gain of the ground station to correspond to a half-wave dipole. The construction of these curves involved a certain amount of blending from one propagation mechanism to another.

Long-term variability, short-term fading, and the effective gain variations of the airborne antenna were treated statistically. Long-term variability is described by the time availability function $V(p, d)$ for $\theta < 10$ milliradians and $V(p, \theta)$ for $\theta \geq 10$ milliradians. The angular distance, θ , is defined to be the angle between horizon rays from the transmitter and receiver [Norton, Rice, and Vogler, 1955], and is defined on Fig. 1 of the main body of this report. For within-the-horizon cases, θ is negative, and not explicitly used. Equations and curves from NBS Report 6767 [1961] along with the curve by Rice, et al. [1959] giving effective heights for high antennas were used to calculate the $V(p, d)$ and $V(p, \theta)$ functions applicable to all hours of the year.

Short-term fading was described by a cumulative distribution function $V'_F(p, \theta)$; it includes the summing of a constant vector and a Rayleigh-distributed vector. An auxiliary distribution function $V'_F(p, \theta)$ was developed using, (1) fading range data, $R(0.1) - R(0.9)$, for 100 Mc/s from a paper by Janes [1955] to express fading range as a function of θ , and (2) Fig. 6 and Table I from Norton, Vogler, Mansfield, and Short [1955] to specify a cumulative distribution, $V'_F(p, \theta)$, for the fading range given by a particular value of θ . For any percentage level λ , $R(\lambda/100)$ is the magnitude level of a cumulative distribution representing the sum of a constant vector and a

Rayleigh-distributed vector expressed in decibels relative to the constant component. Fading range as a function of the angular distance, θ , in degrees, was approximated by

$$R(0.1) - R(0.9) = 0 \text{ for } \theta < 0, \quad (\text{I-26a})$$

$$R(0.1) - R(0.9) = 1 + 12.4\theta \text{ for } 0 \leq \theta < 1^\circ, \quad (\text{I-26b})$$

and
$$R(0.1) - R(0.9) = 13.4 \text{ for } \theta \geq 1^\circ. \quad (\text{I-26c})$$

The distribution functions $V_F(p, \theta)$ and $V'_F(p, \theta)$ are related by

$$V_F(p, \theta) = V'_F(p, \theta) - V'_F(50, \theta) \quad (\text{I-27})$$

Only $V_F(p, \theta)$, which has the median of $V'_F(p, \theta)$ as a reference value, was used in determining short-term variability.

It was unnecessary to consider a different aircraft antenna gain for the direct and reflected rays because their arrival angles are nearly equal as would be more apparent if Fig. I-1 were drawn to scale. This made calculations considerably simpler since the aircraft antenna gain could be described statistically by a cumulative distribution $V_A(p, \gamma_{o2})$, which is a function of γ_{o2} only.

$V_A(p, \gamma_{o2})$ distributions were developed using data from an aircraft antenna modeling study, employing a passenger type aircraft with an E-cavity VOR antenna in its vertical stabilizer [Convair, 1959]. The data used were gain measurements taken around the model with γ_{o2} constant. For each γ_{o2} from 0° through -60° the measured data were expressed as a cumulative distribution and this distribution approximated by using segments of normal distributions drawn through

the 1, 10, 50, 90, and 99% points as shown in Fig. 2 of the main body of the report. Linear interpolation was used to obtain distributions for angles at which data were not available.

Distributions of transmission loss values were calculated as follows using the terms discussed:

$$L(p, d) = L_m - [V(p, \theta \text{ or } d) * V_F(p, \theta) * V_A(p, \gamma_{O2})] \quad (I-28)$$

In this equation all terms except L_m are cumulative distributions for the reliability p , so that the calculation of $L(p, d)$ required several successive convolution processes which are indicated by the operational symbol $*$, and will be further discussed later on.

2. TACAN PROPAGATION MODEL

The TACAN propagation model differs from the VOR model discussed above principally by the use of vertical instead of horizontal polarization and by the assumption of a uniformly rough earth model for transmission loss calculations at the 1150 Mc/s center frequency of the TACAN band. The vertical radiation pattern of the ground station was shown on Fig. 3 of the main body of this report. It is based on a typical center array [Casabona, 1956], with the antenna located 18 ft above the center of the VOR counterpoise and 30 ft above ground.

Median transmission loss L_m , again including the gain of the transmitting antenna, was calculated using geometric optics methods for distances within the radio horizon, but the reflected energy was treated statistically. Thus L_m becomes mainly a function of the direct ray path distance and the gain of the transmitting antenna in the appropriate directions.

The statistical treatment of reflections from the counterpoise was based on the assumption that the complex lobe structure due to the high frequency and the high antenna can best be described by a cumulative distribution function obtained by adding vectorially two rays, one at random phase relatively to the other, where the "constant" vector represents the direct ray, and the vector at random phase has a magnitude r times the magnitude of the "constant" vector which is given by the assumed reflection coefficient and the voltage gains of the transmitting and the receiving antenna as a function of the grazing angle and the other auxiliary angles described by the geometry of Fig. I-1. This distribution function can be considered another factor entering the short-term variability, as the movement of the aircraft through space can be assumed to be random with respect to the complex lobe pattern described by the distribution. The median value of this distribution represents a term added to the free-space median L_m calculated as a function of ray path length, and the distribution itself with respect to the median will be used later as a component of the total variability of the signal.

This concept is illustrated on Fig. I-2. The cumulative distribution, designated $V'_C(p, r)$, due to the vector addition of a unity component and a component r at random phase, in decibels, is given by Norton, Vogler, Mansfield, and Short [1955]:

$$V'_C(p, r) = -10 \log_{10} [1 + r^2 + 2r \cos \pi (p/100)] \quad (\text{I-29})$$

where p is the percentage of time, and the argument $\pi(p/100)$ is in radians. The median of this distribution is obtained from setting p equal to 50:

$$V'_C(50, r) = -10 \log_{10} (1 + r^2) \quad (\text{I-30})$$

This median value is added to the median transmission loss L_m , and takes into account the median power contained in the ray reflected from the counterpoise.

The short-term variability $V_C(p, r)$ due to this distribution, to be used in the same manner as previously shown for VOR, is given by:

$$V_C(p, r) = V'_C(p, r) - V'_C(50, r) \quad (\text{I-31})$$

The relative magnitude r of the random component, assumed to be 0.9 for the illustrative example of Fig. I-2, is given by:

$$r = (R_C g_{r1})/g_{o1} \quad (\text{I-32})$$

where R_C is the reflection coefficient of the counterpoise, and g_{o1} and g_{r1} are the voltage gain factors of the transmitting antenna relative to an isotropic radiator in the direction of the direct, and of the ground-reflected ray, respectively; similar to the VOR case. The dependence of the voltage gain on the elevation angles γ_{o1} and γ_{r1} (defined previously for the VOR case and on Fig. I-1) is shown for the TACAN ground antenna on Fig. 3 of the main body of the report.

Values for the reflection coefficient R_C were assumed as follows as functions of the grazing angle ψ :

For $\psi \leq 30^\circ$, $R_C = 0$ (no reflection from the counterpoise)

For $30^\circ < \psi \leq 43^\circ$, $R_C = 4.19\psi - 2.19$, where ψ is in radians

For $\psi > 43^\circ$, $R_C = 0.95$

Reflection from the uniformly rough ground was assumed to occur for grazing angles less than 30 degrees. In this case a cumulative distribution function $V'_F(p, K)$ represents the energy scattered from the ground, similar to the function $V'_C(p, r)$ used to represent reflections from the counterpoise. Here, the parameter $K = 20 \log_{10} k$ where k is the ratio of the root-mean-square value of the field due to scattering of the reflected ray to that due to the direct ray. With an assumed effective ground reflection coefficient R_G , and antenna voltage gain values g_{o1} and g_{r1} as before, k is given by:

$$k = (R_G g_{r1})/g_{o1} \quad (\text{I-33})$$

The distribution function $V'_F(p, K)$ was discussed and tabulated by Norton, Vogler, Mansfield, and Short [1955] for various values of K . The effective ground reflection coefficient R_G was assumed as follows as a function of the grazing angle ψ :

For $\psi \leq 30^\circ$, $R_G = 0.3$

For $30^\circ < \psi \leq 43^\circ$, $R_G = -0.132\psi + 0.992$, where ψ is in radians

For $\psi > 43^\circ$, $R_G = 0$ (no reflection from the ground due to the presence of the VOR counterpoise)

From the distribution of $V'_F(p, K)$, the median value for $p = 50$ was determined and subtracted from the median transmission loss value L_m in order to take into account the median power reflected by the rough earth. The short-term variability $V_F(p, K)$ due to this distribution, and to be used later on, is given by:

$$V_F(p, K) = V'_F(p, K) - V'_F(50, K) \quad (\text{I-34})$$

The geometric parameters according to Fig. I-1 are the same for TACAN as for the VOR case discussed above. The treatment of reflections from the ground eliminates the need for calculating a divergence factor. For reflection from the counterpoise the divergence factor is assumed to be unity, as before. The carrier frequency used in the calculations was 1150 Mc/s, and the height of the ground antenna is 30 ft above ground and 18 ft above the counterpoise. The maximum gain of the ground antenna is 8.15 db relative to an isotropic antenna. This value occurs at an elevation angle of approximately 5 degrees (see Fig. 3 of the main body of the report, where the ordinate scale designates the voltage gain g_{o1} relative to this maximum).

The median transmission loss, L_m , for the TACAN case, in view of the procedures described above, is now given by:

$$L_m = 36.58 + 20 \log_{10} f_{Mc} + 20 \log_{10} r_o - 20 \log_{10} g_{o1} - 8.15 + V'_C(50, r) - V'_F(50, K) \quad (I-35)$$

Corrections for excess ray bending were made in the same way as for the VOR model, using the same exponential atmosphere.

Calculations of median transmission loss beyond the radio horizon were made by combining smooth-earth diffraction with tropospheric scatter in the same way as was done for VOR. However, the method of calculating diffraction according to Vogler [1961] could not be used, because it does not apply to vertical polarization. It was replaced by more general methods described by Norton, Rice, and Vogler [1955], and in NBS Report 6767 [1961]. Again, for beyond-the-horizon calculations the grazing angles are essentially zero, and the effect of the counterpoise is neglected. The construction of final

propagation curves (L_m versus d) for various discrete aircraft altitudes involved again a certain amount of blending from one propagation mechanism to another.

Long-term variability was described statistically for all distances by the function $V(p, d)$, using the same methods as in the VOR propagation model. For the TACAN model the function $V(p, \theta)$ was not used at all

Short-term (within-the-hour) fading within the radio horizon was described by cumulative distribution functions $V_C(p, r)$ and $V_F(p, K)$, which result from the random addition of the direct and the counterpoise or ground-reflected ray as described above. Equations (I-31) and (I-34) defined these functions. For distances beyond the radio horizon, $V_F(p, K)$ was used with K determined in a way similar to the one described for the VOR model, but based on 1,000 Mc/s fading range data from the paper by Janes [1955]. The two curves for K obtained were blended in the vicinity of the radio horizon in order to obtain a continuous function of K versus distance.

As in the case of VOR, variations in the gain of the aircraft antenna also enter as a short-term fading term, and are described by a cumulative distribution function $V_A(p, \gamma_{02})$, where γ_{02} is the arrival angle of the direct ray at the aircraft (see Fig. I-1). For the type of aircraft antenna used in these calculations, typical distributions for various values of γ_{02} are shown on Fig. 4 of the main body of the report.

All time variability functions were combined by statistical convolution, and the resulting cumulative distribution of transmission loss as a function of the time variability p and the distance d is given by:

$$L(p, d) = L_m - \{V(p, d) * V_A(p, \gamma_{o2}) * V_F(p, K) * [-V_C(p, r)]\} \quad (I-36)$$

All terms in (I-36) except L_m are cumulative distributions, so that several successive convolutions are required, which are denoted by the symbol *. The choice of the values for the reflection coefficient from the ground and the counterpoise assured proper use of the components $V_F(p, K)$ and $V_C(p, r)$: for grazing angles less than 30 degrees the cumulative distribution $V_C(p, r)$ degenerates into a constant.

3. COMPUTATION PROCEDURES

a. General Methods and VOR Calculations

The model on which the computation methods and the numerical results in this report are based considers levels of signals from the desired and from the interfering station, with the receiving aircraft located directly above the great circle path between the two. First, the computer program applicable to the VOR system will be discussed in detail as representative of the overall approach. Variations introduced by consideration of the TACAN system will be pointed out later. Although the program has been written in a way so that it is applicable in the future to a multi-station interference study, its organization is better understood if the discussion is limited first to the two-station model described above. Once this has been understood possible extensions of the program to more complicated situations are easier to follow.

The machine program consists essentially of three parts which may be taken as three different "levels" of control. Actual computations are performed in Levels I and II, with Level III being a catalogue of computer routines available on call. Level II acts principally to

insure proper sequencing of the routines involved and keeps track of the operations performed. Fig. I-3 is a block diagram showing the relations between these levels and the sequence of computations.

Level I uses as its input a set of basic physical data in the form of tables, which have been previously assembled by separate machine programs and other computations. These basic data include transmission loss as a function of great-circle distance and aircraft height in the way defined in the previous sections, together with other geometric and equipment parameters necessary for the problem. The spatial relationship of the ground stations involved is also part of the basic data, but the aircraft antenna pattern (given by its cumulative gain distribution $V(p, \gamma_{o2})$) is brought in only at Level II.

It has been noted before that in this application the term transmission loss includes the gain of the transmitting ground antenna as well as the effect of reflections from the ground or the counterpoise. The construction of the basic data tables is accomplished independently of the main computer program and involves a combination of graphical and computer methods. The tables contain as the argument the distance d along the great circle path on the ground from the transmitting station considered to the aircraft location, and as functional values various geometric parameters defined in Fig. I-1, the angular distance θ and other parameters used in the calculation of the median transmission loss, L_m . A separate table is used for each aircraft height considered; the specific heights used were listed in Section 6 of the main body of this report. Although the formulation of these tables is an involved process, they are useful as they ultimately result in a saving of machine time in the main program. Once a table of transmission loss values is available, the machine calculation of a

value for a specific distance is accomplished by a table look-up and an interpolation.

The characteristics of the tables dictate the following order of calculations in Level I, as illustrated on Fig. I-4. Tables of all basic data for a specific value of aircraft altitude are read into storage. Then input information is read which specifies the separation $S = (d_D + d_U)$, where d_D and d_U , respectively, are the distances along the great circle path on the ground from the desired and the undesired station to the aircraft. An initial value for d_D is contained in the input and appropriate information regarding increments is part of the program. In Level I, the median transmission loss value L_m and other parameters are calculated for d_D and d_U , and presented to Level II for further calculations. Thus control alternates between Level I and Level II for each aircraft position with respect to the two ground stations at the given specific altitude. The schedule is repeated for all desired values of transmitter separation at this altitude; subsequently new tables for a different altitude are read into the machine, and the entire procedure repeated until all available input values are exhausted.

The parameters calculated by Level I of the program are used in Level II for the calculation of the various cumulative distributions which make up the expression for the time distribution of transmission loss previously shown as (I-28):

$$L(p, d) = L_m - [V(p, \theta \text{ or } d) * V_F(p, \theta) * V_A(p, \gamma_{O2})] \quad (\text{I-28})$$

Here the term $V(p, \theta \text{ or } d)$ is the cumulative distribution representing long-term variability of hourly medians (in the VOR case, either as a function of the angular distance, θ , for beyond-the-horizon

paths, or as a function of the path distance, d , for within-the-horizon paths). $V_F(p, \theta)$ represents the short-term (within-the-hour) variability and $V_A(p, \gamma_{O2})$ represents the variability introduced by the aircraft antenna as a function of the elevation angle γ_{O2} defined on Fig. I-1. The percentage of time is represented by the symbol p , and $L(p, d)$ denotes the resulting cumulative distribution of transmission loss. In this program, $L(p, d)$ is calculated for both distances d_D and d_U defined above.

The symbol $*$ in (I-28) denotes the statistical convolution of cumulative distributions. Basically, if two variables x and y are statistically independent and given by their cumulative distributions, their statistical convolution is the cumulative distribution of either the variable $z = x + y$, or the variable $z' = x - y$, depending on the application of the result, and determined in the machine program by an appropriate input code. The cumulative distribution of z is obtained most simply by selecting n equally spaced percentage values from the individual distributions of both x and y calculating all possible sums $z_k = x_i + y_j$, and forming the cumulative distribution of all values of z_k obtained in this manner. Similarly, the cumulative distribution of z' is obtained by forming all possible differences $z'_k = x_i - y_j$.

For the convolution of the individual distributions used in this study, a somewhat more sophisticated method was used in selecting percentage intervals, which provides greater accuracy at the "tails" of the distributions. All individual distributions are contained in storage in tabular form, and the convolution process itself takes the form of a program routine. Successive convolutions (as in I-28) are handled by first convoluting two distributions and then using this intermediate result in a convolution with the third individual distribution.

The convolution process is commutative; i. e., the order in which the individual distributions are used does not matter.

For each given aircraft elevation and spacing of ground station, the distribution of transmission loss $L(p, d)$ is determined for $d = d_D$ and $d = d_U$, the distances of the aircraft from the two ground stations considered. From the distribution $L(p, d_U)$, which is determined first, the values $L(0.05, d_U)$ and $L(0.95, d_U)$ are extracted, converted to relative voltages $E(0.05, d_U)$ and $E(0.95, d_U)$ by a special program routine, and stored for later use. Next, the transmission loss distribution $L(p, d_D)$ corresponding to the path from the desired station to the aircraft is determined. Finally, the cumulative distribution of the difference in transmission loss values, $L(p, d_U) * [-L(p, d_D)]$ is obtained by a convolution. As discussed above, this is equivalent to the distribution of the desired to the undesired signal strength ratios D/U at the receiver input in the aircraft. From this last distribution, a number of percentage values between $D/U(0.01)$ and $D/U(0.99)$ are selected and stored. They are also punched on cards, together with the values d_U and d_D as well as the voltages $E(0.05, d_U)$ and $E(0.95, d_U)$, previously obtained, which designate the extent of the noise-limited service as a function of distance and aircraft height. The subscript U in this case has no further significance; it only denotes that the data for the path identified by U were used for this purpose. The output in the form of punched cards facilitates graphical presentation of the results using an automatic plotter with card input.

Many of the distribution functions which enter into the machine calculation of $L(p, d)$ are empirical and can be stored in the machine in tabular form only. For the purpose of consistency and simplicity, all distribution functions entering the program routines are handled in tabular form, even if they can be expressed analytically. Consequently

a large number of tables is involved and a considerable amount of "bookkeeping" is necessary, which, together with the sequencing of computation and output routines, is the principal function of the Level II control.

Fig. I-5 is a flow diagram of Level II computations and illustrates the interplay between Level II and the program routines contained in Level III. These routines are designated by code names on Fig. I-5, which are tabulated and further explained below.

Table of Program Routines Contained in Level III

<u>Code Designation</u>	<u>Function</u>
(a) Major Routines	
ZEBRA	Computes a table describing the cumulative distribution function of the receiving antenna pattern, $V_A(p, \gamma_{02})$.
FALTG	Calculates the convolution of cumulative distribution functions; results are available to the program in form of a table.
VPT	Calculates the cumulative distribution function $V(p, \theta)$; results are in tabular form.
VPD	Calculates the average cumulative distribution function $V(p, d)$ from summer and winter values available from BRAP; results are in tabular form.

Table of Program Routines Contained in Level III (Continued)

<u>Code Designation</u>	<u>Function</u>
(b) Subroutines	
INTERP	This is an interpolation program, using the n^{th} Lagrangian approximation, with n specified in any particular case. It is used as a part of ZEBRA and FALTG, where interpolation between tabulated values is necessary.
ENDPNT	This is a routine similar to an interpolation, but it fits Gaussian distribution functions between given points of cumulative distributions like $V(p, d)$, etc. It is used in ZEBRA and VPD.
BRAP	This routine handles the actual calculation of summer and winter values for $V(p, d)$ at selected values of p . It is used for VPD, but ENDPNT is needed to find intermediate values.

Summarizing the program steps, it is seen that the group of programs contained in Level I are called by Level II to carry out the actual computations of transmission loss values and necessary geometric parameters. Level II control makes decisions based on information furnished by Level I as to which programs of that level are pertinent; subsequently Level II control calls these programs in their proper sequence, provides them with proper input, and keeps track of their output. This output eventually becomes input for additional Level III program steps also controlled by Level II, unless it constitutes an end result to be read out of the machine.

There is a specific routine for each component distribution which can enter into the transmission loss distribution given by (I-28). Upon being given a particular value of the elevation angle γ_{o2} , the program for the antenna gain distribution function $V_A(p, \gamma_{o2})$ extracts values of this function for $p = 1, 10, 50, 90,$ and 99% from the tables contained in storage. These and the corresponding percentage values used are presented to the ENDPNT routine which constructs a new table by a process equivalent to plotting the available points on normal probability paper and drawing straight lines between them. Thus a more complete table of the distribution function is obtained for use in the calculations.

The calculation of the long-term variability function $V(p, d)$ uses a similar procedure, but in this case two distributions $V_1(p, d)$ and $V_2(p, d)$ must first be calculated, corresponding to summer and winter data [NBS Report 6767]. These two distributions are averaged to give the desired $V(p, d)$ by means of the BRAP routine.

Tables are used exclusively for the long- and short-term variability functions $V(p, \theta)$, and $V_F(p, \theta)$ used in the VOR study.

With the extensive use of tables, the need to interpolate arises often, and linear interpolation will not always suffice. Therefore, a subroutine was included in the program which calculates the n^{th} Lagrangian approximation [Lance, 1960], where $n \leq m - 1$ with m being the number of entries in the table. The special case $n = 1$ results in linear interpolation. As a practical matter, n is usually required to be less than five. This is necessitated by the fact that Lagrangian interpolation may exhibit large oscillations between tabular entries whenever they do not lie on rather smooth analytic functions.

b. TACAN Calculations

The program for the TACAN system is only slightly different from the one discussed above for VOR. In Level I, the tables containing data for use in transmission loss calculations are different due to the changes in the propagation model discussed in Section 2 of this Appendix. These tables contain the great-circle distance d as the argument as before, but in addition to the TACAN median transmission loss L_m the parameters r and K defined by (I-32) and (I-33), respectively, are also listed as functions of d . These parameters enter two component distributions $V_F(p, K)$ and $V_C(p, r)$ used for TACAN which represent the variability introduced by the scattered ground- (or counterpoise-) reflected power and by the multiple lobes of the ground antenna. The distribution function $V_F(p, K)$ replaces $V_F(p, \theta)$ used for VOR. The long-term variability in the TACAN case is always represented by the $V(p, d)$ functions. The resulting transmission loss distribution for the TACAN case is now given by (I-36), which contains the additional term $-V_C(p, r)$:

$$L(p, d) = L(m) - \{V(p, d) * V_A(p, \gamma_{o2}) * V_F(p, K) * [-V_C(p, r)]\} \quad (I-36)$$

Level II differs from VOR only by the substitution of different tables corresponding to the TACAN distribution functions mentioned, and Level III is changed accordingly by deleting routines not needed and including new routines for the calculation of the distribution functions $V_C(p, r)$ and $V_F(p, K)$. Also, the tables used to calculate the antenna gain distribution function $V_A(p, \gamma_{o2})$ are changed in accordance with the TACAN aircraft antenna model used. For TACAN, the noise-limited service (without regard to interference from another station)

is denoted by receiver input power levels rather than by voltage levels as used for VOR. Consequently, power levels $P_a(0.95, d_U)$ and $P(0.05, d_U)$ are calculated from the corresponding transmission loss values and stored for output.

c. Extension of the Program to the Case of
Multiple-Station Interference

The present study is limited to a single interfering station acting on the reception of the desired signal at the aircraft receiver terminals. The computer program, however, can be expanded to permit a generalization of the problem; i. e., the consideration of interference from more than one station. In this case it would be necessary to provide more input information than given by the station separations in order to specify completely their positions relative to each other and relative to the aircraft. This requirement affects Level I routines by demanding more input parameters in several sets. Furthermore, an additional input to Level II is needed which indicates the number of interfering stations involved.

When considering n stations, Level II of the program would first calculate $L(p, d_{U(1)})$, $L(p, d_{U(2)})$, $\dots\dots L(p, d_{U(n-1)})$, which are the transmission loss distributions corresponding to each interfering station. These must then be converted to relative power units, and the distribution of their sum is determined by successive convolutions under the simplified assumption that no correlation exists between the various distributions. The result is converted back to a transmission loss distribution and substituted for the $L(p, d_U)$ distribution used in the single-interference case. No other changes are necessary in Level II, neither is Level III affected by the number of stations considered.

GEOMETRY FOR RAY INTERFERENCE WITHIN THE RADIO HORIZON

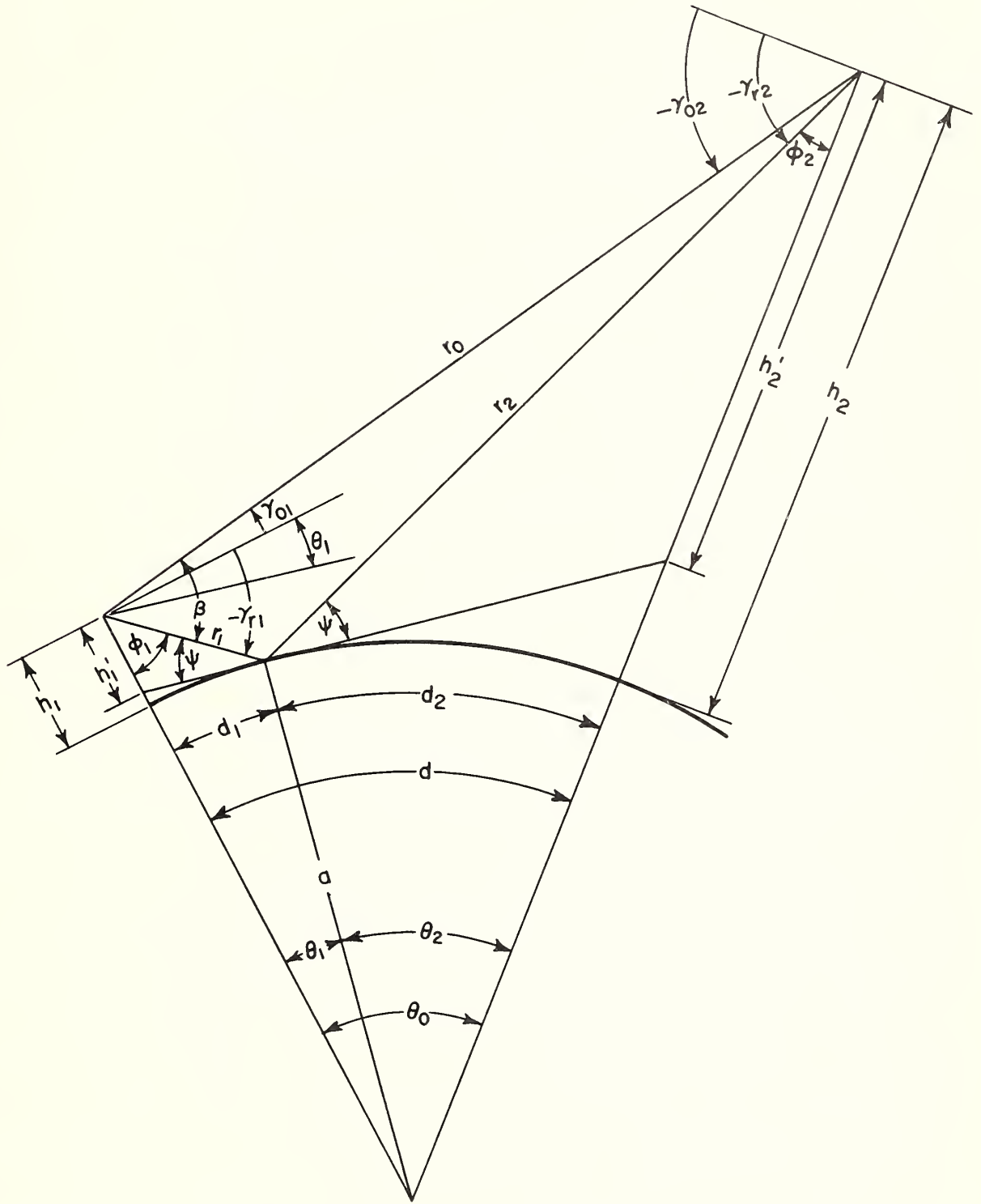


Figure I-1

THE CUMULATIVE DISTRIBUTION FUNCTION $V'_c(p, r)$ FOR $r=0.9$

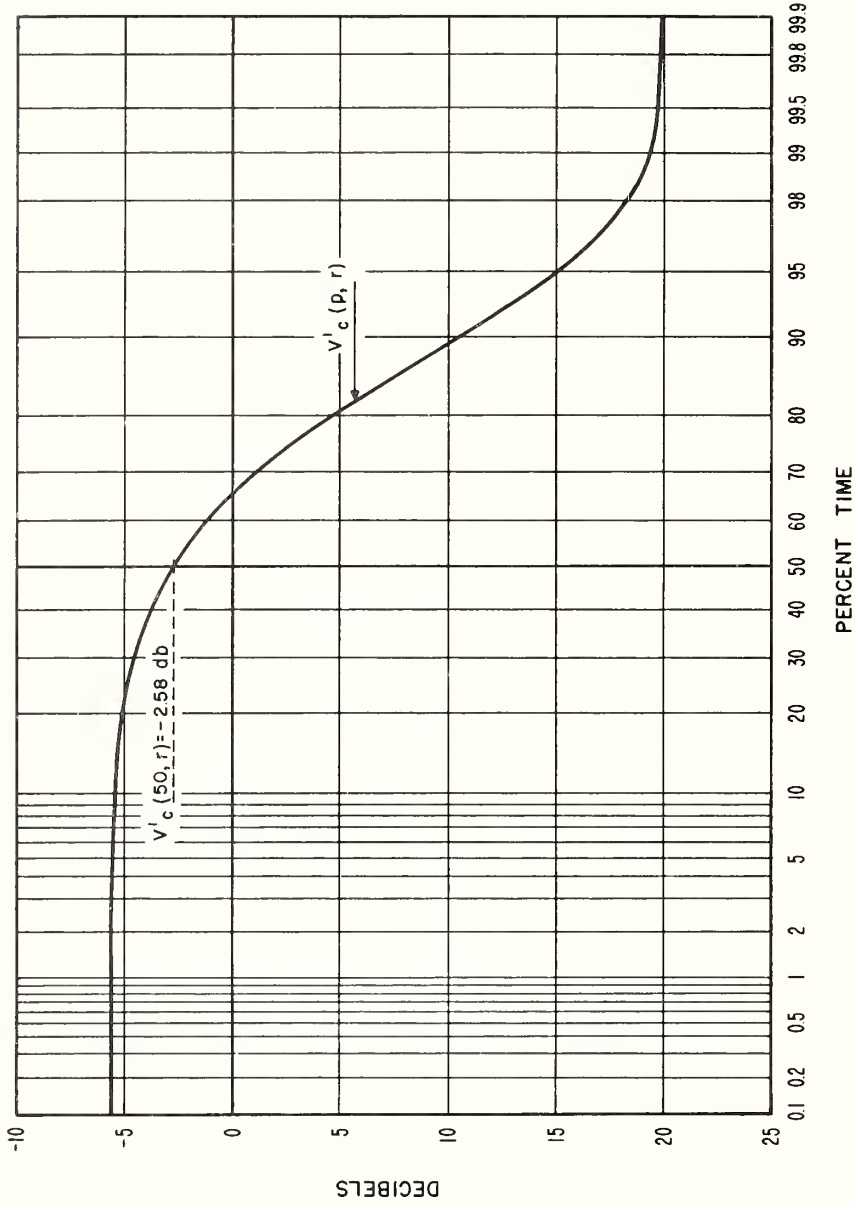


Figure I-2

BLOCK DIAGRAM OF COMPUTATION PROCEDURE

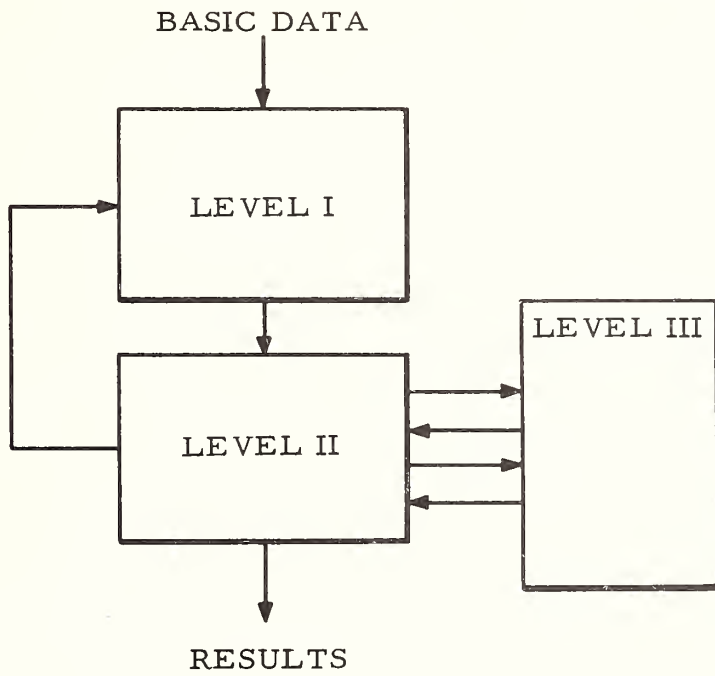


Figure I-3

FLOW DIAGRAM FOR LEVEL I OF MAIN COMPUTER PROGRAM

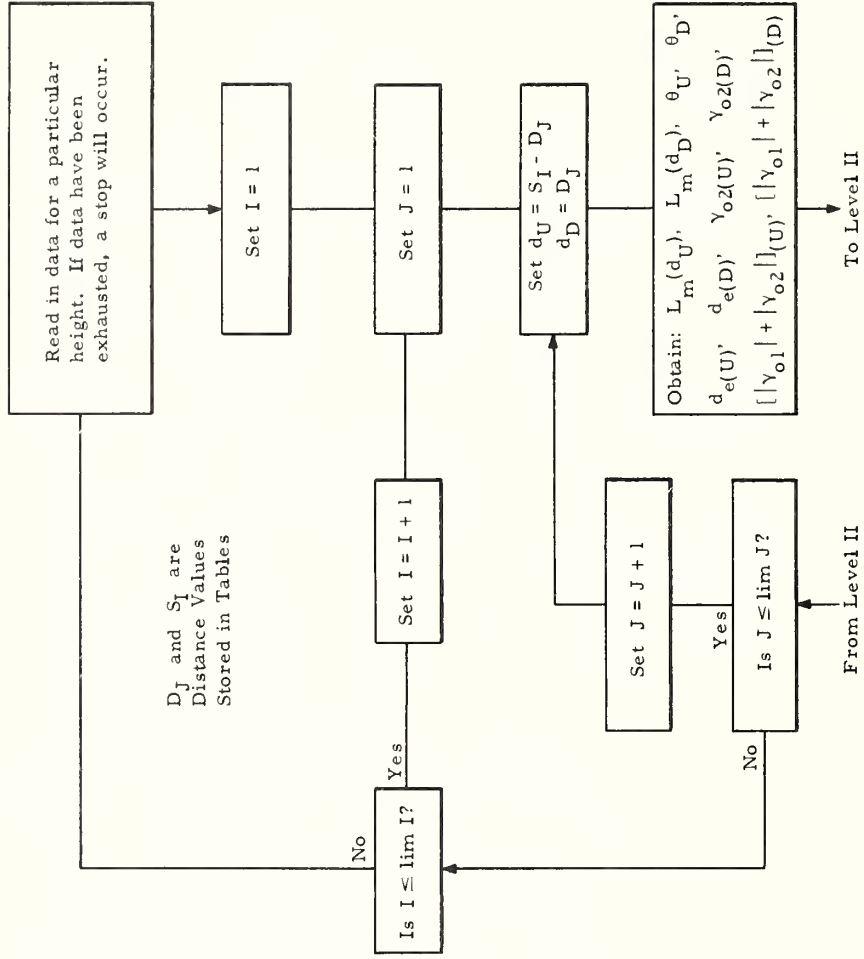


Figure I-4

FLOW DIAGRAM FOR LEVEL II COMPUTATIONS
(CODED ROUTINES ARE CONTAINED IN LEVEL III)

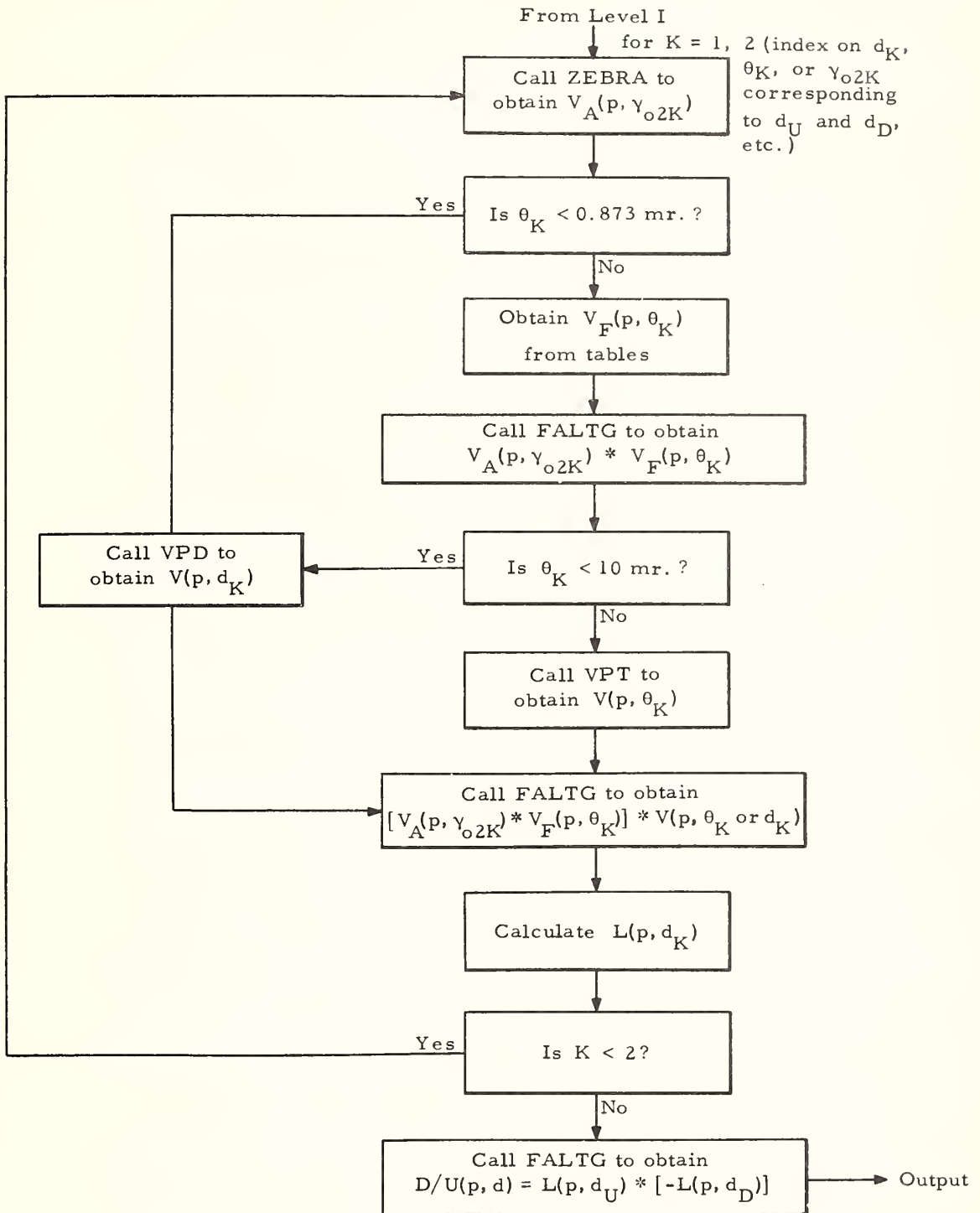


Figure I-5

REFERENCES

- Barsis, A. P., K. A. Norton, P. L. Rice, and P. H. Elder, Performance predictions for single tropospheric communication links and for several links in tandem, NBS Technical Note No. 102, PB 161603 (August 1961). \$3.00*
- Casabona, A. M., Antenna for the AN/URN-3 TACAN beacon, Electrical Communication, Vol. 33, No. 1, 35-59 (March 1956).
- Commercial Jetstar antenna installation, Report No. ER-3938 (October 1959). (Company Confidential)
- Convair 880 jet-liner antennas, Report No. ZN-22-006 (January 1959).
- Decker, M. T., TACAN coverage and channel requirements, NBS Report 5025 (1956).
- Decker, M. T., TACAN coverage and channel requirements, IRE Transactions on Aeronautical and Navigational Electronics, ANE-4, No. 3, 135-143 (September 1957).
- Janes, H. B., An analysis of within-the-hour fading in 100- to 1,000-Mc transmissions, J. Research NBS 54, No. 4, 231-250 (April 1955).
- Kirby, R. S., J. W. Herbstreit, and K. A. Norton, Service range for air-to-ground and air-to-air communications at frequencies above 50 Mc, Proc. IRE 40, No. 5, 525-536 (May 1952).
- Lance, G. N., Numerical methods for high speed computers, 142-144 (Iliffe, London, 1960).
- McGavin, R. E., and L. J. Maloney, Study at 1,046 megacycles per second of the reflection coefficient of irregular terrain at grazing angles, J. Research NBS 63D (Radio Prop.), No. 2, 235-248 (Sept. -Oct. 1959).

* Order by PB number from the Office of Technical Services, U. S. Department of Commerce, Washington 25, D. C. Foreign remittances must be in U. S. exchange and must include one-fourth of the publication price to cover mailing costs.

NBS Report 6767, Ground Telecommunications Performance Standards, Part 5 of 6, Tropospheric Systems, prepared by the Central Radio Propagation Laboratory of the National Bureau of Standards under sponsorship of the Ground Electronics Engineering and Installation Agency (Directorate of Engineering, ROZM). Also published as United States Air Force T.O. 31Z-10-1, under authority of the Secretary of the Air Force (June 15, 1961).

Norton, K. A., The calculation of ground-wave field intensity over a finitely conducting spherical earth, Proc. IRE 29, No. 12, 623-639 (December 1941).

Norton, K. A., Transmission loss in radio propagation, Proc. IRE 41, No. 1, 146-152 (January 1953).

Norton, K. A., System loss in radio-wave propagation, Proc. IRE 47, No. 9, 1661 (September 1959).

Norton, K. A., P. L. Rice, and L. E. Vogler, The use of angular distance in estimating transmission loss and fading range for propagation through a turbulent atmosphere over irregular terrain, Proc. IRE 43, No. 10, 1488-1526 (October 1955).

Norton, K. A., L. E. Vogler, W. V. Mansfield, and P. J. Short, The probability distribution of the amplitude of a constant vector plus a Rayleigh-distributed vector, Proc. IRE 43, No. 10, 1354-1361 (October 1955).

Rice, P. L., A. G. Longley, and K. A. Norton, Prediction of the cumulative distribution with time of ground wave and tropospheric wave transmission loss, NBS Technical Note No. 15, PB 151374 (July 1959). \$1.50*

Staras, H., P. L. Rice, and J. W. Herbstreit, An analysis of propagation phenomena as affecting VOR communication systems, NBS Report 1038 (1951).

Vogler, L. E., Smooth earth diffraction calculations for horizontal polarization, J. Research NBS 65D (Radio Prop.), No. 4, 397-399 (July-Aug. 1961).

* Order by PB number from the Office of Technical Services, U. S. Department of Commerce, Washington 25, D. C. Foreign remittances must be in U. S. exchange and must include one-fourth of the publication price to cover mailing costs.

U. S. DEPARTMENT OF COMMERCE

Luther H. Hodges, *Secretary*

NATIONAL BUREAU OF STANDARDS

A. V. Astin, *Director*



THE NATIONAL BUREAU OF STANDARDS

The scope of activities of the National Bureau of Standards at its major laboratories in Washington, D.C., and Boulder, Colorado, is suggested in the following listing of the divisions and sections engaged in technical work. In general, each section carries out specialized research, development, and engineering in the field indicated by its title. A brief description of the activities, and of the resultant publications, appears on the inside of the front cover.

WASHINGTON, D.C.

Electricity. Resistance and Reactance. Electrochemistry. Electrical Instruments. Magnetic Measurements. Dielectrics.

Metrology. Photometry and Colorimetry. Refractometry. Photographic Research. Length. Engineering Metrology. Mass and Scale. Volumetry and Densimetry.

Heat. Temperature Physics. Heat Measurements. Cryogenic Physics. Equation of State. Statistical Physics.

Radiation Physics. X-ray. Radioactivity. Radiation Theory. High Energy Radiation. Radiological Equipment. Nucleonic Instrumentation. Neutron Physics.

Analytical and Inorganic Chemistry. Pure Substances. Spectrochemistry. Solution Chemistry. Analytical Chemistry. Inorganic Chemistry.

Mechanics. Sound. Pressure and Vacuum. Fluid Mechanics. Engineering Mechanics. Rheology. Combustion Controls.

Organic and Fibrous Materials. Rubber. Textiles. Paper. Leather. Testing and Specifications. Polymer Structure. Plastics. Dental Research.

Metallurgy. Thermal Metallurgy. Chemical Metallurgy. Mechanical Metallurgy. Corrosion. Metal Physics.

Mineral Products. Engineering Ceramics. Glass. Refractories. Enameled Metals. Crystal Growth.

Physical Properties. Constitution and Microstructure.

Building Research. Structural Engineering. Fire Research. Mechanical Systems. Organic Building Materials. Codes and Safety Standards. Heat Transfer. Inorganic Building Materials.

Applied Mathematics. Numerical Analysis. Computation. Statistical Engineering. Mathematical Physics.

Data Processing Systems. Components and Techniques. Digital Circuitry. Digital Systems. Analog Systems. Applications Engineering.

Atomic Physics. Spectroscopy. Radiometry. Solid State Physics. Electron Physics. Atomic Physics.

Instrumentation. Engineering Electronics. Electron Devices. Electronic Instrumentation. Mechanical Instruments. Basic Instrumentation.

Physical Chemistry. Thermochemistry. Surface Chemistry. Organic Chemistry. Molecular Spectroscopy. Molecular Kinetics. Mass Spectrometry. Molecular Structure and Radiation Chemistry.

• Office of Weights and Measures.

BOULDER, COLO.

Cryogenic Engineering. Cryogenic Equipment. Cryogenic Processes. Properties of Materials. Gas Liquefaction.

Ionosphere Research and Propagation. Low Frequency and Very Low Frequency Research. Ionosphere Research. Prediction Services. Sun-Earth Relationships. Field Engineering. Radio Warning Services.

Radio Propagation Engineering. Data Reduction Instrumentation. Radio Noise. Tropospheric Measurements. Tropospheric Analysis. Propagation-Terrain Effects. Radio-Meteorology. Lower Atmosphere Physics.

Radio Standards. High Frequency Electrical Standards. Radio Broadcast Service. Radio and Microwave Materials. Atomic Frequency and Time Interval Standards. Electronic Calibration Center. Millimeter-Wave Research. Microwave Circuit Standards.

Radio Systems. High Frequency and Very High Frequency Research. Modulation Research. Antenna Research. Navigation Systems. Space Telecommunications.

Upper Atmosphere and Space Physics. Upper Atmosphere and Plasma Physics. Ionosphere and Exosphere Scatter. Airglow and Aurora. Ionospheric Radio Astronomy.

Department of Commerce
National Bureau of Standards
Boulder Laboratories
Boulder, Colorado

Official Business



Postage and Fees Paid
U. S. Department of Commerce